

การโคลนและลักษณะสมบัติของอัลเทอร์เนนซุเกรสจาก *Leuconostoc citreum* ABK-1 และ
บทบาทของกรดอะมิโนชนิดเอโรแมติกบริเวณผิวต่อขนาดของผลิตภัณฑ์



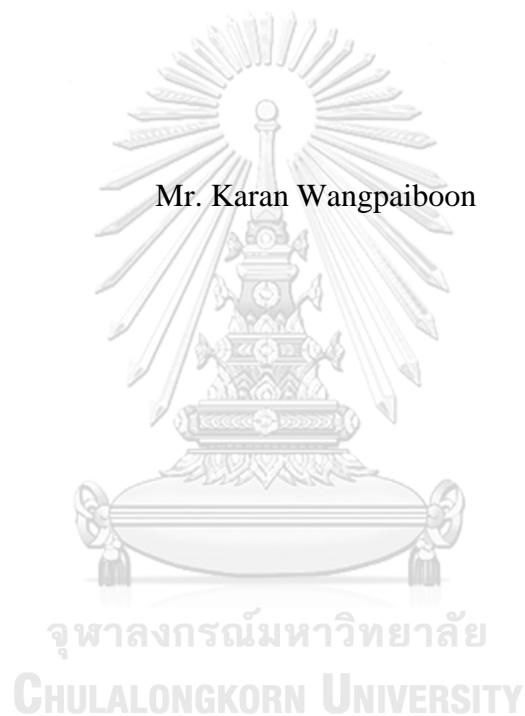
บทคัดย่อและแฟ้มข้อมูลฉบับเต็มของวิทยานิพนธ์ตั้งแต่ปีการศึกษา 2554 ที่ให้บริการในคลังปัญญาจุฬาฯ (CUIR)
เป็นแฟ้มข้อมูลของนิสิตเจ้าของวิทยานิพนธ์ ที่ส่งผ่านทางบัณฑิตวิทยาลัย

The abstract and full text of theses from the academic year 2011 in Chulalongkorn University Intellectual Repository (CUIR)
are the thesis authors' files submitted through the University Graduate School.

วิทยานิพนธ์นี้เป็นส่วนหนึ่งของการศึกษาตามหลักสูตรปริญญาวิทยาศาสตรดุษฎีบัณฑิต
สาขาวิชาชีวเคมีและชีววิทยาโมเลกุล ภาควิชาชีวเคมี
คณะวิทยาศาสตร์ จุฬาลงกรณ์มหาวิทยาลัย
ปีการศึกษา 2560
ลิขสิทธิ์ของจุฬาลงกรณ์มหาวิทยาลัย

CLONING AND CHARACTERISATION OF ALTERNANSUCRASE FROM
Leuconostoc citreum ABK-1 AND ROLE OF SURFACE AROMATIC ACIDS ON
PRODUCT SIZE

Mr. Karan Wangpaiboon



A Dissertation Submitted in Partial Fulfillment of the Requirements
for the Degree of Doctor of Philosophy Program in Biochemistry and Molecular
Biology
Department of Biochemistry
Faculty of Science
Chulalongkorn University
Academic Year 2017
Copyright of Chulalongkorn University

Thesis Title	CLONING AND CHARACTERISATION OF ALTERNANSUCRASE FROM <i>Leuconostoc citreum</i> ABK-1 AND ROLE OF SURFACE AROMATIC ACIDS ON PRODUCT SIZE
By	Mr. Karan Wangpaiboon
Field of Study	Biochemistry and Molecular Biology
Thesis Advisor	Assistant Professor Rath Pichyangkura, Ph.D.

Accepted by the Faculty of Science, Chulalongkorn University in Partial
Fulfillment of the Requirements for the Doctoral Degree

..... Dean of the Faculty of Science
(Professor Polkit Sangvanich, Ph.D.)

THESIS COMMITTEE

..... Chairman
(Associate Professor Teerapong Buaboocha, Ph.D.)

..... Thesis Advisor
(Assistant Professor Rath Pichyangkura, Ph.D.)

..... Examiner
(Assistant Professor Kuakarun Krusong, Ph.D.)

..... Examiner
(Assistant Professor Manchumas Prousoontorn, Ph.D.)

..... External Examiner
(Professor Emeritus Piamsook Pongsawasdi, Ph.D.)

กรินทร์ วังไพบูลย์ : การโคลนและลักษณะสมบัติของอัลเทอร์เนนชูเครสจาก *Leuconostoc citreum* ABK-1 และบทบาทของกรดอะมิโนชนิดแอมโรแมติกบริเวณผิวต่อขนาดของผลิตภัณฑ์ (CLONING AND CHARACTERISATION OF ALTERNANSUCRASE FROM *Leuconostoc citreum* ABK-1 AND ROLE OF SURFACE AROMATIC ACIDS ON PRODUCT SIZE) อ.ที่ปรึกษาวิทยานิพนธ์หลัก: ผศ. ดร. รัฐ พิชญางกูร, 153 หน้า.

อัลเทอร์เนนชูเครส (ALT, EC 2.4.1.140) เร่งปฏิกิริยาการโยกย้ายกลูโคสจากซูโครสเพื่อสร้างพอลิเมอร์ที่เชื่อมต่อกันด้วยพันธะ α -1,6 และ α -1,3 เรียกว่า “อัลเทอร์เนน” ยีนของอัลเทอร์เนนชูเครสจาก *Leuconostoc citreum* ABK-1 (WTalt) ถูกนำมาโคลนและแสดงออกใน *Escherichia coli* BL21 (DE3) ได้สำเร็จ และได้สร้างอัลเทอร์เนนที่ถูกตัดบางส่วนของ SH3-like โดเมนสองแบบ ได้แก่ Δ 3SHALT และ Δ 7SHALT ได้สำเร็จ WTALT, Δ 3SHALT and Δ 7SHALT แสดงออกภูมิที่เหมาะสมในการเร่งปฏิกิริยาที่ 40 องศาเซลเซียส ในขณะที่ pH ที่เหมาะสมของการเร่งปฏิกิริยาของ WTALT อยู่ที่ pH 5.0 และ ของ Δ 3SHALT and Δ 7SHALT อยู่ที่ pH 4.0 นอกจากนี้การเร่งปฏิกิริยาของทั้งสามสามารถถูกกระตุ้นได้ด้วย Mn^{2+} การศึกษาจลนพลศาสตร์ของเอนไซม์ของทั้งสามแสดงแอกทิวิตีทรานส์ไกลโคซิลเลชันเป็นหลักอย่างเด่นชัด แต่ Δ 3SHALT และ Δ 7SHALT สามารถแสดงแอกทิวิตีไฮโดรไลซิสได้เล็กน้อย การตัด SH3-like domain ส่งผลต่อความเสถียรของเอนไซม์และขนาดของผลิตภัณฑ์เมื่อเทียบกับ WTALT ลักษณะของผลิตภัณฑ์ที่ได้จากอัลเทอร์เนนชูเครสทั้งสามไม่ได้แตกต่างกันตรวจสอบโดย เทคนิค NMR การวิเคราะห์ methylation และ HPAEC-PAD อย่างไรก็ตาม Δ 3SHALT และ Δ 7SHALT ให้ผลิตภัณฑ์เป็นโอลิโกแซคคาไรด์ที่สูงกว่าเมื่อเปรียบเทียบกับ WTALT ที่สำคัญยิ่ง รูปแบบการเชื่อมต่อพันธะในสายพอลิเมอร์ประกอบด้วยการสลับกันระหว่าง α -1,6 และ α -1,3 อย่างไม่สม่ำเสมอ ยืนยันด้วย เทคนิค NMR การวิเคราะห์ methylation และการวิเคราะห์พอลิเมอร์ด้วยการย่อยด้วยกรดอย่างไม่สมบูรณ์ พอลิเมอร์สามารถเกิดการรวมตัวเป็นอนุภาคนาโนได้โดยอัตโนมัติเมื่ออยู่ในสารละลาย ที่ความเข้มข้นสูงกว่า 15% (w/v) พอลิเมอร์ไม่เกิดการรวมตัวเป็นอนุภาคนาโนแต่เกิดการรวมตัวเป็นสารละลายที่มีความหนืดสูง และสามารถเปลี่ยนเป็นฟิล์มที่โปร่งแสงได้เมื่อถูกทำให้แห้ง นอกจากนี้การกลายพันธุ์ที่ตำแหน่ง W675 มีผลกระทบต่อขนาดผลิตภัณฑ์โดยไม่สามารถตรวจพบพอลิเมอร์ W675A สูญเสียความสามารถในการจับโมเลกุลตัวรับอย่างมีนัยสำคัญ ทำให้ได้ผลิตภัณฑ์ที่มีลักษณะเปลี่ยนไปเมื่อเปรียบเทียบกับ WT (Δ 7SHALT)

ภาควิชา ชีวเคมี ลายมือชื่อนิสิต

สาขาวิชา ชีวเคมีและชีววิทยาโมเลกุล ลายมือชื่อ อ.ที่ปรึกษาหลัก

ปีการศึกษา 2560

5571910623 : MAJOR BIOCHEMISTRY AND MOLECULAR BIOLOGY

KEYWORDS: LEUCONOSTOC CITREUM, ALTERNANSUCRASE, INSOLUBLE POLYMER, SH3 DOMAIN, MUTAGENESIS AND ACCEPTOR BINDING SITE

KARAN WANGPAIBOON: CLONING AND CHARACTERISATION OF ALTERNANSUCRASE FROM *Leuconostoc citreum* ABK-1 AND ROLE OF SURFACE AROMATIC ACIDS ON PRODUCT SIZE. ADVISOR: ASST. PROF. RATH PICHYANGKURA, Ph.D., 153 pp.

The alternansucrase (ALT, EC 2.4.1.140) catalyses transferring of glucose from sucrose to produce a polymer with α -1,6 and α -1,3 linkages, so-called "alternan". The ALT-encoding gene from *Leuconostoc citreum* ABK-1 (WTalt) was successfully cloned and expressed in *Escherichia coli* BL21 (DE3). The two versions of truncated SH3-like domains, Δ 3SHALT and Δ 7SHALT, were successfully constructed. The WTALT, Δ 3SHALT and Δ 7SHALT possessed optimum temperature of 40 °C, while optimum pH of WTALT was at 5.0 but Δ 3SHALT's and Δ 7SHALT's were shifted to pH 4.0. Their activities could be enhanced by Mn^{2+} . Kinetic studies of all ALTs were mainly responsible for transglycosylation activity with less detectable hydrolytic activity in the Δ 3SHALT and Δ 7SHALT. Deletion of SH3-like domains affected enzyme stability and size of products compared with WTALT. The ALTs' product patterns were not significantly dissimilar judged by NMR, methylation analysis and HPAEC-PAD. However, Δ 3SHALT and Δ 7SHALT produced higher the amount of oligosaccharides compared to WTALT. Importantly, the polymer product harbours irregular pattern of alternating α -1,6 and α -1,3 glycosidic linkages as confirmed by NMR, methylation analysis, and partial hydrolysis. The polymer can undergo self-assembly, forming nanoparticles in solution. At concentrations above 15% (w/v), nanoparticles disassembled and formed a high viscous solution, while a transparent film was formed once polymer was dried. Additionally, the mutation at W675 position effected on sizes of products without detectable polymer. W675A significantly revealed the loss of acceptor binding ability, resulted in the production of different product patterns compared with the WT (Δ 7SHALT).

Department: Biochemistry Student's Signature

Field of Study: Biochemistry and Molecular Biology Advisor's Signature

Biology

Academic Year: 2017

ACKNOWLEDGEMENTS

I would like to gratefully thank my advisor, Asst. Prof. Rath Pichyangkura, Ph.D., for his ideas, kindness, and suggestions throughout this project.

My gratitude is also extended to Assoc. Prof. Teerapong Buaboocha, Ph.D., Asst. Prof. Kuakarun Krusong, Ph.D., Asst. Prof. Manchumas Prousunthorn, Ph.D., and Prof. Emeritus Piamsook Pongsawasdi, Ph.D. for serving as thesis committees. I am very thankful to Prof. Robert A. Field, Ph.D. at John Innes Centre, for his suggestion, support and kindness.

I would like to thank Asst. Prof. Panuwat Padungros, Ph.D. from Department of Chemistry, Faculty of Science, Chulalongkorn University for great NMR analysis, Asst. Prof. Surasak Chunsrivirod, Ph.D. and Mr. Thassanai Sitthiyotha for molecular docking technique, Prof. Suwabun Chirachanchai, Ph.D., Petroleum and Petrochemical College, Chulalongkorn University, for the Zetasizer Nano ZS analysis, Santhana Nakapong, Ph.D. from Department of Chemistry, Faculty of Science, Ramkhamhaeng University, who isolated L. citreum ABK-1, and Martin Rejzek, Ph.D. at John Innes Centre, for supporting linkage analysis technique.

My sincerely thanks are extended to all members of 709 lab including senior members, Starch and Cyclodextrin Research Unit and friends, and all supporting staffs of the Department of Biochemistry, Faculty of Science, Chulalongkorn University as well as R.A.F lab members at John Innes Centre, for their assistance and friendship. I would like to give special thanks to Pawinee Panpetch, Ph.D., my beloved girlfriend, for her supporting and thesis proofreading. Finally, I wish to express my deepest gratitude to my family and my aunt's family for all their continuous support, helpful and understanding.

The thesis is supported by research grant from Chulalongkorn University Graduate School scholarship, Commemorating the 72nd Anniversary of His Majesty King Bhumibol Aduladej, Doctoral Degree Chulalongkorn University 100th Year Birthday Anniversary, the 90th Anniversary of Ratchadaphiseksomphot

CONTENTS

	Page
THAI ABSTRACT	iv
ENGLISH ABSTRACT.....	v
ACKNOWLEDGEMENTS	vi
CONTENTS.....	vii
Table contents	ix
Figure contents.....	x
CHAPTER I INTRODUCTION.....	1
1.1 Lactic acid bacteria.....	1
1.2 Glucansucrase	2
1.3 Structure of glucansucrase	6
1.4 Mechanism of glucansucrase	10
1.5 Alternansucrase.....	10
1.6 Alternan properties	13
1.7 SH3 domain	13
1.8 Role of aromatic residue on carbohydrate active enzyme	14
CHAPTER II MATERIALS AND METHODS.....	17
2.1 Equipments	17
2.2 Chemicals	18
2.3 Enzymes and Restriction enzymes	20
2.4 Bacterial strains and plasmid	21
2.5 General techniques for molecular cloning and gene expression.....	22
2.6 General techniques for protein characterisation	30
2.7 Product characterisation.....	34
CHAPTER III RESULTS	40
3.1 Cloning of <i>WTalt</i> , $\Delta 3SHalt$ and $\Delta 7SHalt$ genes	40
3.3 Characterisation of WTALT, $\Delta 3SHALT$ and $\Delta 7SHALT$	62
3.4 Product characterisation.....	66
3.4.1 Oligosaccharide characterisation.....	66

	Page
3.4.2 Polymer characterisation	74
3.4.2.1 NMR analysis	74
3.4.2.2 Linkage analysis by methylation experiment	82
3.4.2.3 Polymer analysis by partial hydrolysis	82
3.4.2.4 Solubility of polymer	86
3.5 Mutagenesis of <i>alt</i> gene	96
3.6 Characterisation of W675A	107
CHAPTER IV DISCUSSION.....	121
4.1 Cloning of WT <i>alt</i> , Δ 3SH <i>alt</i> and Δ 7SH <i>alt</i> genes	121
4.2 Expression of WT <i>alt</i> , Δ 3SH <i>alt</i> and Δ 7SH <i>alt</i> genes	122
4.3 Characterisation of WTALT, Δ 3SHALT and Δ 7SHALT	123
4.4 Characterisation of ALT products	127
4.4.1 Oligosaccharide characterisation.....	127
4.4.2 Polymer characterisation.....	129
4.4.3 Solubility properties of the polymer.....	130
4.5 Mutagenesis of ALT by alanine scanning	132
4.6 Characterisation of W675A	133
CHAPTER V CONCLUSION.....	136
REFERENCES	138
VITA.....	153

Table contents

Table 1. The lists of primer for alt amplification and sequencing	25
Table 2. Primer lists for alanine scanning mutation.....	28
Table 3. Primer lists for saturation mutagenesis at W675 position.....	29
Table 4 Purification table of WTALT.....	59
Table 5 Purification table of Δ 3SHALT	59
Table 6 Purification table of Δ 7SHALT	59
Table 7 The kinetic parameters of WTALT, Δ 3SHALT and Δ 7SHALT	65
Table 8 Mole percentage of methylated glucoses in hydrolysates of glucans	83

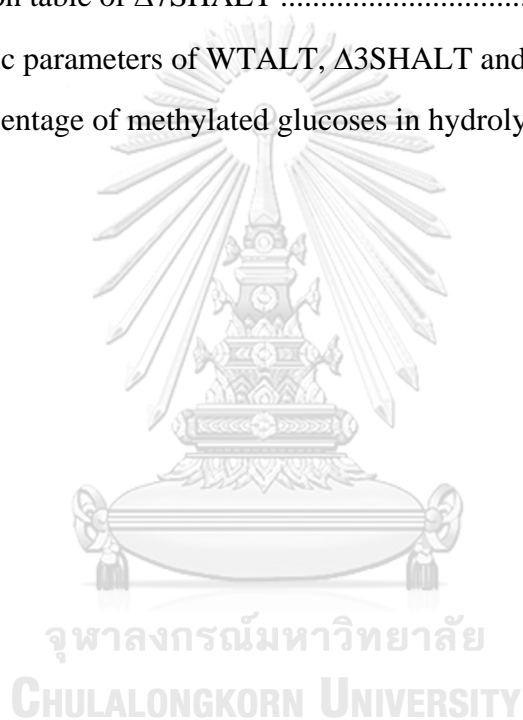


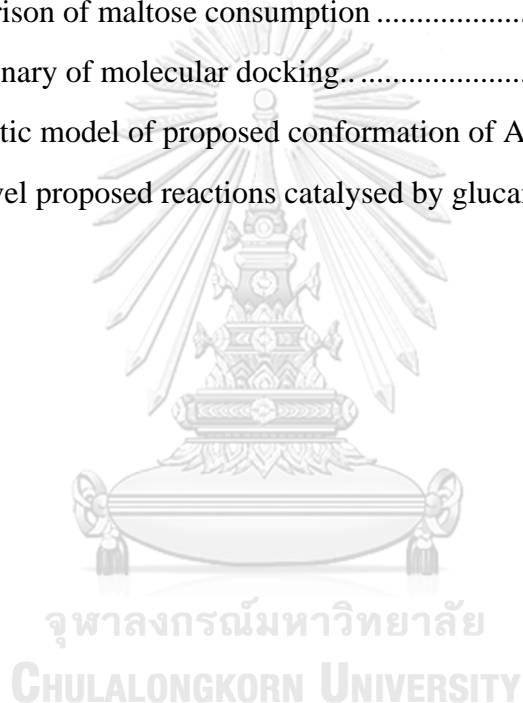
Figure contents

Figure 1 Four different reactions catalysed by glucansucrases.....	4
Figure 2 Various types of α -glucan produced	5
Figure 3 Comparison of domain organisation.....	7
Figure 4 Comparison of 2 crystal structures of glucansucrase from <i>L. reuteri</i> 180.	8
Figure 5 Crystal structure of E715Q truncated dextransucrase from <i>L. citreum</i> NRRL B-1299.....	9
Figure 6 Insertion mechanism of dextran biosynthesis.....	12
Figure 7 <i>Leuconostoc citreum</i> ABK-1 grown on sucrose-containing LB agar plat....	16
Figure 8 Site-directed mutagenesis by PCR driven overlapping extension.....	27
Figure 9 Cloning result analysed on 0.8 % (w/v) agarose gel	41
Figure 10 Amino acid sequences alignment of bacterial ALT from various species .	42
Figure 11 Amino acid sequences alignment of WTALT and <i>Lm</i> ALT	43
Figure 12 The protein diagram of WTALT, Δ 3SHALT and Δ 7SHALT.....	48
Figure 13 Amino acid sequences alignment of 7 repeat SH3-like domains	49
Figure 14 The 7 SH3-like domains of <i>L. citreum</i> ABK-1 alternansucrase.....	49
Figure 15 SDS-PAGE analysis of crude extract of WTALT	51
Figure 16 SDS-PAGE analysis of optimisation of WTALT production.	52
Figure 17 SDS-PAGE analysis of optimisation of WTALT production in <i>E. coli</i> BL21 (DE3) at 16 °C	53
Figure 18 The effect of IPTG concentration on WTALT activity	54
Figure 19 Determination of enzyme activity in different fractions.	55
Figure 20 SDS-PAGE analysis of production of WTALT, Δ 3SHALT and Δ 7SHALT in soluble and insoluble fractions	56
Figure 21 SDS-PAGE analysis of the purified WTALT, Δ 3SHALT and Δ 7SHALT after purification by Toyopearl® DEAE and Phenyl-650M columns.....	58
Figure 22 Affinity analysis of WTALT, Δ 3SHALT and Δ 7SHALT proteins on nondenaturing-PAGE.....	60

Figure 23 Relative mobility of WTALT, Δ 3SHALT and Δ 7SHALT proteins on native gel.....	61
Figure 24 Optimum pH (A) and optimum temperature (B).....	63
Figure 25 Effect of metal ions and detergent on enzyme activities.....	63
Figure 26 Determination of enzyme stability of WTALT, Δ 3SHALT and Δ 7SHALT in various conditions.....	65
Figure 27 Comparison oligosaccharide pattern of WTALT, Δ 3SHALT and Δ 7SHALT by HPAEC-PAD.....	67
Figure 28 Separation of oligosaccharides by GPC	67
Figure 29 Complete hydrolysis of WTALT oligosaccharides	68
Figure 30 Oligosaccharides (DP2-8) pattern of WTALT	69
Figure 31 Mass analysis by MALDI-TOF MS.	69
Figure 32 Hydrolysis of WTALT oligosaccharide by WTALT	70
Figure 33 Product mass of WTALT oligosaccharide after incubating with WTALT.....	70
Figure 34 Effect of enzyme on product formation.....	72
Figure 35 Effect of temperature on product formation.	73
Figure 36 ^1H NMR spectrum of polymeric products.....	75
Figure 37 ^{13}C NMR spectra.....	76
Figure 38 COSY spectrum of WTALT polymer	77
Figure 39 ^1H NMR spectrum of WTALT polymer (400 MHz, DMSO- d_6 +TFA).....	79
Figure 40 COSY spectrum of WTALT polymer (400 MHz, DMSO- d_6 +TFA).....	79
Figure 41 Multiplicity-edited HSQC spectrum of WTALT polymer	80
Figure 42 HMBC spectrum of WTALT polymer	81
Figure 43 Separation of partially hydrolysed product by size exclusion.....	83
Figure 44 TLC analysis of partially hydrolysed WTALT polymer separated.....	84
Figure 45 Analysis of partially hydrolysed WTALT polymer.. ..	85
Figure 46 Comparison of solubility of three glucan polymers in water.. ..	87
Figure 47 Determination of sizes of WTALT , Δ 3SHALT and Δ 7SHALT nanoparticle.....	88

Figure 48 Comparison of solubility of WTALT (A), Δ 3SHALT (B) and Δ 7SHALT (C) polymers.	89
Figure 49 Comparison of viscosity of WTALT (●), Δ 3SHALT (■) and Δ 7SHALT (▲) polymers	90
Figure 50 Solubility, nanoparticle and film formation properties of WTALT polymer	91
Figure 51 TEM images of WTALT, Δ 3SHALT and Δ 7SHALT polymers.....	92
Figure 52 Purification of WTALT polymer by GPC.....	93
Figure 53 MALDI-TOF MS analysis of purified WTALT polymer.	94
Figure 54 Analysis of the purified WTALT polymer by high resolution ESI-TOF MS.....	95
Figure 55 Homology model of Δ 7SHALT.	97
Figure 56 Ramachandran plot of Δ 7SHALT homology model.	98
Figure 57 SDS-PAGE analysis of purified ALTs produced by alanine scanning mutants.....	99
Figure 58 TLC analysis of glucan products produced by alanine scanning mutants.....	101
Figure 59 Comparison of oligosaccharide patterns of alanine scanning mutants.....	102
Figure 60 Determination of masses of oligosaccharide products of W675A by MALDI-TOF MS.....	103
Figure 61 Comparison of three conserved sequence motifs of various glucansucrases.....	103
Figure 62 SDS-PAGE analysis of purified ALTs produced by alanine scanning mutants.....	104
Figure 63 TLC analysis of glucan products produced by alanine scanning mutants.....	105
Figure 64 Comparison of oligosaccharide patterns of saturation mutagenesis.....	106
Figure 65 Optimum temperature (A) and optimum pH (B) of W675A mutant.....	107
Figure 66 Kinetic study of W675A).	108
Figure 67 Comparison of oligosaccharide patterns of Δ 7SHALT and W675A.	109
Figure 68 Separation of W675A products by GPC column.....	110
Figure 69 Analysis of masses of W675A products by MALDI-TOF MS	110

Figure 70 TLC analysis of W675A products	111
Figure 71 HPAEC-PAD analysis of W675A products	112
Figure 72 Analysis of acceptor reaction between WT and W675A on TLC.....	114
Figure 73 Comparison of products from maltose acceptor reaction.....	115
Figure 74 Comparison of oligosaccharide patterns produced by maltose acceptor reactions	116
Figure 75 Effect of maltose concentration on WT products.....	117
Figure 76 Effect of concentration of maltose acceptor on W675A products.....	118
Figure 77 Comparison of maltose consumption	119
Figure 78 Preliminary of molecular docking.....	120
Figure 79 Schematic model of proposed conformation of ALT.....	127
Figure 80 The novel proposed reactions catalysed by glucansucrases.	128



CHAPTER I

INTRODUCTION

Carbohydrates are one of the most important biomolecules in the world. They play essentially role in participating in cell communication, cell structure and energy providing. Carbohydrates are found in various sources; plants, animals and microorganisms^{1,2}. Bacterial-derived exopolysaccharides or EPSs are important carbohydrates utilised in biotechnological field. Some types of EPSs such as xanthan gum and gellan gum were improved in terms of their physical properties for being used as an alternative source of carbohydrates from plants and algae (e.g. guar gum, pectin, carrageenan and alginate)³⁻⁵. Furthermore, some EPSs provided the high quality polysaccharide in terms of purity such as bacterial cellulose⁶. In addition to applications in food industry (e.g. sweeteners, prebiotics and food extenders), the EPSs can be applied in medical field as blood plasma extender and adjuvant because of their biocompatible property. Moreover, they are also used as matrix supports of chromatography^{7,8}.

1.1 Lactic acid bacteria

Lactic acid bacteria (LAB) are well-known bacteria that efficiently produce large amount of EPSs. Some of them were classified as GRAS (Generally Recognised as Safe) that is considered safe by experts to be added in foods such as *Leuconostoc* spp.⁹ and *Lactobacillus* spp.¹⁰ and some strains of *Streptococcus* spp.¹¹. EPSs were used to colonise or embed and reserved as extracellular energy form. Additionally, the tolerance of microorganism embedded in biofilm to antibiotics is increased by 1,500 times¹². Furthermore, EPSs can also protect bacterial cells from drying, phage

attacking, protozoa predating, and osmotic stressing¹³. Another benefit is that the EPSs can serve closely communication among cells due to the cells aggregation¹⁴. The EPSs are mainly classified into 2 classes depends on the monosaccharide building blocks: heteropolysaccharides and homopolysaccharides. The heteropolysaccharides comprised several species of monosaccharide in the chain and multiple steps and several types of enzymes are needed for synthesis¹⁵. On the other hand, the homopolysaccharides produced by LAB were synthesised from only sucrose substrate via a single type of enzyme. The homopolymers produced by sucrose-metabolising enzyme consisted of either fructose (as fructopolysaccharides or fructans) or glucose (as glucopolysaccharides or glucans)¹⁶.

1.2 Glucansucrase

Glucansucrases, one of the sucrose-metabolising enzymes, produced glucans, used only sucrose as substrate not the nucleotide sugar donors, which was contrast to the previous report of other glycosyltransferase, Leloir-type glycosyltransferase which used nucleotide-activated sugar as substrate. Several glucansucrases from different sources have been reported¹⁶⁻¹⁹. They catalyse the transferring of glucose from sucrose to produce oligosaccharides and polymers with different linkages. To investigate the hydrolysis rate of sucrose, its ΔG^0 value was 24.5 ± 1.0 kJ/mol. This energy was approximately twofold greater than those of other disaccharides such as lactulose, melibiose, palatinose, trehalose and turanose and 3-o- β -D-galactopyranosyl-D-arabinose²⁰. However, this energy level is enough to drive the formation of new glycosidic bond similar to that of nucleotide sugar²¹. In addition to glycosyltransferase activity, the glucansucrases also catalyse other reactions such as hydrolysis, acceptor reaction and isotropic exchange¹⁷ as shown in Fig. 1.

Glucansucrases can be categorised into either the CAZy glycoside hydrolase family 13 (GH13) or 70 (GH70) based on their conserved protein sequences^{7,22,23}. Nevertheless, the amylosucrase belongs to only GH13 family. The amylosucrase generates α -1,4-linked glucan. The polymer exhibited as amylose-like glucan. In contrast, the other glucansucrases belonging to GH70 produce glucans with different linkages and branching patterns. To date, four main types of glucansucrases in GH70 have been reported: dextransucrase, mutansucrase, alternansucrase and reuteransucrase²⁴. The species of glucansucrase are distinguished by the type of major linkage on main chain product²³. Dextran polymer is an example of glucan products produced by glucansucrases from 96 bacterial strains of *Leuconostoc citreum* and *Leuconostoc mессenteroides* which has been characterised since 1954. Moreover, different bacterial strains apparently produced different characteristics and physical properties of dextrans²⁵. On the other hand, other glucansucrases or reuteransucrases from *Lactobacillus reuteri* 121²⁶ and *L. reuteri* ATCC 55730²⁷ obviously showed different hydrolytic rates.

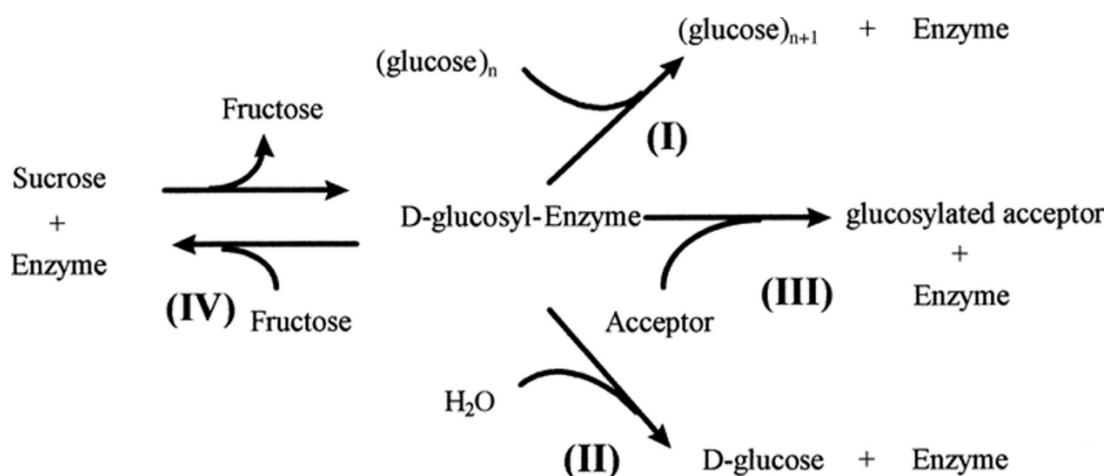


Figure 1 Four different reactions catalysed by glucosyl-enzymes. (I) glucan synthesis by successive transfer of glucosyl units; (II) sucrose hydrolysis by transferring of the glucosyl unit to water acceptor; (III) oligosaccharide synthesis by transferring of the glucosyl unit to an acceptor molecule; and (IV) isotopic exchange by reverse reaction of glucosyl-enzyme complex formation¹⁷.

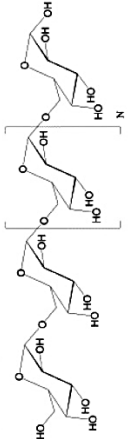
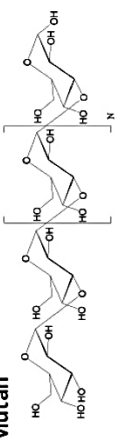
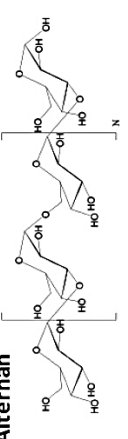
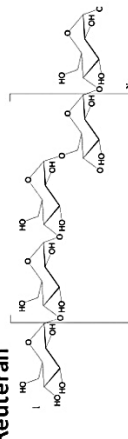
α -Glucan	Enzyme	Linkage composition of the product (%) ($\alpha 1 \rightarrow 2$) ($\alpha 1 \rightarrow 3$) ($\alpha 1 \rightarrow 4$) ($\alpha 1 \rightarrow 6$)	References		
Dextran 	<i>Leuconostoc mesenteroides</i> NRRL B-512F DSRs	5	95	(Monchoiset al., 1997)	
	<i>Leuconostoc citreum</i> B-1299 DSRE ^a	5	3	81	(Fabre et al., 2005)
	<i>Leuconostoc citreum</i> B-1299 BSR-A ^b	37		63	(Passerini et al., 2017)
	<i>Leuconostoc citreum</i> BSR-B ^b	50		50	(Vuillemin et al., 2016)
	<i>Weissella cibaria</i> DSRWC			100	(Kang et al., 2009)
Mutan 	<i>Lactobacillus reuteri</i> 180 Gtf180	31	69	(van Leeuwen et al., 2008)	
	<i>Streptococcus mutans</i> GS5 GtfD	30	70		(Hanada and Kuramitsu, 1989)
	<i>Streptococcus mutans</i> GS5 GtfB	88		12	(Shiroza et al., 1987)
	<i>Lactobacillus reuteri</i> ML1	65		35	(Krajc et al., 2004)
	<i>Leuconostoc mesenteroides</i> NRRL B-1118 DSRI	50		50	(Cote and Skory, 2012)
Alternan 	<i>Leuconostoc mesenteroides</i> NRRL B-1355 ASR	43	57	(Côté and Robyt, 1982b)	
	Reuteran 	<i>Lactobacillus reuteri</i> 121 GtfA	58	42	(van Leeuwen et al., 2008c)
<i>Lactobacillus reuteri</i> ATCC 55730 GtfO		79	21		(Krajc et al., 2005)

Figure 2 Various types of α -glucan produced by different types of lactic acid bacteria²⁴

1.3 Structure of glucansucrase

Based on the 3D structures of GH70 glucansucrases family, this enzyme essentially comprise 5 domains (Fig. 3). The catalytic core domain consists of A, B and C domains also found in GH13⁷. The catalytic triad located within TIM barrel structure of domain A. Moreover, Ca²⁺ ion was present in C domain of many glucansucrases as a cofactor. Additionally, domains IV and V have been reported only in GH70 and showed high flexibility. The IV domain behaves like “hinge” that support the movement of V domain towards the catalytic site²⁸. This was supported by the previous study of two different crystal structures of glucansucrase from *L. reuteri* 180 which were shown as stretch and boomerang-like structures as well as confirmation of the dynamic movement of enzyme in solution by Small-angle X-ray scattering (SAXS) technique²⁹ (Fig. 4). The DSR-MΔ2 crystal structure of domain V showed that this domain folded closely to catalytic domain A at 5 Å of distance³⁰ (Fig. 5). Furthermore, domain V also harboured multi-copies of glucan binding domain (GBD or YG repeat) with β-solenoid folding that facilitated the glucan synthesis in active site¹⁶. The stepwise deletion of GBD resulted in glucan binding ability and glucan production^{31,32}. Moreover, the point mutation of aromatic and basic amino acid residues at conserved sequence in GBD affected glucan binding ability of *S. downei* Gtfl³³. At present, only crystal structures derived from the truncated glucansucrases are available in database. Hence, complete information of structure especially domain V and enzyme mechanism are still debated.

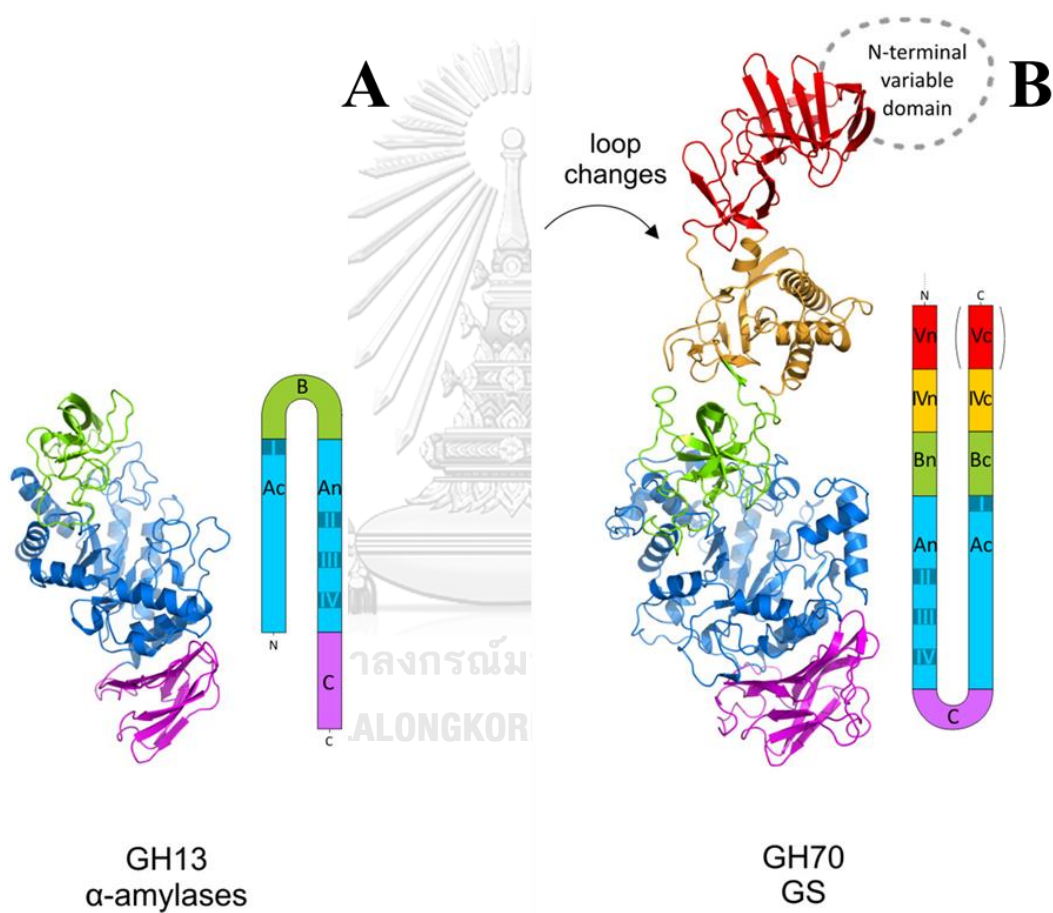


Figure 3 Comparison of domain organisation of (A) α -amylase from GH13 family and (B) glucansucrase from GH70 family (adjusted from Gangoiti et al, 2018).

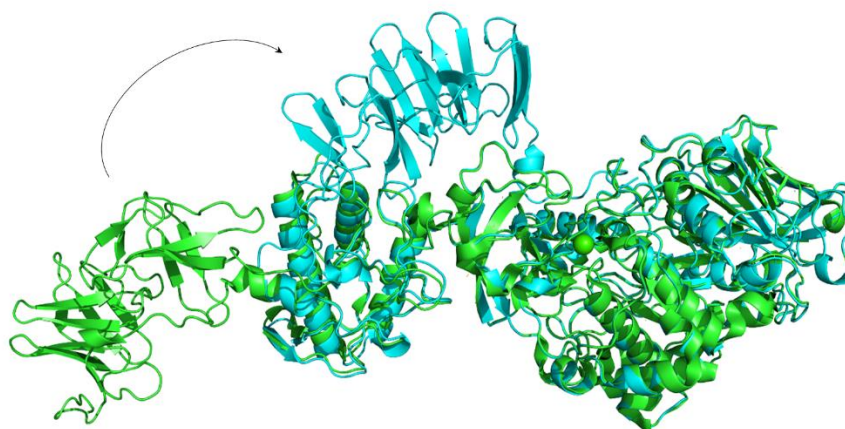


Figure 4 Comparison of 2 crystal structures of glucansucrase from *L. reuteri* 180. (GTF180- Δ N). Green colour represent GTF180- Δ N in triclinic apo-form (PDB code: 3KLK), while GTF180- Δ N in orthorhombic apo-form (PDB code: 4AYG) was shown in cyan.

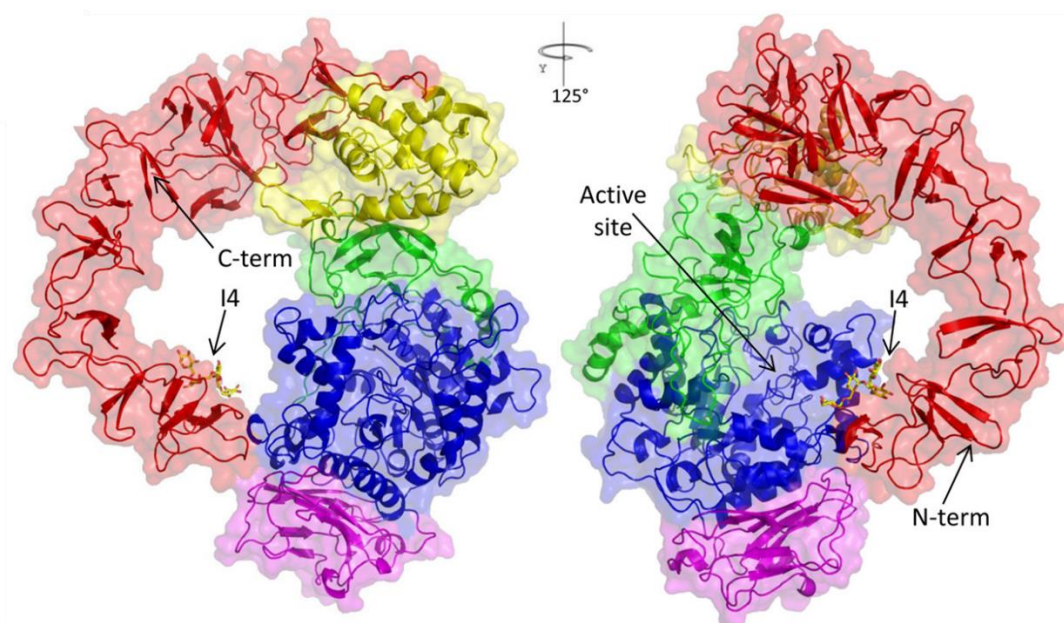


Figure 5 Crystal structure of E715Q truncated dextranucrase from *L. citreum* NRRL B-1299 (DSRM- Δ 2 E715Q, PDB code: 5NGY) (Claverie et al, 2017). Magenta, blue, green, yellow and red colours represent C, A, B, IV and V domains, respectively. I4 indicated tetraisomaltose molecule.

1.4 Mechanism of glucansucrase

Although the mechanism of glucan synthesis is still unclear especially the linkage type formation, three catalytic residues of GH70 are identified based on the crystal structures of were studied^{28,34}. However, the mechanism of GH70 enzymes was proposed to similar to that of amylosucrase from *Neisseria polysaccharea* belonging to GH13^{28,35}. Moreover, glucosyl- and dextransyl-intermediates were successfully detected in dextransucrases³⁶⁻³⁸. Robyt et al. (2008)³⁹, proposed the mechanism dextran synthesis using two nucleophiles in a single active site of *L. messenteroides* B-512F dextransucrase, so-called “insertion mechanism”. Three catalytic residues, Asp551, Glu589 and Asp662, play roles in acid/base catalysis. The reaction is initiated by the attack of sucrose donor by Asp551 nucleophile generating the carboxyl acetal ester with glucose moiety of sucrose, while the fructose moiety is then released by proton transferring from Glu589. Then, the second nucleophile (Asp662) is protonated by Glu589 and attacks to another molecule of sucrose. After that, the fructose moiety is released by receiving proton from Glu589 whereas the glucose moiety is covalently linked with Asp662. The proton of C6-OH is covalently linked with second sucrose, and pulled off by Glu589 releasing a hydroxyl ion that attacks to C1 of the first glucosyl intermediate. The elongation mechanism of dextran polymer was shown in Fig. 6. Moreover, the longer chains of dextran were obtained when decreased amount of enzyme, suggesting the enzyme possessivity³⁹.

1.5 Alternansucrase

Alternansucrase (ALT, EC 2.4.1.140), a member of glucansucrases, has been reported to produce glucans with alternating α -1,3 and α -1,6 linkages namely “alternan”. The first ALT was reported in *Leuconostoc messenteroides* NRRL-B1335.

In 2000, alternansucrase gene of *L. messenteroides* NRRL-B1335 (*Lmalt*) was successfully cloned and expressed in *E. coli*⁴⁰. However, the recombinant *LmALT* was unstable and rapidly degraded. The C-terminal deletion of 2 repeat CW-like domains (YG repeat) and 7 tandem repeat SH3-like domains (APY domain) of *LmALT* increased solubility and thermal stability of enzyme without different linkage pattern of product judged by NMR⁴¹. In addition, alternansucrase has also been reported to efficiently catalyse several acceptor reactions greater than dextransucrase⁴². The products of acceptor reactions catalyzed by ALT obtained from various types of acceptor molecules such as maltose, nigerose, isomaltose, methylglucose⁴³, cellobiose⁴⁴, α -octylglucopyranoside⁴⁵ exhibited prebiotic property and selectively promoted growth of probiotic bacteria⁴⁶. Moreover, the partially purified *Leuconostoc citreum* SK24.002 alternansucrase was used in stevioside biotransformation⁴¹.

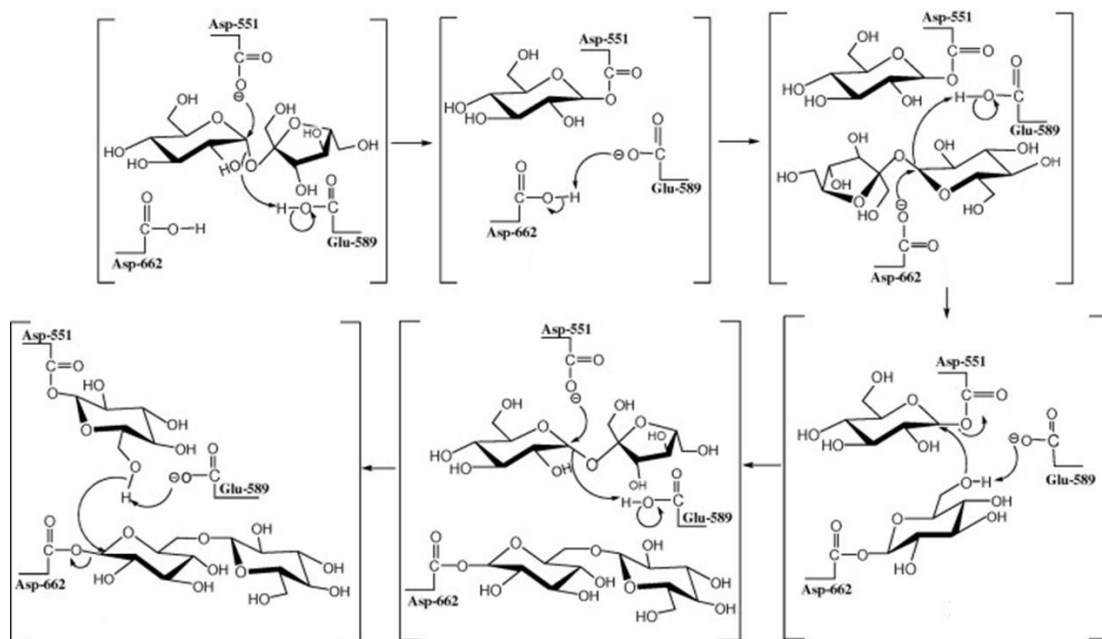


Figure 6 Insertion mechanism of dextran biosynthesis from *L. messenteroides* B-512F dextranase proposed by Robyt et al. (2008)³⁹.

1.6 Alternan properties

On the other hand, the alternan products exhibited endo-dextranase and endo-mutanase resistance, and insoluble properties⁴⁷. Characterisation of alternan by ¹³C NMR and methylation analysis confirmed the presence of α -1,3 and α -1,6 linkages in the polymer backbone⁴⁸. Moreover, there were reports on glucans representing α -1,3 and α -1,6-linked backbone such as glucan from *Lactobacillus reuteri* strain 180⁴⁹ and *Lactobacillus brevis* E25⁵⁰. Alternan polymer was also reported to be opalescent insoluble polymer. The viscosity of polymer was increased when the concentration was increased. At the concentration of more than 25% (w/v) in H₂O, the polymer showed non-Newtonian characteristic⁵¹. In addition, alternan was stable at pH 4.0 – 7.0 at up to 70 °C for at least one week. Moreover, it has no emulsifier property unlike gum Arabic. However, viscosity of alternan could be improved by ultra-sonication and enzymatic degradation and the modified alternan exhibited similar property to that of the commercial gum Arabic⁵².

1.7 SH3 domain

SH3 domains containing approximately 60 amino acids are widely present in eukaryotic proteins and involved in cell signaling and cytoskeletal protein system such as Ras proteins and Src kinase which control some cellular pathways^{53,54}. Many researches of SH3 domains demonstrated that these domains caused protein aggregation and amyloid fibril formation. Thus, SH3 domains were considered to be a model for studying of neurodegenerative diseases such as Alzheimer, Parkinson and Huntington diseases⁵⁵ resulted from amyloid fibril formation and protein aggregation. Besides, the SH3 domains were also identified in bacterial proteins and showed different functions in different proteins. For example, the SH3 domains in

peptidoglycan cysteine peptidase of *Anabaena variabilis* participated in protein interaction with its ligand⁵⁶. The N-terminal tandem repeat SH3 domains in peptidoglycan cysteine peptidase of *Bacillus cereus* enhanced the recognition of substrate of murein peptides⁵⁷. The C-terminus of glycylglycine endopeptidase of *Staphylococcus simulans* (ALE-1) contained SH3-like folding domain which strongly bound to pentaglycine of bacterial cell wall⁵⁸. The C-terminal 3 tandem repeat SH3 domains in Internalin of *Listeria monocytogenes* (InlB) bound to lipoteichoic acid and glycosaminoglycan heparin on the bacterial cell surface during pathogen invasion⁵⁹⁻⁶¹. The SH3 domains in *Diphtheria* toxin repressor (DtxR) bound to Co^{2+} and then proper conformation of DtxR was induced for DNA binding⁶². Bacterial ferrous iron-transport activating factor (FeoA) folded like as SH3 domains structure in dimeric form using two zinc ion crosslink⁶³. Furthermore, C-terminal sequences of some glucansucrases^{41,64,65} and fructansucrases⁶⁶ exhibited SH3-like folding, making them have larger C-terminal domains than general enzymes. However, the function of these domains is still unclear.

1.8 Role of aromatic residue on carbohydrate active enzyme

Several researches on carbohydrate active enzymes demonstrated that aromatic residues usually play important role in their mechanism or substrate/product binding. For example, F183 and F259 in CGTase were crucial in cyclisation and disproportionation activities⁶⁷. Tryptophan located in N-terminal domain of chitinase of *Serratia* sp. TU09, was shown to bind to colloidal chitin substrate⁶⁸. The crystal structure of glucansucrase-maltose from *Streptococcus mutans* showed that W517 served hydrophobic platform for maltose binding²⁸. Moreover, aromatic residues

located in glucan binding domain (GBD) of some other glucansucrases were reported to play essential role in glucan binding^{30,33}.

Previously, our lab could screen lactic acid bacteria isolated from kow-tom-mud, a Thai dessert. It was identified as *Leuconostoc citreum* ABK-1 by 16SrRNA sequencing. This strain can obviously produce high level of polysaccharide on LB agar containing sucrose. The mixtures of glucan polymers were harbored α -1,6 as major linkage using ¹H NMR technique. Furthermore, the complete genome sequence of *Leuconostoc citreum* KM20 has been reported. Putative glucansucrase genes consisting of 3 dextransucrases and alternansucrase were successfully identified in the genome sequence

Therefore, this work aims to (1) clone, express and characterise alternansucrase from *L. citreum* ABK-1 as well as their products, (2) study the possible functions of 7 tandem repeat SH3-like domains at C-terminus of alternansucrase from *L. citreum* ABK-1, and (3) observe the role of surface aromatic residues on product size.



Figure 7 *Leuconostoc citreum* ABK-1 grown on sucrose-containing LB agar plate. *L. citreum* ABK-1 was streak on LB plate containing 20% (w/v) sucrose and incubated at 30 °C for overnight.

CHAPTER II

MATERIALS AND METHODS

2.1 Equipments

AND Vibro Viscometer: SV-10, Japan

Autoclave: Model 29MLS-2400. Sanyo, Japan

Autoflex maX MALDI-TOF and TOF/TOF: Bruker, Germany

Autopipette: Pipetteman Gilson, France

Centrifuge, refrigerated centrifuge: Model J2-21, Beckman Instrument, Inc., U.S.A.
and Sorvall Legend XTR, ThermoFisher Scientific, Inc., Germany

Centrifuge, microcentrifuge: Model 5430, Eppendorf Co., Ltd., Germany

Dark Reader blue transilluminators, Dark Reader[®], Clare Chemical Research, Inc.,
U.S.A.

Electrophoresis unit:

- Mini protein, Bio-Rad, U.S.A.
- Mini Horizontal Gel Electrophoresis System, Major Science, U.S.A.
- Submarine agarose gel electrophoresis unit, Bio-Rad, U.S.A.

Eppendorf Biospectrometer[®] basic: Eppendorf, Germany

Fraction collector: Frac-920, GE Healthcare Bio-Sciences AB, Sweden

Gene Pulser[®]/ *E. coli* Pulser[™] cuvette: Bio-Rad, U.S.A.

Gel Document: SYNGEND, England

Gel permeation chromatography (GPC): Gilson, France

High-performance anion-exchange chromatography (HPAEC): ThermoFisher
Scientific, Inc., U.S.A.

Incubator, shaker: Innova™ 4000 and 4080, New Brunswick Scientific, U.S.A.

Incubator, waterbath: Model M20S, Lauda, Germany and Biochiller 2000, FOTODYNE Inc., U.S.A. and ISOTEMP 210, Fisher Scientific, U.S.A.

Laminar flow: HT123, ISSCO, U.S.A. and Streamline® Vertical Laminar Flow Cabinet Model SCV-4A1, Gibthai Co., Ltd., Singapore

Magnetic stirrer: Model Fisherbrand, Fisher Scientific, U.S.A.

Magnetic spinbar: Teflon® PTFE, Scienceware®, Capitol Scientific, Inc., U.S.A.

Microplate reader: Synergy™ H1, Biotek Instruments, Inc., U.S.A.

MicroPulser™ electroporator: Bio-Rad, U.S.A.

NMR 400 MHz: Bruker, Germany

pH meter: Model MP220, Mettler-Toledo International, Inc., U.S.A.

Spectrophotometer: Model G10S UV-Vis, ThermoFisher Scientific, Inc., U.S.A.

Thermal Cycler Block: Type 5020, ThermoFisher Scientific, Inc., Finland

Transmission electron microscopy (TEM) model H-7650: Hitachi, Japan

Vortex: Model G560E, Scientific Industries, Inc., U.S.A.

Water bath: Charles Hearson Co. Ltd., England

Zetasizer Nano ZS: Malvern, England

2.2 Chemicals

Absolute ethanol (Merck)

Acrylamide (AppliChem PanReac)

Agarose (Invitrogen)

Ammonium hydroxide (Sigma-Aldrich)

Ammonium persulfate (AppliChem)

Ampicillin (Affymetrix)

Beta-mercaptoethanol (Bio Basic)

Citric acid (Univar)

Cobalt (II) chloride (Merck)

Copper (II) sulphate (Sigma-Aldrich)

Dipotassium phosphate (Univar)

Ethylenediaminetetraacetic acid (EDTA) (AppliChem)

Glacial acetic acid (Merck)

Glucose (Univar)

Glycerol (Univar)

Glycine (Norgen Biotek)

Calcium (II) chloride (Univar)

Chloroform (Carlo Erba)

Dinitrosalicylic acid (Sigma-Aldrich)

Hydrochloric acid (Labscan)

Iron (III) chloride (Univar)

Isopropyl β -D-1-thiogalactopyranoside (IPTG) (ThermoFisher Scientific)

Magnesium (II) chloride (Univar)

Magnesium chloride hexahydrate (USB)

Manganese (II) chloride (Univar)

Methanol (Honeywell)

Potassium chloride (Univar)

Potassium dihydrogen phosphate (Univar)

Phenol (Merck)

Sodium chloride (Univar)

Sodium citrate (Univar)

Sodium azide (Univar)

Sodium dodecyl sulfate (Univar)

Sodium hydroxide (Lab-Scan)

Sodium potassium tartrate (Univar)

Tetramethylethylenediamine (TEMED) (ThermoFisher Scientific)

TriColor Broad Protein Ladder (Biotechrabbit)

Trifluoroacetic acid (ThermoFisher Scientific)

Tris (Vivantis)

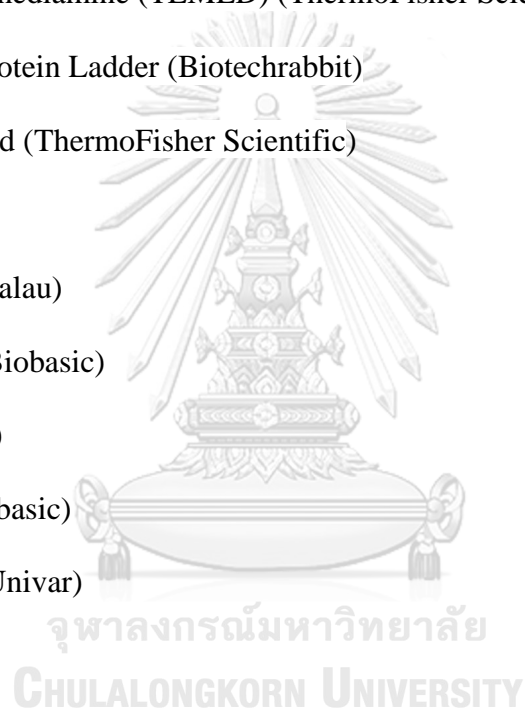
Triton X-100 (Schalau)

Tryptone type-I (Biobasic)

Tween-20 (Sigma)

Yeast extract (Biobasic)

Zinc (II) sulfate (Univar)



2.3 Enzymes and Restriction enzymes

T4 DNA Ligase (NEB)

*Nco*I (NEB)

*Xho*I (NEB)

PrimeSTAR[®] DNA polymerase (Takara)

Glucose oxidase kit (Glucose liquiColor[®], Human, German)

2.4 Bacterial strains and plasmid

Leuconostoc citreum **ABK-1**, isolated from Khow-tom-mud (Thai traditional dessert) and identified by 16SrRNA sequencing, was provided by Dr. Santhana Nakapong.

Escherichia coli **TOP10** (Invitrogen™, Thermo Scientific), genotype: F⁻ *mcrA* Δ (*mrr*⁻ *hsdRMS*⁻ *mcrBC*) ϕ 80*lacZ* Δ M15 Δ *lacX74* *recA1* *araD139* Δ (*ara-leu*)7697 *galU* *galK* *rpsL* (Str^R) *endA1* *nupG*, was used as a host for plasmid propagation.

Escherichia coli **BL21 (DE3)** (Novagen), genotype: F⁻ *ompT* *gal* *dcm* *lon* *hsdS_B*(*r_B*⁻ *m_B*⁻) λ (DE3 [*lacI* *lacUV5-T7p07* *ind1* *sam7* *nin5*]) [*malB*⁺]_{K-12}(λ^S), was used as an expression host for protein production.

Escherichia coli **Rosetta (DE3) pLysS** (Novagen), genotype:

F⁻ *ompT* *gal* *dcm* *lon* *hsdS_B*(*r_B*⁻ *m_B*⁻) λ (DE3 [*lacI* *lacUV5-T7p07* *ind1* *sam7* *nin5*]) [*malB*⁺]_{K-12}(λ^S)

pLysSRARE[*T7p20* *ileX* *argU* *thrU* *tyrU* *glyT* *thrT* *argW* *metT* *leuW* *proL* *ori_{p15A}*](C^m^R), was used as an expression host for protein production.

Escherichia coli **Origami (DE3) pLysS** (Novagen), genotype: Δ (*ara-leu*)7697 Δ *lacX74* Δ *phoA* *PvuII* *phoR* *araD139* *ahpC* *galE* *galK* *rpsL* (DE3) F'[*lac*⁺ *lacI*^q *pro*] *gor522::Tn10* *trxB* pLysS (Cam^R, Str^R, Tet^R), was used as an expression host for protein production.

Escherichia coli **Rosetta-gami (DE3) pLysS** (Novagen), genotype: Δ (*ara-leu*)7697 Δ *lacX74* Δ *phoA* *PvuII* *phoR* *araD139* *ahpC* *galE* *galK* *rpsL* (DE3) F'[*lac*⁺ *lacI*^q *pro*] *gor522::Tn10* *trxB* pLysSRARE (Cam^R, Str^R, Tet^R), was used as an expression host for protein production.

pET19b (Novagen) was used as an expression vector.

pETMus was synthesised by Genscript. The mutansucrase (*gtf-I*) gene from *Streptococcus sorbinus*⁶⁹ was inserted into pET21b.

2.5 General techniques for molecular cloning and gene expression

2.5.1 Genome extraction

The 1 mL of overnight culture was harvested by centrifugation at 8,000xg for 5 min. The cell pellets were resuspended with 0.5 mL SET buffer. The cells were lysed by adding 30 μ L of 10% SDS and gently mixed by inverting the tube. Then, 50 μ L of 5 M sodium acetate was added and gently mixed. The cell lysate were centrifuged at 10,000xg for 10 min and the supernatant was collected. The protein contaminant was gently extracted by phenol: chloroform: isoamylalcohol and then centrifuged at 10,000xg for 10 min. This step was repeated twice. Then, upper phase was transferred into nuclease-free microcentrifuge tube. Genomic DNA was precipitated by adding of 2.5 volumes of absolute ethanol and pellet by centrifugation at 10,000xg for 5 min. The DNA pellet was washed by 70 % (v/v) ethanol and dried to remove the residual ethanol at 60 °C for 10 min. The genomic DNA was dissolved in sterile nuclease-free ultrapure (UP) water and stored at 4 °C.

2.5.2 Plasmid preparation

Cells harbouring plasmid were cultured in 4 mL of LB broth containing appropriate antibiotics at 37 °C with shaking at 250 rpm for overnight. Cells were then harvested by centrifugation at 10,000xg for 30 sec and applied to Presto™ Mini Plasmid Kit (Geneaid).

2.5.3 Electrocompetent cell preparation

The method was modified based on Sambrook et al. 1989⁷⁰. Overnight *E. coli* culture was diluted in fresh LB medium with ratio of 1:100. The culture was then grown in at 37 °C shaking 250 rpm. The bacterial growth was monitored until OD₆₀₀ reached ~0.3-0.35. Cells were immediately kept on ice for 10 min. After that, cells were collected by centrifugation at 2,000xg, 4 °C for 10 min. The cell pellets were gently washed by cold sterile UP-water and collected by centrifugation at 2,000xg, 4 °C for 10 min (repeat this step twice). Then, cells were washed by cold 10 % (v/v) glycerol and collected by centrifugation at 2,000xg, 4 °C for 12 min. Finally, the cell pellets were suspended with ratio of 500 µL of cold 10 % (v/v) glycerol:1 L of cell culture. The 40 µL of cell suspension was aliquoted into microcentrifuge tube and immediately stored at -80 °C freezer.

2.5.4 Transformation of recombinant plasmid into *E. coli* host cell ⁷⁰

The 3 µL of plasmid solution or purified ligation mixture was gently mixed with the competent cells on ice. Then, cells mixture was transferred to a 0.1 or 0.2 cm-gap cold sterile electroporation cuvette and electroporated by using 25 µF, 200 Ω of the pulse controller unit with 18 kV. Then, 0.5 mL of LB medium was added to the cells mixture for recovery and cells were culture at 37 °C with shaking at 250 rpm for 45 min. The recovered culture was thoroughly plated on LB agar containing appropriate antibiotic and incubated at 37 °C for overnight.

2.5.5 Agarose gel electrophoresis

The 8 % (w/v) agarose gel was prepared. Eight gram of agarose was dissolved in 100 mL of 1xTAE buffer and heated until completely dissolved. The gel was then cast. After gel was set completely, the DNA samples were mixed well with 6x loading dye and subsequently loaded into the wells. Electrophoresis was constantly run at 100 Volts for 30-45 min. The gel was stained with 50 mg/L ethidium bromide solution and visualised under UV light by Gel Document device.

2.5.6 Construction of recombinant plasmids

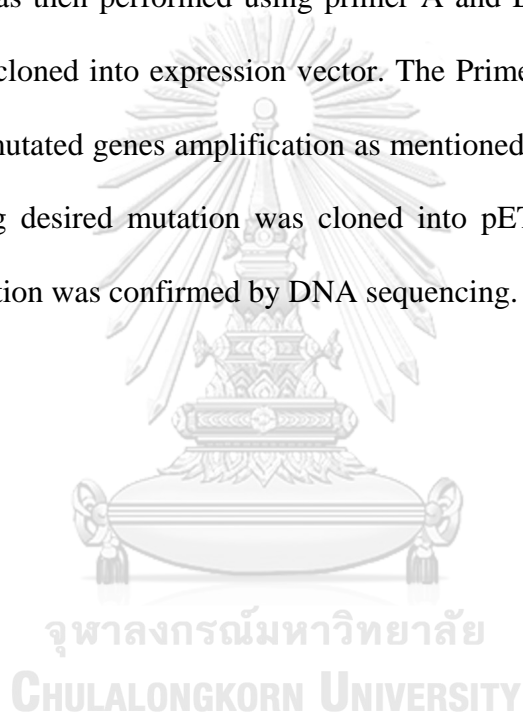
The genes were amplified by PrimeSTAR[®] DNA polymerase (Takara) using genomic DNA as template followed the manufacturer's manual. The PCR products were purified by PCR/Gel extraction kit (Geneaid) and analysed by agarose electrophoresis. The purified PCR products and pET19b were excised by 30 U of *Nco*I and *Xho*I restriction enzymes for overnight at 37 °C. After purification of the digested PCR products and linearised pET19b by using the same kit, the ligation was performed at 16 °C for overnight. The ligation mixtures were cleaned by Phenol:Chloroform extraction prior to transforming into *E. coli* TOP10. The transformants were randomly picked and grown in antibiotics-containing LB broth for overnight. The recombinant plasmids were isolated and analysed by restriction enzyme analysis. Nucleotide sequences of the positive clones were further verified by DNA sequencing (1st BASE).

Table 1. The lists of primer for *alt* amplification and sequencing

primer name	primer sequence (5'-3')	remark
F_alt_pro	GCTATGGCGTCATGCAGGAACCACTTTATC	first amplification of <i>alt</i>
F_altNdeI	GGGAGAGTAATCCATGGAACAACAAG	secondary amplification of <i>alt</i>
R_altxhoI	CCGCTCGAGTTAAGCTTGCAAAGCACGCTTATC	<i>alt</i> amplification
F_alt1	GATGGTAATGGCCAACCGTTAATC	for sequencing
F_alt2	GTACTGAGTGGTTACGTGATGCAATTG	for sequencing
R_alt3	TACGTTTGTGAAGCAAGATGGAAC	for sequencing
R_alt4Sal	GGGTCGACTCTAGTAGCAGTAACAACCTTCCTTCC	for sequencing
F_alt5	CGGTGGCATGTCATTCTTAGATTC	for sequencing
R_alt6	GATGCCTACGGTGCACAATGGCGT	for sequencing
T7promotor	AATACGACTCACTATAG	for sequencing
T7terminator	GCTAGTTATTGCTCAGCGG	for sequencing
R_Del3	GCATCTCGAGCTAGCTCAAAGCGCGA	Δ SH3alt construction
R_Del7	CAGCCGGATCCTCGAGTTAAGCTTGC	Δ SH7alt construction

2.5.7 Mutagenesis by PCR driven overlap extension method⁷¹

The method was shown in Fig. 8. The 2 fragments of PCR products were primarily generated by two pairs of primer; forward primer A and reverse primer B, and forward primer C and reverse primer D, respectively. Primers B and C harboured the codon for desired mutated amino acid. The 2 PCR products with overlapping region from the first PCR were purified and mixed before using as a template for the second PCR. The PCR was then performed using primer A and D. After that the new PCR product was then cloned into expression vector. The PrimeSTAR[®] DNA polymerase was used for the mutated genes amplification as mentioned in section 2.5.6. The PCR product containing desired mutation was cloned into pET19b vector by restriction cloning. The mutation was confirmed by DNA sequencing.



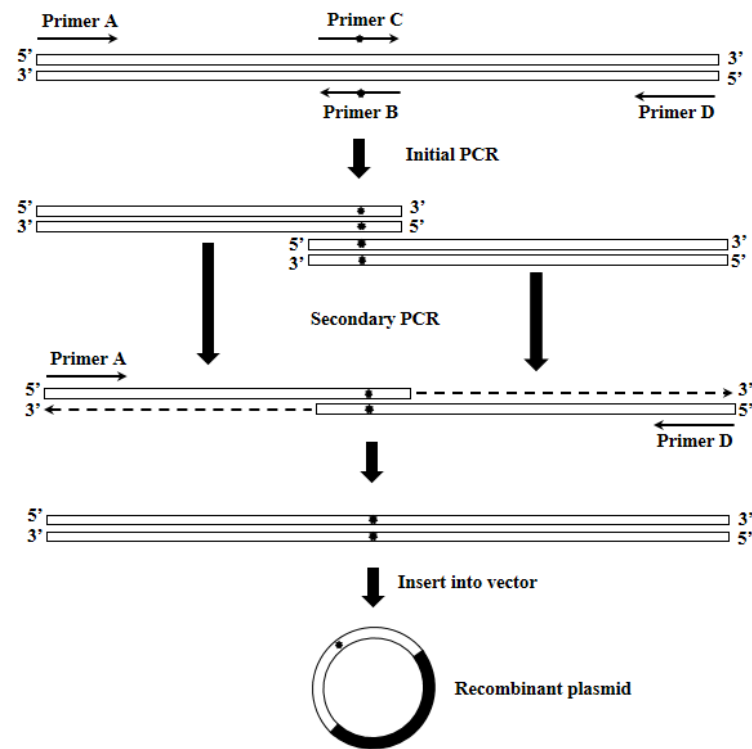


Figure 8 Site-directed mutagenesis by PCR driven overlapping extension. The asterisks indicated the desired point mutation.

Table 2. Primer lists for alanine scanning mutation

primer name	primer sequence (5'-3')	remark
F_F538A	CAGACAGAAGACGAAGCTGCTGATGGATTG	mutation at F538
R_F538A	CTTGAAGCCACTGCAATCCATCAGCAGCTTCG	mutation at F538
F_W543A	GCTTTTGATGGATTGCAGGCGCTTCAAGG	mutation at W543
R_W543A	GCTAGGAATCCCCCTTGAAGCGCCTGCAATC	mutation at W543
F_W675A	GCATTTGTCTATTTTAGAAGACGCGAATGGC	mutation at W675
R_W675A	CATATTGAGGATCTTTGCCATTCGCGTCTTC	mutation at W675
F_Y695A	GCGCAATTAACAATGGATGCCACAGTACTT	mutation at Y695
R_Y695A	CCAAACTGTGAAGTAAGTGTGGCATCCATTG	mutation at Y695
F_F701A	CACAGTTACTTCACAGGCTGGCAATTCTC	mutation at F701
R_F701A	GGCACCATGTGTTAGAGAATTGCCAGCCTGTGAAG	mutation at F701
F_W716A	CAACAGGAGTAACATGGCGTATTTCTTAG	mutation at W716
R_W716A	GATAATAGCCAGTATCTAAGAAATACGCCATGTTAC	mutation at W716
F_Y717A	CAACAGGAGTAACATGTGGGCTTTCTTAG	mutation at Y717
R_Y717A	GATAATAGCCAGTATCTAAGAAAGCCCACATG	mutation at Y717
F_Y768A	GTTTTATTAGAGCGCATGATGCCGATGCTCAAG	mutation at Y768
R_Y768A	CTAATTGGATCTTGAGCATCGGCATCATGC	mutation at Y768
F_F802A	CTGGCTCAGGGAATGGAAGCCTACTATC	mutation at F802
R_F802A	GATTATTTTGATCTTGATAGTAGGCTTCCATTC	mutation at F802
F_F813A	CAAATAATCCGTCTGGTGCCAAAAAGTATAA	mutation at F813
R_F813A	GTTATAATCGTTATACTTTTTGGCACCAGAC	mutation at F813
F_Y816A	TCCGTCTGGTTTCAAAAAGGCTAACGATTA	mutation at Y816
R_Y816A	GGCACTAGGTAAGTTATAATCGTTAGCCTTTTTGAAAC	mutation at Y816
F_Y1110A	CTAGTGGTGACACTAATGCCGGTGCC	mutation at Y1110
R_Y1110A	CTAAGAATGACATGCCACCGCATTAGTG	mutation at Y1110
F_Y1124A	CTTCTTAAATAATGGTGCTGCATTTAC	mutation at Y1124
R_Y1124A	CATATCTATCCGTAAATGCAGCACCATTA	mutation at Y1124

Table 3. Primer lists for saturation mutagenesis at W675 position

primer name	primer sequence (5'-3')	remark
F_W675Y	CTATTTTAGAAGACT <u>TATA</u> ATGGCAAAGATCCTC	mutation at W675 to Y
R_W675Y	GAGGATCTTTGCCATT <u>ATAG</u> TCTTCTAAAATAG	mutation at W675 to Y
F_W675F	CTATTTTAGAAGACT <u>TTT</u> AATGGCAAAGATCCTC	mutation at W675 to F
R_W675F	GAGGATCTTTGCCATT <u>AAA</u> GTCTTCTAAAATAG	mutation at W675 to F
F_W675L	CTATTTTAGAAGAC <u>CTGA</u> ATGGCAAAGATCCTC	mutation at W675 to L
R_W675L	GAGGATCTTTGCCATT <u>CAG</u> GTCTTCTAAAATAG	mutation at W675 to L
F_W675I	CTATTTTAGAAGAC <u>ATTA</u> AATGGCAAAGATCCTC	mutation at W675 to I
R_W675I	GAGGATCTTTGCCATT <u>AATG</u> TCTTCTAAAATAG	mutation at W675 to I
F_W675S	CTATTTTAGAAGACT <u>TCCA</u> ATGGCAAAGATCCTC	mutation at W675 to S
R_W675S	GAGGATCTTTGCCATT <u>GGAG</u> TCTTCTAAAATAG	mutation at W675 to S
F_W675H	CTATTTTAGAAGAC <u>CATA</u> ATGGCAAAGATCCTC	mutation at W675 to H
R_W675H	GAGGATCTTTGCCATT <u>ATGG</u> TCTTCTAAAATAG	mutation at W675 to H
F_W675N	CTATTTTAGAAGAC <u>ACA</u> CAATGGCAAAGATCCTC	mutation at W675 to N
R_W675N	GAGGATCTTTGCCATT <u>GTTG</u> TCTTCTAAAATAG	mutation at W675 to N
F_W675D	CTATTTTAGAAGAC <u>GATA</u> AATGGCAAAGATCCTC	mutation at W675 to D
R_W675D	GAGGATCTTTGCCATT <u>ATCG</u> TCTTCTAAAATAG	mutation at W675 to D

2.5.8 Expression of alt and all constructs

The overnight culture of cells harbouring recombinant plasmid were inoculated into new LB broth containing 100 µg/mL ampicillin (1:100), and cultured at 37 °C with shaking at 250 rpm. The growth was monitored until OD₆₀₀ reached 0.4-0.6. The culture was induced by 0.4 mM IPTG and continuously grown at 16 °C with shaking at 250 rpm for overnight. Cells were collected by centrifugation at 8,000xg for 10 min at 4 °C, and suspended in cold extraction buffer (50 mM sodium citrate buffer, 0.1 % (V/V) Triton X-100 and 75 mM NaCl, pH 6.2) with ratio of buffer to cell culture, 0.3:1. Cells were lysed by sonication with trapper probe for 1.30 min of pulse-on using 30% power at 4 °C. The insoluble fraction was removed by centrifugation at 10,000xg for 15 min at 4 °C. The soluble protein was dialysed against 25 mM sodium citrate pH 6.2. Finally, the crude enzyme was kept at 4 °C for further experiments.

2.6 General techniques for protein characterisation

2.6.1 Polyacrylamide gel electrophoresis (PAGE) analysis

2.6.1.1 Sodium Dodecyl Sulfate-Polyacrylamide Gel Electrophoresis (SDS-PAGE) ⁷²

The 8% (w/v) of separating gel and 5% (w/v) of stacking gel containing 0.1% (w/v) of SDS were set. The protein samples were mixed with 5X sample buffer. Then, the sample was carefully loaded into wells of the gel and the electrophoresis was run in electrophoresis buffer pH 8.3 containing 0.1% (w/v) of SDS by using 15 mA/gel. The protein bands were visualised by Coomassie staining.

2.6.1.1 Affinity electrophoresis⁷³

The 8% (w/v) of separating gel was set containing various concentration of dextran 0-1% (w/v) without SDS. The 5% acrylamide gel was used as stacking gel. The proteins sample were run under non-denaturing condition at 4 °C using 15 mA/gel.

2.6.2 Modified Dinitrosalicylic acid assay (DNS assay)⁷⁴

The standard reaction was consist of 50 mM citrate buffer in optimum pH and 2 % (w/v) sucrose (20 % (w/v) sucrose was used for W675A characterisation) in 0.5 mL of total volume. The reaction was then initiated by adding the enzyme. The 0.5 mL enzymatic reaction was terminated by adding of equal volume of DNS solution and boiled for 10 min. The reaction was diluted by adding of 4 mL of deionised water. The enzyme activity was measured at A₅₄₀ by comparing the amount of reducing sugars produced in the reaction with fructose standard. One enzyme unit was defined by the amount of enzyme that release 1 μmol of reducing sugar from sucrose substrate in a minute per enzyme (mL).

2.6.3 Protein assay by Bradford method⁷⁵

The 25 μL of protein solution was mixed with 300 μL of Bradford's reagent, and incubated at room temperature for 10 min. The mixture was immediately subjected to A₅₉₅ measurement and the amount of protein was compared with BSA standard.

2.6.4 Periplasmic protein extraction

The cell pellet was re-suspended in 0.5 M sorbitol and chilled on ice for 30 min. the cell were collected by centrifugation at 4 °C. The osmotic shock was provided by suspending the cell pellet in the 50 mM citrate buffer pH 6.2 and stored on ice for 10

min. The cells were separated by centrifugation and supernatant were kept to activity assay.

2.6.5 Purification of full length ALT

2.6.5.1 Purification by DEAE Toyopearl 650M column

The crude enzyme was loaded onto column equilibrated with 25 mM sodium citrate buffer pH 6.2 and washed with the same buffer. Then, proteins were eluted by linear gradient of 0–1 M NaCl in 25 mM sodium citrate buffer pH 6.2. The protein and activity in each fraction were monitored by measuring at A_{280} and A_{540} , respectively. Finally, the activity fractions were pooled and stored at 4 °C.

2.6.5.2 Purification by Phenyl Toyopearl 650M column

The pooled activity fractions from DEAE toyopearl 650M column was slowly added ammonium sulfate power at 4 °C until concentration was raised up to 0.4 M. After that, the protein solution was loaded onto Phenyl Toyopearl 650M column equilibrated with 25 mM sodium citrate buffer containing 0.4 M ammonium sulfate, pH 6.2 and washed with the same buffer. Then, proteins were eluted by linear gradient of 0.35–0.15 M ammonium sulfate in 25 mM sodium citrate buffer pH 6.2. The protein and activity were monitored by measuring at A_{280} and A_{540} , respectively. Finally, ammonium sulfate in the pooled activity fractions was removed by using Amicon® ultrafiltration. Then, the purified protein in 25 mM sodium citrate buffer pH 6.2 was stored at 4 °C.

2.6.6 Characterisation of ALT and all mutants

All characterisations (optimum pH and temperature, effect of metal ion and detergents, pH stability, storage stability, and enzyme kinetics) were monitored by DNS assay.

2.6.6.1 Optimum pH

The purified enzyme was incubated with 2 % (w/v) sucrose in 50 mM of various buffers [sodium citrate buffer (pH 3.0-6.0) and potassium phosphate buffer (pH 6.0-8.0)] at 37 °C.

2.6.6.2 Optimum temperature

The purified enzyme was incubated with 2 % (w/v) sucrose in 50 mM citrate buffer pH 5.5 and 4.0 for wild type and mutants, respectively, at different temperatures (20-60 °C).

2.6.6.3 Effect of metal ions and detergents

The reaction was carried out by incubating of the purified enzyme in 50 mM acetate buffer pH 5.5 and 4.0 for wild type and mutants, respectively, at 40 °C containing metal ion or detergent (with final concentration of 10 mM of Ca²⁺, Co²⁺, Cu²⁺, Fe³⁺, Mg²⁺, Mn²⁺, Zn²⁺, EDTA, and 0.1% (v/v) Triton X-100).

2.6.6.4 pH stability

Firstly, the enzyme was pre-incubated in 20 mM Britton-Robinson buffer pH 3.0-8.0 for 2 hr at 30 °C, and enzyme activity was then measured at optimum pH and temperature. Secondly, the enzyme was incubated in 50 mM citrate buffer pH 6 at 30 °C for 24 hr, and enzyme activity was detected. Finally, the enzyme was incubated in 50 mM citrate buffer at optimum pH and temperature for 12 hr, and enzyme activity was measured.

2.6.6.5 Storage stability

The enzyme was stored in 25 mM citrate buffer pH 6.2 at 4 °C for 28 days. Enzyme activity was measured under optimal condition by DNS assay for every week.

2.6.6.6 The kinetic study

The kinetics was studied under optimal condition of each enzyme at initial velocity using 100 mU of enzyme. The reactions were carried out in 0.5 mL and terminated by adding of 15 or 35 μ L of 1 N NaOH to the reaction containing 50 mM citrate buffer pH 5.5 or pH 4.0, respectively. The reactions were then initiated by adding the enzyme. The reactions were analysed by DNS and glucose oxidase kit. The hydrolysis activity was calculated from amount of free glucose in reaction whereas the difference between free fructose and glucose in reaction exhibited the transglycosylation activity of enzyme.

2.7 Product characterisation

2.7.1 Production of polymer

Alternan polymer was synthesised by 20% (w/v) sucrose with 5 U of enzyme per gram of sucrose in 50 mM sodium citrate buffer pH 5.0 (pH 4.0 for truncated enzymes) at 37 °C in 100 mL total volume for overnight. The polymer was then precipitated by addition of 1:1 volume of acetone then chilled on ice for 1 hr. The reaction was then centrifuged at $10,000 \times g$ for 20 min. The polymer pellet was collected, re-suspended in deionised water, and dialysed against deionised water. The sample was lyophilised and stored for further experiments. For reduce viscosity of polymer, the polymer was dissolved in deionised water at 20% (w/v) and pre-treated to reduce the viscosity by ultrasonication

(Sonics Vibra-Cell, at 50% power output) on ice, for 15 min. The sonicated polymer was lyophilised for further experiments.

2.7.1 Thin layer chromatography (TLC)

The mobile phase system I comprises 2-butanol:Acetic acid:Water (3:3:2). The system I was equilibrated at room temperature ($\sim 30\text{ }^{\circ}\text{C}$) at least 48 hr⁷⁶. On the other hand, the mobile phase system II consists of Acetonitrile:Ethyl acetate:1-propanol:Water (85:20:50:60)⁷⁷. The system II was equilibrated at room temperature for 30 min. The samples were carefully spotted on TLC aluminium plate and run in saturated tanks for 3 ascends or twice for system II. The products were visualised by spraying with orcinol solution and burning at $110\text{ }^{\circ}\text{C}$ for 10 min.

2.7.2 Partial hydrolysis of WTALT polymer

The 0.5 g of WTALT polymer was dissolved in 2 mL of 1 M HCl, and boiled for 15 min. The reaction was cooled down and neutralised by NaOH.

2.7.3 Purification of oligosaccharides and polymer by gel filtration chromatography

The oligosaccharides were purified by Bio gel-P2 column ($22 \times 1000\text{ mm}$) using DI water as mobile phase at $50\text{ }^{\circ}\text{C}$ with flow rate of 0.5 mL/min. The signals were monitored by RI detector. For polymer sample, using Toyopearl HW44S under the same condition.

2.7.4 High Performance Anion Exchange Chromatography-Pulse Amperometric Detection (HPAEC-PAD) analysis

The samples were filtered through 0.45 μm syringe filter prior to injection. The samples from partial hydrolysis of polymer and oligosaccharides from wild type reaction, were analysed by CarboPac PA100 (2 or 4 mm. i.d. x 250 mm. length) and eluted with linear gradient of 0-150 mM of sodium acetate in 150 mM NaOH. To compare the pattern of oligosaccharide among the mutants, the gradient 0-300 mM of sodium acetate in 150 mM NaOH was used.

2.7.5 Complete hydrolysis of oligo-alternan

The oligo-alternans from alternansucrase reaction were separated by gel filtration and their molecular masses were verified by MALDI-TOF. Each oligosaccharide was incubated in 3 M Trifluoroacetic acid (TFA) at 100 °C for 4 hr. Then, the TFA was evaporated. The samples were dissolved in DI water and analysed by HPAEC-PAD.

2.7.6 Acetolysis of mutan polymer

The mutan polymer was produced by expression of mutansucrase (*gtf-I*) gene from *S. sorbinus* in *E. coli* BL BL21(DE3). The mutan polymer was primarily treated by sonication, then dissolved in mixture of acetic anhydride, acetic acid and sulfuric acid in the ratio 5:4:0.5, with stirring for overnight at room temperature. The sulfuric acid was gently added up to ratio of 1. The reaction was heated at 100 °C for 25 min and then gently neutralised at 4 °C by adding of saturated NaHCO_3 . The reaction was extracted by dichloromethane (DCM) and evaporated. The pre-acetylated

oligosaccharides were dissolved in 0.1 M sodium methoxide in anhydrous methanol, and incubated for overnight at room temperature. The oligosaccharide mixture was then neutralised by adding of Amberlite™ ion exchange resins. Finally, the oligosaccharides were dried and dissolved in DI water.

2.7.7 Methylation of polymer⁷⁸

The 0.3 mg of purified alternan polymer was mixed with 50 μ L of DMSO and 50 μ L of NaOH/DMSO, and sonicated in ultrasonic bath for 10 min. Then, 20 μ L of methyl iodide was added and sonicated continuously for 45 min (repeated 3 times). After that, 0.5 mL of DCM and 1 mL of 100 mg/mL sodium thiosulfate were added and vortex vigorously. The DCM phase was collected, and washed by DI water for 3 times, and evaporated. All methylation processes were performed twice.

2.7.8 Linkage analysis⁷⁸

The 20 μ g of polymer was methylated as described above. Then, the sample was completely hydrolysed by using 3 M TFA at 100 °C for 4 hr. After that, the TFA was evaporated. One μ g of myo-inositol was added as an internal standard. The sample was then reduced by adding of 50 μ L of 2 M NH_4OH and 50 μ L of 2 M sodium boroduteride dissolved in 2 M NH_4OH , and incubated at room temperature for 2.5 hr. Then, 15 μ L of glacial acetic acid was gradually dropped to the sample and evaporated. The 250 μ L of 5 % (v/v) acetic acid in methanol was then added to the sample and evaporated (repeated this step for 3 times). Then, the sample was acetylated by adding of 250 μ L of acetic anhydride, and incubated for 2.5 hr at 100 °C. The excess acetic anhydride were removed by adding of 2 mL of DI water. Pre-methylated pre-acetylated sugars were extracted twice by 0.5 mL of DCM. The DCM phase was washed twice by

DI water and dried under Nitrogen condition. Finally, the sample was dissolved in 20 μL of DMC and analysed by GC-MS.

2.7.9 NMR analysis

The polymer was dissolved in DI water with 20 % (w/v) final concentration and sonicated (50 % Amplitude for 15 min at 4 °C). The sample was precipitated by equal volume of acetone and suspended in DI water, and lyophilised. The dried polymers were dissolved in D₂O or DMSO-d₆ and NMR analysis was performed.

2.7.10 Size determination by Dynamic light scattering (Zetasizer Nano ZS)

The dialysed polymer without sonication and acetone precipitation and 1 % (w/v) lyophilised polymer were pre-equilibrated for 1 min at 25 °C. The size determination of the polymer was carried out by Zetasizer Nano ZS using a refractive index value of 1.33, with 90 ° scattering optics at 633 nm.

2.7.11 Transmission electron microscopy (TEM)

The dialysed polymer without sonication and acetone precipitation and 1 % (w/v) lyophilised polymer were diluted (1-10,000 times) prior to dropping onto copper grids. The grids were dried in desiccator for overnight. The TEM images were obtained by Hitachi H-7650 transmission electron microscope.

2.7.12 Soluble and film-forming abilities of the polymer

The solubility of polymer was investigated by dissolving in DI water, DMSO and 50 % (w/v) NaOH at various concentrations. To observe film-forming property, the 2 % (w/v) of polymer was cast on polypropylene surface and air dried for overnight.

2.7.13 Viscosity determination by viscometer

The 15 % (w/v) of lyophilised polymer was dissolved in DI water for overnight. The polymer solution was serially diluted and its viscosity was measured by using viscometer at 25-27 °C.



CHAPTER III

RESULTS

3.1 Cloning of WT*alt*, Δ 3SH*alt* and Δ 7SH*alt* genes

The alternansucrase gene (*alt*) was amplified using genomic DNA of *L. citreum* ABK-1 as a template. The size of putative full length gene was around 6 kb analysed on 8 % (w/v) agarose gel (lane 2, Fig. 9A). The WT*alt* gene harboured 6,174 bp of a single open reading frame (ORF) encoding 2,057 residues of deduced amino acids. The theoretical mass and pI value were 228,950.74 Da and 5.16, respectively, predicted by ExPASy translate tool. The sequence was deposited in GenBank database with accession number, KM083061.2. WTALT was aligned with ALT sequences of various bacterial species as shown in Fig. 10. Three conserved sequence motifs were exhibited, and three catalytic residues were shown by underlines. In addition, WTALT was also compared with *L. messenteroides* NRRL B-1355 *LmALT* reported in NCB database (accession no. CAB65910.2). They shared 97 % identity which 32 out of 45 different residues highlighted in yellow were present in catalytic domain (shown in red letters) (Fig. 11).

On the other hand, deletion of 3 and 7 of C-terminal SH3-like domains (Δ 3SH*alt* and Δ 7SH*alt*, respectively) were successfully constructed. The 5,454 and 4,485 bp of Δ 3SH*alt* and Δ 7SH*alt* (Fig. 9B and 9C, respectively) encoding 1,817 and 1,494 amino acids of Δ 3SHALT and Δ 7SHALT were shown. The theoretical masses of these two truncated proteins were 202,207.06 and 166,028.02 kDa, respectively.

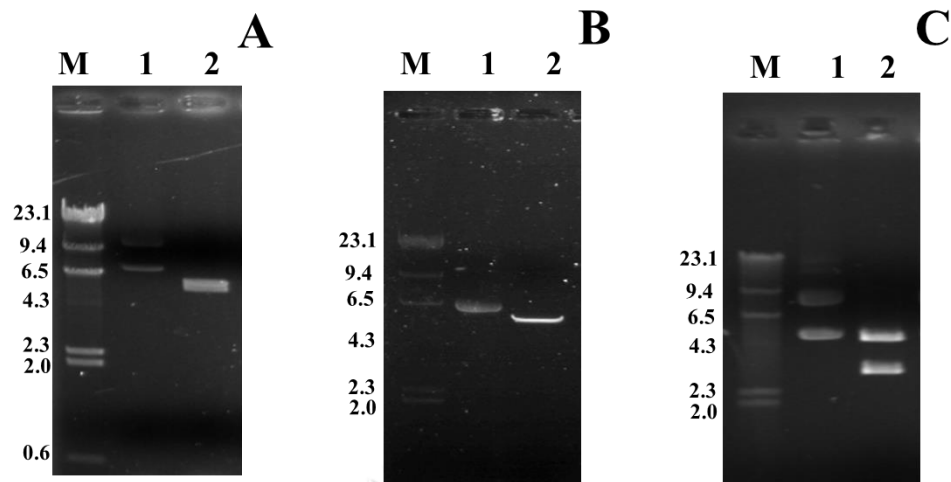


Figure 9 Cloning result analysed on 0.8 % (w/v) agarose gel; (A) WTalt, (B) Δ 3SHalt and (C) Δ 7SHalt

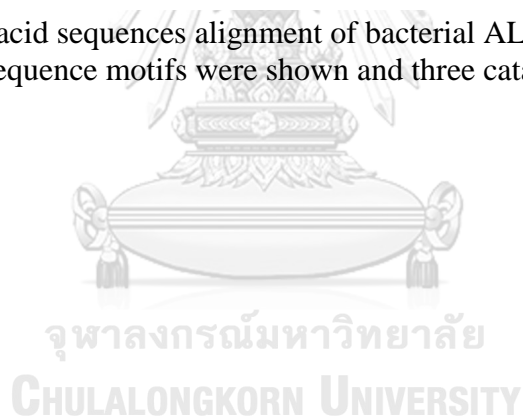
Lane M: λ /HindIII marker

Lane 1: Uncut recombinant plasmid (pETALT (A), pET Δ 3SHalt (B) and pET Δ 7SHalt (C))

Lane 2: Double digestion of recombinant plasmid with *Nco*I and *Xho*I (pETALT (A), pET Δ 3SHalt (B) and pET Δ 7SHalt (C))

Bacterial strain		conserved I		conserved II		conserved III	Accession No.
<i>L. citreum</i> ABK-1	627	ANFDGIRV <u>DA</u> VNDADLLKI	668	HLSI <u>LE</u> DWNGKDPQY	760	YSFIRAH <u>DY</u> DAQDPI	This work
<i>L. mesenteroides</i> NRRL B-1355	627	ANFDGIRV <u>DA</u> VNDADLLKI	668	HLSI <u>LE</u> DWNGKDPQY	760	YSFVRAH <u>DY</u> DAQDPI	CAB65910.2
<i>L. citreum</i> B/110-1-2	547	ANFDSIRV <u>DA</u> VNDADLLDI	588	HISI <u>LE</u> DWSGLDPNE	658	YSFVRAH <u>D</u> SEVQGII	ACY92456.2
<i>S. sobrinus</i> OMZ176	439	ANFDSIRV <u>DA</u> VNDADLLQI	480	HVSIV <u>E</u> AWSDNDTPY	551	YSFARAH <u>D</u> SEVQDII	BAA02976.1
<i>L. mesenteroides</i> NRRL B-1299	519	ANFDGYRV <u>DA</u> VNDADLLQI	560	HISI <u>LE</u> DWDNDSAY	631	YAFIRAH <u>D</u> SEVQTVI	CAD22883.1
<i>L. mesenteroides</i> NRRL B-512F	543	ANFDGIRV <u>DA</u> VNDADLLQI	584	HLSI <u>LE</u> DWSHNDPLY	655	YSFVRAH <u>D</u> SEVQTVI	AAD10952.1
<i>L. reuteri</i> 121	1016	ANFDSVRV <u>DA</u> PDNIDADLMNI	1056	HINIL <u>E</u> DWNHADPEY	1126	YSFVRAH <u>D</u> NNSQDQI	OJ111530.1
<i>S. mutans</i> GS-5	457	ANFDGVRV <u>DA</u> VNDVNADLLQI	498	HLSI <u>LE</u> AWSDNDPQY	577	YIFIRAH <u>D</u> SEVQTVI	AAA26895.1
<i>L. reuteri</i> 180	1017	ANFDGIRV <u>DA</u> VNDVDLLSI	1058	HINIL <u>E</u> DWGDDPAY	1129	YNFVRAH <u>D</u> SNAQDQI	AAU08001.1
		****. **** *: :. *: : *		* : . * : * . *		* * * * * : * *	

Figure 10 Amino acid sequences alignment of bacterial ALT from various species. Three conserved sequence motifs were shown and three catalytic residues were underlined.



```

WTALT      MEQQETVTRKKLYKSGKVVWAAATAFAVLGVSTVTTVNADTNENVAVKQINNTGTNDSGE
LmALT      MKQQETVTRKKLYKSGKVVWAAATAFAVLGVSTVTTVHADTSENVAVKQINNTGTNDSGE
*::*****::*****::*****
WTALT      KKAVPVSTNNDLQGTDFGWYDSGDRVDQKTNQILLTAEQLKKNNEKNLSVISDDTSK
LmALT      KKVVPVSTNNDLQGTDFGWYDSGDRVDQKTNQILLTAEQLKKNNEKNLSVISDDTSK
**.*****
WTALT      KDDENISKQTKIANQQTVDTAKGLTTSNLSDPITGGHYENHNGYFVYIDASGKQVTGLQN
LmALT      KDDENISKQTKIANQQTVDTAKGLTTSNLSDPITGGHYENHNGYFVYIDASGKQVTGLQN
*****
WTALT      IDGNLQYFDDNGYQVKGSFRDVNGKHIYFDSVTGKASSNVDIVNGKAQGYDAQGNQLKKS
LmALT      IDGNLQYFDDNGYQVKGSFRDVNGKHIYFDSVTGKASSNVDIVNGKAQGYDAQGNQLKKS
*****
WTALT      YVADSSGQTYFDGNGQPLIGLQTIIDGNLQYFNQQGVQIKGGFQDVNNKRIYFAPNTGNA
LmALT      YVADSSGQTYFDGNGQPLIGLQTIIDGNLQYFNQQGVQIKGGFQDVNNKRIYFAPNTGNA
*****
WTALT      VANTEIINGKLQGRDANGNQVKNAFSTDVAGNTFYFDANGVMLTGLQTIISGKTYYLDEQG
LmALT      VANTEIINGKLQGRDANGNQVKNAFSKDVAGNTFYFDANGVMLTGLQTIISGKTYYLDEQG
*****.*****
WTALT      HLRKNYAGTFNNQFMYFDADTGAGKTAIEYQFDQGLVVSQSNENTPHNAAKSYDKSSFENV
LmALT      HLRKNYAGTFNNQFMYFDADTGAGKTAIEYQFDQGLVVSQSNENTPHNAAKSYDKSSFENV
*****

```

Figure 11 Amino acid sequences alignment of WTALT and *Lm*ALT. The 2,057 residues of WTALT and *Lm*ALT were compared using Clustal OMEGA. Catalytic domain sequences of GH70 were shown in red. The different residues between WTALT and *Lm*-ALT were highlighted in yellow. Three conserved sequence motifs were boxed, and three catalytic residues were underlined.

WTALT DGYL TADTWYRPTDILKNGDTWTASTETDMRPLLMTWVDPKQTQANYLNFMSKGLGITT
LmALT DGYL TADTWYRPTDILKNGDTWTASTETDMRPLLMTWVDPKQTQANYLNFMSKGLGITT

WTALT TYTAATSQKTLNDAAFVIQTAIEQQISLKKSTEWLRDAIDSFVTTQANWNKQTEDEAFDG
LmALT TYTAATSQKTLNDAAFVIQTAIEQQISLKKSTEWLRDAIDSFVKTQANWNKQTEDEAFDG

WTALT LQWLQGGFLAYQDDSHRTPNTDSGNNRKLGRQPVNIDGSKDITDGKGFLLANDIDNSN
LmALT LQWLQGGFLAYQDDSHRTPNTDSGNNRKLGRQPINIDGSKDITDGKGFLLANDIDNSN

WTALT PIVQAEQLNWLHYLMNFGSITGNNDNANFDGIRVDAVDNVDADLLKIAGDYFKALYGTDK
LmALT PIVQAEQLNWLHYLMNFGSITGNNDNANFDGIRVDAVDNVDADLLKIAGDYFKALYGTDK

WTALT SDANANKHLSILEDWNGKDPQYVNVQGNNAQLTMDYTVTSQFGNSLTHGANNRNSNMWYFLD
LmALT SDANANKHLSILEDWNGKDPQYVNVQGNNAQLTMDYTVTSQFGNSLTHGANNRNSNMWYFLD

WTALT TGYLNGDINKKIVDKNRQNSGTLVNRIANAAGDTQVIPNYSFIRAHDYDAQDPIRRAMID
LmALT TGYLNGDINKKIVDKNRENSGTLVNRIANSAGDTKVIPNYSFVRAHDYDAQDPIRKAMID

WTALT HGI IKNMQDTFTFDQLAQGMEFYQDQNNPSGFKKYNDYNLPSAYAMLLTNKDTIPRVYY
LmALT HGI IKNMQDTFTFDQLAQGMEFYKDQENPSGFKKYNDYNLPSAYAMLLTNKDTVPRVYY

Figure 11 Continued

WTALT GDMY^YEGGQYMQ^{NET}TIY^NR^SVISALLKARIKYVSGGQTMATDSSGKDLKDG^ETDLLTSVRF

*Lm*ALT GDMY^LEGGQYME^{KGT}TIY^NR^SVISALLKARIKYVSGGQTMATDSSGKDLKDG^ETDLLTSVRF

*****^Y*****[:]*****^Y*****

WTALT GKGIMTSDQTTTQDNSQDYKNQGIGVIVGNPDLKLNNDKTITLHMGKAHK^NQLYRAL^AL

*Lm*ALT GKGIMTSDQTTTQDNSQDYKNQGIGVIVGNPDLKLNNDKTITLHMGKAHK^NQLYRAL^VL

*****^Y*****

WTALT SNDSGIDVY^NSD^DE^AP^TL^RT^ND^NG^DL^IF^HK^TN^TF^VK^QD^GT^II^NY^EM^KG^SL^NA^LI^SG^YL^GV

*Lm*ALT SNDSGIDVY^DSD^KA^PT^LR^TN^DN^GD^LI^FH^KT^NT^FV^KQ^DG^TI^IN^YE^MK^GS^LN^AL^IS^GY^LG^V

*****[:]***[:]*****

WTALT WVPVGASDSQDARTVATE^ASSNDGSVFHSNAALDSNVIYEGFSNFQAMPTSPEQSTNVV

*Lm*ALT WVPVGASDSQDARTVATE^SSSNDGSVFHSNAALDSNVIYEGFSNFQAMPTSPEQSTNVV

*****^Y*****

WTALT IA^AN^AE^MF^KK^LG^IT^SF^EL^AP^QY^RS^SG^DT^NY^GG^MS^FL^DS^FL^NN^GY^AF^TD^RY^DL^GF^NK^AD^G^T

*Lm*ALT IA^TK^AN^LF^KE^LG^IT^SF^EL^AP^QY^RS^SG^DT^NY^GG^MS^FL^DS^FL^NN^GY^AF^TD^RY^DL^GF^NK^AD^G^N

[:]*[:]***[:]*****

WTALT PNPTKYGTDQDLR^NAIEALHKN^GM^QA^IADWVPD^QIYALPGKEVVTATR^VDERGNQLK^DT^D

*Lm*ALT PNPTKYGTDQDLR^NAIEALHKN^GM^QA^IADWVPD^QIYALPGKEVVTATR^VDERGNQLK^DT^D

WTALT FVNLLYVANTKSSGV^DY^QS^KYGG^EFLDKL^REE^YS^SLFKQ^NQ^VSTG^QPIDASTKIK^QWSAK

*Lm*ALT FVNLLYVANTKSSGV^DY^QA^KYGG^EFLDKL^REE^YP^SLFKQ^NQ^VSTG^QPIDASTKIK^QWSAK

*****^Y*****[:]***^Y*****

Figure 11 Continued

WTALT YMNGTNI LHRGAYYVLKDWATNQYFN IAKT D EVFLPLQLQNKD E QTGFISDASGVKYYSI
LmALT YMNGTNI LHRGAYYVLKDWATNQYFN IAKT N EVFLPLQLQNKD A QTGFISDASGVKYYSI
***** : * * * : *****

WTALT SGYQAKDTFIEDGNGNWYFDDKDGYM A RSQQGENPIRTVETSVNTRNGNYFMPNGVELR
LmALT SGYQAKDTFIEDGNGNWYFDDKDGYM V RSQQGENPIRTVETSVNTRNGNYFMPNGVELR
***** . *****

WTALT KGFGTDNSGNVYFDDQGKMVRDKYINDDANNFYHLNVDGTMSRGLFKFDSDTLQYFASN
LmALT KGFGTDNSGNVYFDDQGKMVRDKYINDDANNFYHLNVDGTMSRGLFKFDSDTLQYFASN

WTALT GVQIKDSYAKDSKGNKYFDSATGNNDT V KAQA W DGNNGYYITIDSDANNIGVNTDYTAY
LmALT GVQIKDSYAKDSKGNKYFDSATGNNDT G KAQT W DGNNGYYITIDSDANNIGVNTDYTAY
***** * * * : *****

WTALT ITSSLREDGLFANAPYGVVTKDQNGNDLKWQYINHTKQYEGQQVQVTRQYTDSKGVSWNL
LmALT ITSSLREDGLFANAPYGVVTKDQNGNDLKWQYINHTKQYEGQQVQVTRQYTDSKGVSWNL

WTALT ITFAGGDLQGQ K LWVDSRALTMTPFKTMNQISFISYANRNDGLFLNAPYQVKGYQLAGMS
LmALT ITFAGGDLQGQ R LWVDSRALTMTPFKTMNQISFISYANRNDGLFLNAPYQVKGYQLAGMS
***** : *****

WTALT NQYKGQQVTIAGVANVSGKDWSLISFNGTQYWIDSQALNTNFTHDMNQKVFVNTTNSLDG
LmALT NQYKGQQVTIAGVANVSGKDWSLISFNGTQYWIDSQALNTNFTHDMNQKVFVNTTNSLDG

Figure 11 Continued

WTALT LFLNAPYRQPGYKLAGLAKNYNNQTVTVSQQYFDDQGTVWSQVVLGGQTVWVDNHALAQM
*Lm*ALT LFLNAPYRQPGYKLAGLAKNYNNQTVTVSQQYFDDQGTVWSQVVLGGQTVWVDNHALAQM

WTALT QVSDT SQQLYVNSNGRNDGLFLNAPYRGQSQLIGMTADYNGQHVQVTKQGQDAYGAQWR
*Lm*ALT QVSDT DQQLYVNSNGRNDGLFLNAPYRGQSQLIGMTADYNGQHVQVTKQGQDAYGAQWR

WTALT LITLNNQVWVDSRALSTTIMQAMND MYVNS NQRTDGLWLNAPYTMMSGAKWAGDTRSAN
*Lm*ALT LITLNNQVWVDSRALSTTIMQAMND NMYVNS SQRTDGLWLNAPYTMMSGAKWAGDTRSAN

WTALT GRYVHISKAYSNEVGNTYYLTNLNGQSTWIDKRAFT A TFDQVVALNATIVARQRPDGMFK
*Lm*ALT GRYVHISKAYSNEVGNTYYLTNLNGQSTWIDKRAFT V TFDQVVALNATIVARQRPDGMFK

WTALT TAPYGEAGAQFVDYVTNYNQQTVPVTKQHSDAQGNQWYLATVNGTQYWIDQRSFSPVVTK
*Lm*ALT TAPYGEAGAQFVDYVTNYNQQTVPVTKQHSDAQGNQWYLATVNGTQYWIDQRSFSPVVTK

WTALT VVDYQAKIVPRTTRDGVFSGAPYGEVNAKLVNMATAYQNQVVHATGEYTNASGITWSQFA
*Lm*ALT VVDYQAKIVPRTTRDGVFSGAPYGEVNAKLVNMATAYQNQVVHATGEYTNASGITWSQFA

WTALT LSGQEDKLWIDKRALQA
*Lm*ALT LSGQEDKLWIDKRALQA

Figure 11 Continued

For domain organization, WTALT consists of a gram-positive bacterial signal peptide predicted by SignalP 4.1 server, 4 and 3 repeat sequences of glucan-binding domains at N- and C-termini, respectively, catalytic domain of glycoside hydrolase family 70 (GH70), and 7 repeat sequences of SH3-like domains at C-terminus (Fig. 12). While, Δ 3SHALT and Δ 7SHALT harboured C-terminal truncation of 3 and 7 of SH3-like domains, respectively.

Furthermore, sequences of 7 tandem repeats of SH3-like domains were aligned and their 3D-structures predicted by SWISS-MODEL server were shown in Fig. 13 and 14, respectively.

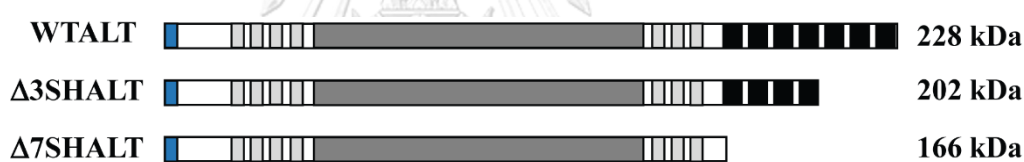


Figure 12 The protein diagram of WTALT, Δ 3SHALT and Δ 7SHALT. Blue boxes represent signal peptides, the light grey boxes represent CW-like repeats, the long dark grey boxes are catalytic domains, and black boxes are SH3-like domains.

```

repeat1  --NTDYTAYITSSLREDGLFANAPYGVVTKDQNGNDLKWQYINHTKQYEGQQVQVTRQYT
repeat2  -KTMNQISFISYANRNDGLFLNAPYQVK-----GYQLAGMSNQYKGQVTVIAG-VA
repeat3  ---MNQKVFVNTTNSLDGLFLNAPYRQP-----GYKLAGLAKNYNNQTVTVSQQYF
repeat4  ---TSQQLYVNSNGRNDGLFLNAPYRQ-----GSQLIGMTADYNGQHVQVTKQGG
repeat5  -QAMNDDMYVNSNQRTDGLWLNAPYTMS-----GAKWAGDTRSANGRYVHISKAYS
repeat6  DQVVALNATIVARQRPDGMFKTAPYGEA-----GAQFVDYVTNYNQQTVPVTKQHS
repeat7  TKVVDYQAKIVPRTTRDGVFSGAPYGEV-----NAKLVNMATAYQNQVVHATGEYT
          :      ***:  ***          : .      : : * :

repeat1  DSKGVSWNLITFAGGDLQGGKLVVDSRALT
repeat2  NVSGKDWSLISF-----NGTQYWIDSQALN
repeat3  DDQGTVWSQVVL-----GGQTVWVDNHALA
repeat4  DAYGAQWRLITL-----NNQQVWVDSRALS
repeat5  NEVGNTYYLTNL-----NGQSTWIDKRAFT
repeat6  DAQGNQWYLATV-----NGTQYWIDQRSFS
repeat7  NASGITWSQFALSG---QEDKLWIDKRALQ
          : * : .          ***: : :

```

Figure 13 Amino acid sequences alignment of 7 repeat SH3-like domains at C-terminus of *L. citreum* ABK-1 alternansucrase. The alignment was performed using Clustal Omega program.

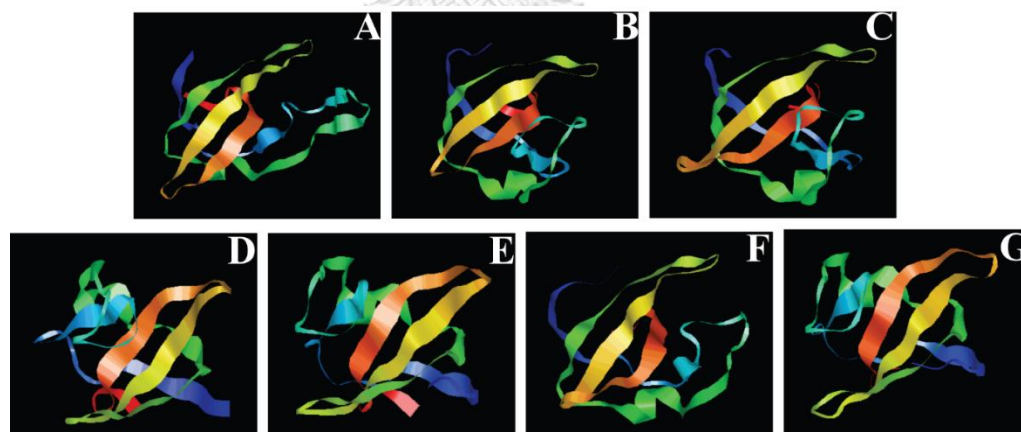


Figure 14 The 7 SH3-like domains of *L. citreum* ABK-1 alternansucrase. A-G represent homology models of 1st - 7th SH3-like domains, respectively, predicted by SWISS MODEL server.

3.2 Expression of WTalt, Δ 3SHalt and Δ 7SHalt genes

The pETALT was successfully constructed and transformed into expressing hosts; *E. coli* BL21 (DE3), *E. coli* Rosetta (DE3) pLysS, *E. coli* Origami (DE3) pLysS and *E. coli* Rosetta-gami (DE3) pLysS. Only *E. coli* BL21 (DE3) strain could apparently show the expression of the WTalt gene via production of WTALT with the size around 230 kDa on SDS gel (as shown in black ring in lane 2, Fig. 15). Although most protein was present in insoluble fraction, the production of soluble WTALT could apparently be increased by lowering the culture temperature together with reduction of IPTG concentration. However, the WTALT could slightly be detected as an extracellular protein after induction at low temperature (Fig. 16). The highest yield of soluble WTALT was obtained under induction of 0.4 mM IPTG at 16 °C for overnight (Fig. 17B) with the highest activity confirmed by DNS assay (Fig. 18).

In addition, Δ 3SHalt and Δ 7SHalt were also expressed under the optimal conditions as described above. The specific activity of crude WTALT, Δ 3SHALT and Δ 7SHALT were 7.16, 5.76 and 14.11 U/mg, respectively, of which more than 97 % of activity (Fig. 19) were derived from proteins predominantly produced in intracellular fraction (Fig. 20).

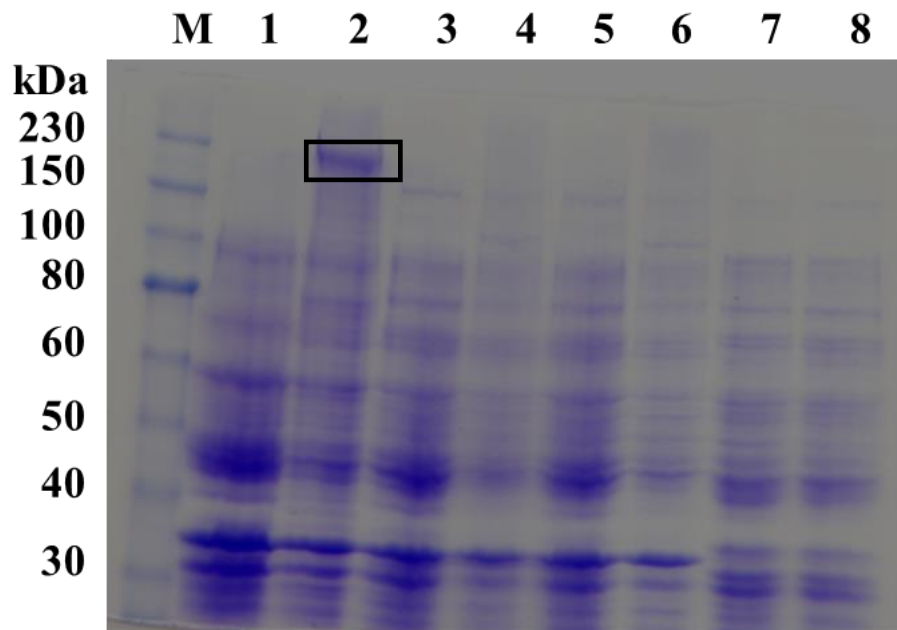


Figure 15 SDS-PAGE analysis of crude extract of WTALT produced by various *E. coli* T7 hosts under 1 mM IPTG induction at 37 °C

Lane M: Molecular weight protein marker

Lane 1: Non-induced *E. coli* BL21 (DE3)

Lane 2: Induced *E. coli* BL21 (DE3)

Lane 3: Non-induced *E. coli* Rosetta (DE3) pLysS

Lane 4: Induced *E. coli* Rosetta (DE3) pLysS

Lane 5: Non-induced *E. coli* Origami (DE3) pLysS

Lane 6: Induced *E. coli* Origami (DE3) pLysS

Lane 7: Non-induced *E. coli* Rosetta-gami (DE3) pLysS

Lane 8: Induced *E. coli* Rosetta-gami (DE3) pLysS

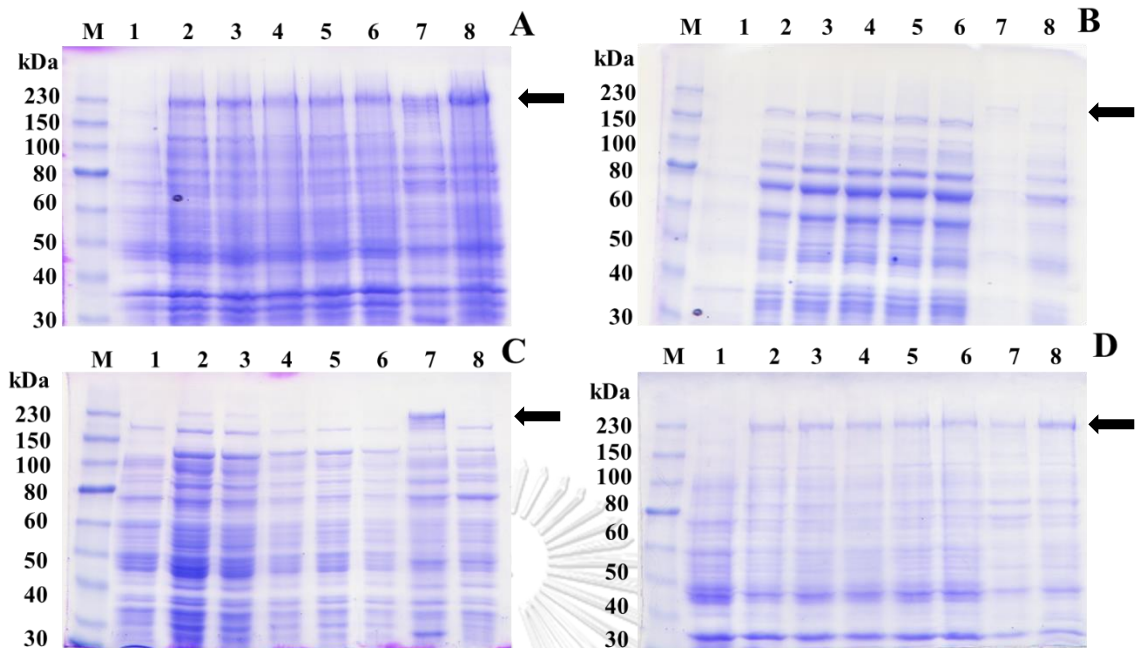


Figure 16 SDS-PAGE analysis of optimisation of WTALT production in *E. coli* BL21 (DE3); (A) whole cell lysate (B) extracellular fraction (C) intracellular fraction and (D) insoluble fraction. Arrows indicated bands of WTALT.

Lane M: Molecular weight protein marker

Lane 1: Non-induction

Lane 2: Induction with 0.2 mM IPTG at 37 °C

Lane 3: Induction with 0.4 mM IPTG at 37 °C

Lane 4: Induction with 0.6 mM IPTG at 37 °C

Lane 5: Induction with 0.8 mM IPTG at 37 °C

Lane 6: Induction with 1 mM IPTG at 37 °C

Lane 7: Induction with 1 mM IPTG at 16 °C

Lane 8: Induction with 1 mM IPTG at 30 °C

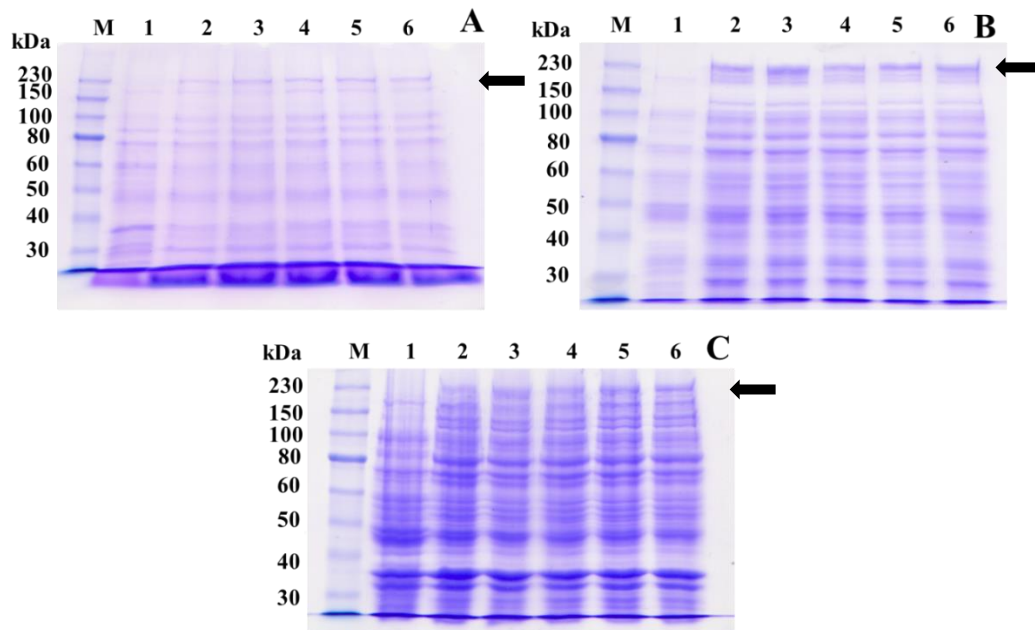


Figure 17 SDS-PAGE analysis of optimisation of WTALT production in *E. coli* BL21 (DE3) at 16 °C under various concentrations of IPTG induction; (A) extracellular fraction (B) intracellular fraction and (C) insoluble fraction. Arrows showed bands of WTALT.

Lane M: Molecular weight protein marker

Lane 1: Non-induction

Lane 2: Induction with 0.2 mM IPTG

Lane 3: Induction with 0.4 mM IPTG

Lane 4: Induction with 0.6 mM IPTG

Lane 5: Induction with 0.8 mM IPTG

Lane 6: Induction with 1 mM IPTG

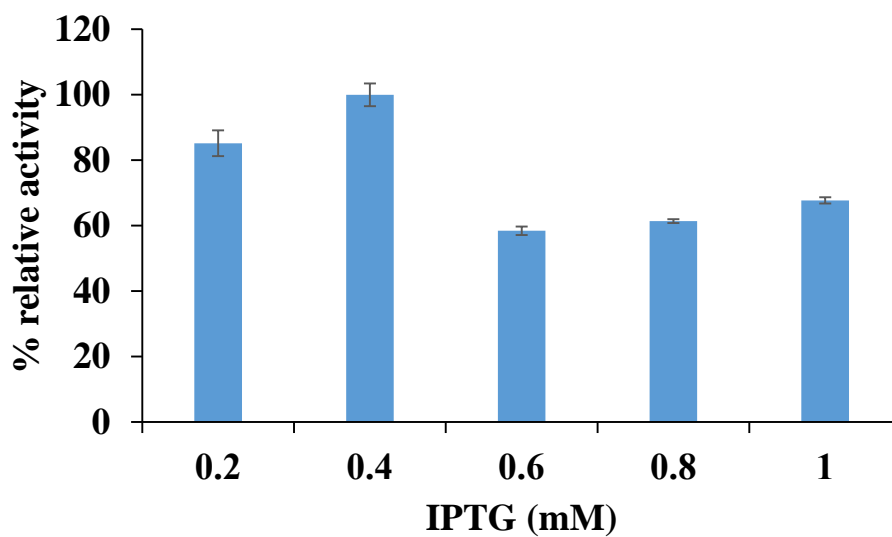


Figure 18 The effect of IPTG concentration on WTALT activity analysed by DNS assay. The WTalt expression was induced by various concentration of IPTG at 16 °C with shaking at 250 rpm for overnight.

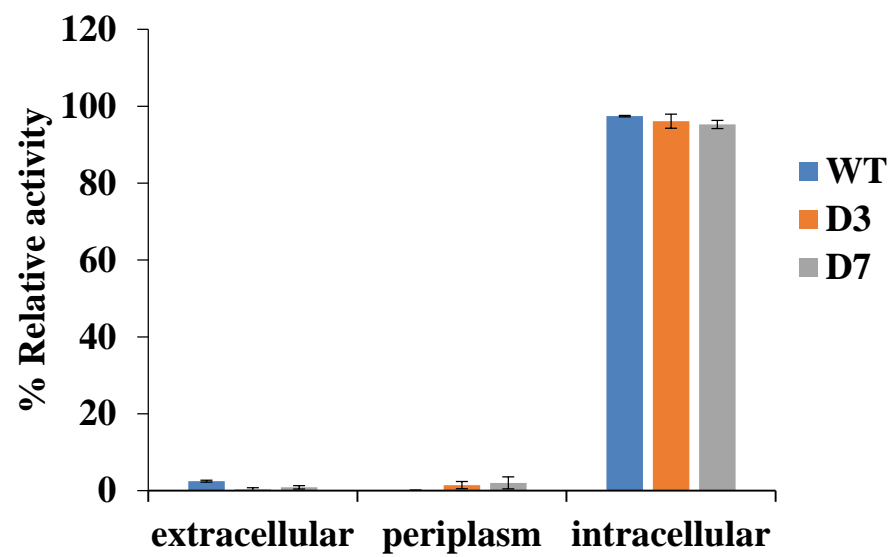


Figure 19 Determination of enzyme activity in different fractions; extracellular, periplasmic and intracellular enzymes of WTALT, $\Delta 3$ SHALT and $\Delta 7$ SHALT, assayed by DNS method.

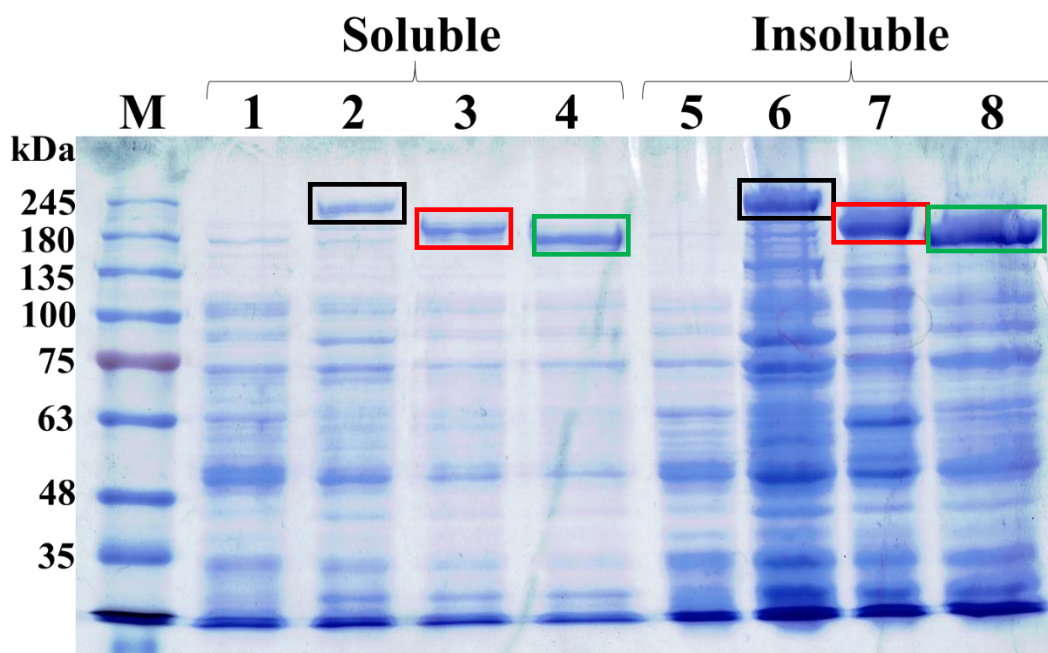


Figure 20 SDS-PAGE analysis of production of WTALT, $\Delta 3$ SHALT and $\Delta 7$ SHALT in soluble and insoluble fractions of *E. coli* BL21 (DE3) under induction with 0.4 mM IPTG at 16 °C for overnight. Each lane was loaded 6 μ g of protein. The proteins of interest were shown in the boxes.

Lane M: Molecular weight protein marker

Lane 1: Soluble proteins uninduced *E. coli* BL21DE(3)

Lane 2: Soluble proteins of WTALT

Lane 3: Soluble proteins of $\Delta 3$ SHALT

Lane 4: Soluble proteins of $\Delta 7$ SHALT

Lane 5: Insoluble proteins uninduced *E. coli* BL21DE(3)

Lane 6: Insoluble proteins of WTALT

Lane 7: Insoluble proteins of $\Delta 3$ SHALT

Lane 8: Insoluble proteins of $\Delta 7$ SHALT

Then, all three proteins were purified by 2 column chromatographies; DEAE followed by Phenyl column. Firstly, WTALT, Δ 3SHALT and Δ 7SHALT were applied onto Toyopearl[®] DEAE-650M column and their enzyme activities were totally found in unbound fractions. Then, the pooled activity fractions of WTALT was subsequently loaded onto Toyopearl[®] Phenyl-650M. The activity fractions were eluted with approximately 265 mM of ammonium sulfate. On the other hand, activity of Δ 3SHALT and Δ 7SHALT were found in flow-through even though the condition similar to that of WTALT was performed. Finally, the proteins with activity fraction were subsequent to buffer exchange by 100 kDa cutoff ultrafiltration. After purification, the purified proteins were primarily analysed on SDS gel which showed a single band of each protein as shown in lane 1, 2 and 3 of WTALT, Δ 3SHALT and Δ 7SHALT, respectively (Fig. 21), and their specific activities were present in Table 4-6.

WTALT, Δ 3SHALT and Δ 7SHALT were run on affinity electrophoresis mixed with various dextran concentration. The trend of all bands were moved shorter when the concentrations of dextran were increased. Furthermore, the Δ 3SHALT and Δ 7SHALT were obviously doublet bands on the gels (Fig. 22). The dextran concentrations were plotted against $1/R_f$ were compared dextran binding ability. The WTALT were apparently exhibited higher binding ability than Δ 3SHALT and Δ 7SHALT, while Δ 3SHALT was slightly higher than Δ 7SHALT as shown in Fig. 23.

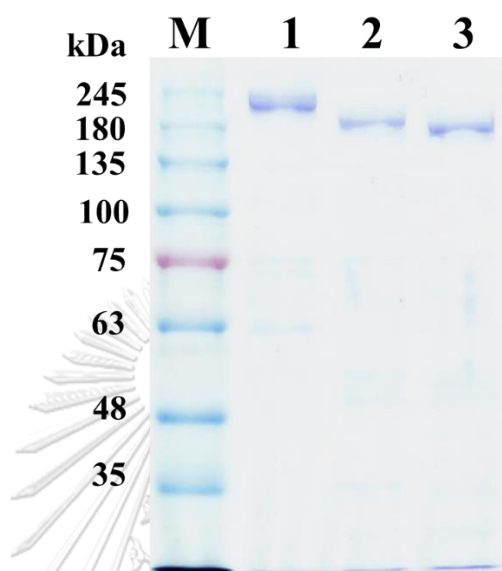


Figure 21 SDS-PAGE analysis of the purified WTALT, Δ 3SHALT and Δ 7SHALT after purification by Toyopearl[®] DEAE and Phenyl-650M columns.

Lane M: Molecular weight protein marker

Lane 1: WTALT

Lane 2: Δ 3SHALT

Lane 3: Δ 7SHALT

Table 4 Purification table of WTALT

Fraction	Protein (mg/mL)	Activity (U/mL)	Volume (mL)	Total activity(U)	Specific activity (U/mg)	% Yield	Purity fold
Crude	0.52	3.70	60	222	7.16	100	1.0
DEAE	0.28	2.66	77	204	9.55	92	1.3
Phenyl	0.03	0.94	108	101	34.9	46	4.8

Table 5 Purification table of Δ 3SHALT

Fraction	Protein (mg/mL)	Activity (U/mL)	Volume (mL)	Total activity(U)	Specific activity (U/mg)	% Yield	Purity fold
Crude	0.53	3.06	122	373.3	5.76	100	1.0
DEAE	0.33	2.50	142	355	7.65	95	1.3
Phenyl	0.15	1.34	110	144	8.97	39	1.5

Table 6 Purification table of Δ 7SHALT

Fraction	Protein (mg/mL)	Activity (U/mL)	Volume (mL)	Total activity(U)	Specific activity (U/mg)	% Yield	Purity fold
Crude	0.50	7.09	62	439	14.11	100	1.0
DEAE	0.29	4.72	89	420	16.43	95	1.1
Phenyl	0.10	2.05	126	258	19.75	59	1.4

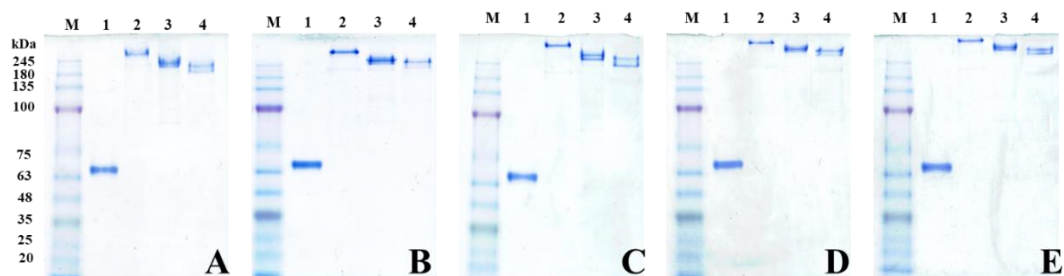


Figure 22 Affinity analysis of WTALT, Δ 3SHALT and Δ 7SHALT proteins on nondenaturing-PAGE. WTALT, Δ 3SHALT and Δ 7SHALT were run on native gel containing 0, 0.25, 0.5, 0.75 and 1% (w/v) dextran (panel A - E, respectively) at 4 °C using 15 mA/gel.

Lane M: Molecular weight protein marker

Lane 1: std. BSA protein

Lane 2: WTALT

Lane 3: Δ 3SHALT

Lane 4: Δ 7SHALT

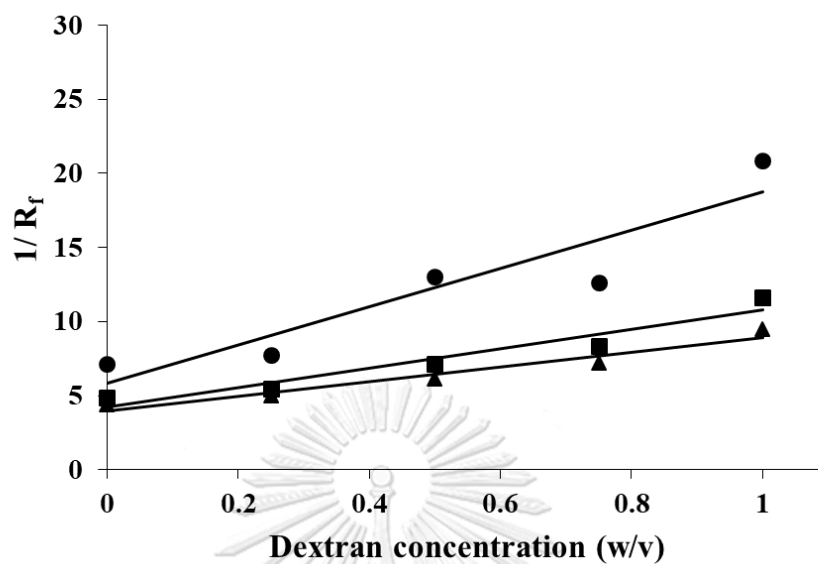


Figure 23 Relative mobility of WTALT, $\Delta 3$ SHALT and $\Delta 7$ SHALT proteins on native gel. The dextran concentrations were plotted against $1/R_f$ values of WTALT (●), $\Delta 3$ SHALT (■) and $\Delta 7$ SHALT (▲).

3.3 Characterisation of WTALT, Δ 3SHALT and Δ 7SHALT

The optimum pHs of these enzymes were in range of weak acidic to neutral pHs. The maximum activity of WTALT was at pH 5.0 whereas Δ 3SHALT and Δ 7SHALT showed the highest activity at pH 4.0. The optimum temperatures of these three enzymes present as narrow bell-like shape graph with the maximum activity at 40 °C. Interestingly, at 37 °C, Δ 3SHALT also showed 100 % of activity, while activities of WTALT and Δ 7SHALT were dramatically decreased approximately 70 % and 40 %, respectively (Fig. 24). In addition, effect of metal ions and detergent on activities of WTALT, Δ 3SHALT and Δ 7SHALT were slightly similar. The Mn^{2+} could obviously promote their activities, while Cu^{2+} and Fe^{3+} were strong inhibitors (Fig. 25). However, activity of Δ 3SHALT was apparently less affected by all metal ions compared to those of WTALT and Δ 7SHALT, whereas Δ 7SHALT's was the most affected enzyme compared to the others. Hence, Δ 3SHALT obviously showed the highest positively response to metal ions and detergent and was greater than WTALT and Δ 7SHALT, respectively.

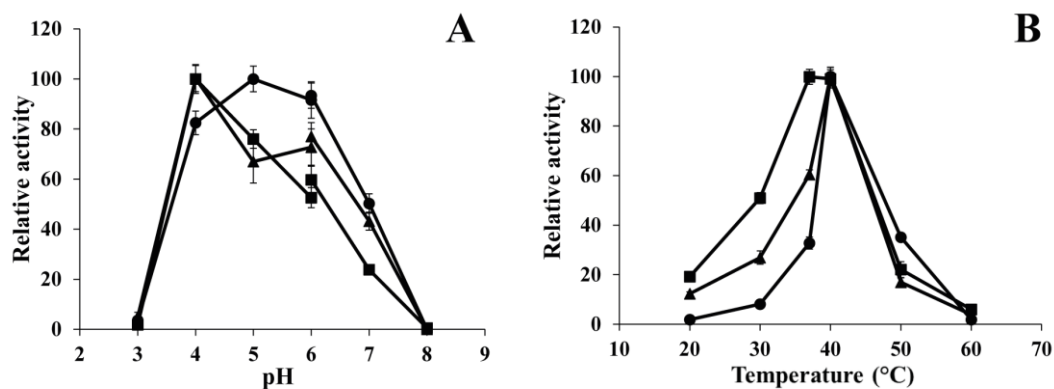


Figure 24 Optimum pH (A) and optimum temperature (B) of WTALT (●), Δ3SHALT (■) and Δ7SHALT (▲).

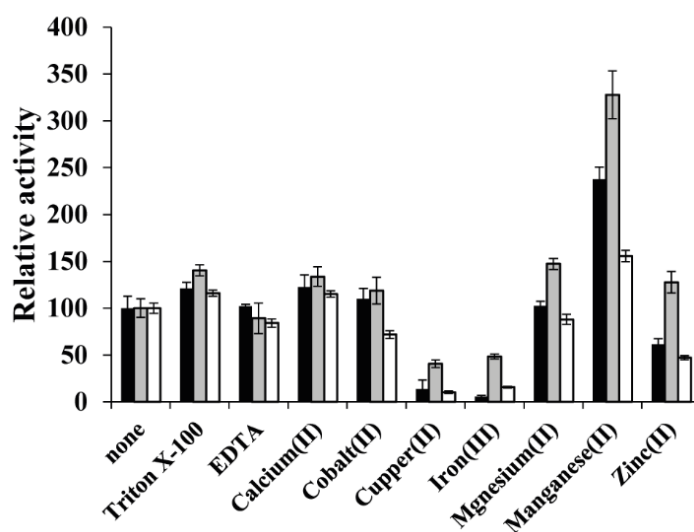


Figure 25 Effect of metal ions and detergent on enzyme activities of WTALT, Δ3SHALT and Δ7SHALT. The black bar represent WTALT, whereas Δ3SHALT and Δ7SHALT were shown in grey and white, respectively.

Moreover, the pH stability of ALTs were also observed. After incubation of ALTs at different pHs at 30 °C for 2 hr, they showed the highest activity at pH 6 (Fig. 26A). Nonetheless, for longer incubation period at 30 °C (pH 6), almost 100 % of activity of WTALT still remained within 6 hr but sharply decreased after then completely lost at 24 hr. While, $\Delta 3$ SHALT and $\Delta 7$ SHALT activity were immediately dropped around 20 % after an hour of incubation time, and then gradually dropped further around 10-20 % within 12 hr. After that, their total activity were nearly disappeared at 24 hr (Fig. 26B). However, investigation of enzyme stability at optimum temperature (40 °C) and pH (pH 5.0 for WTALT and 4.0 for both Δ SHALTs) resulted in complete lost of their activities within 15 min (data not shown). Thus, enzyme stability observed at 37 °C was performed instead. Under this condition, activities of $\Delta 3$ SHALT and $\Delta 7$ SHALT were quickly lost within 2 hr whereas around 60 % of WTALT activity remained (Fig. 26C). Interestingly, when these ALTs were stored in 25 mM citrate buffer pH 6.2 at 4 °C, they could definitely retain their activities for at least 30 days (Fig. 26D).

On the other hand, the kinetic study of WTALT only showed the transglycosylation activity without free glucose detected under glucose oxidase assay, while $\Delta 3$ SHALT's and $\Delta 7$ SHALT's showed transglycosylation activity with slightly low level of detectable hydrolysis. The K_m , k_{cat} and k_{cat}/K_m values of WTALT, $\Delta 3$ SHALT and $\Delta 7$ SHALT were shown in Table 7.

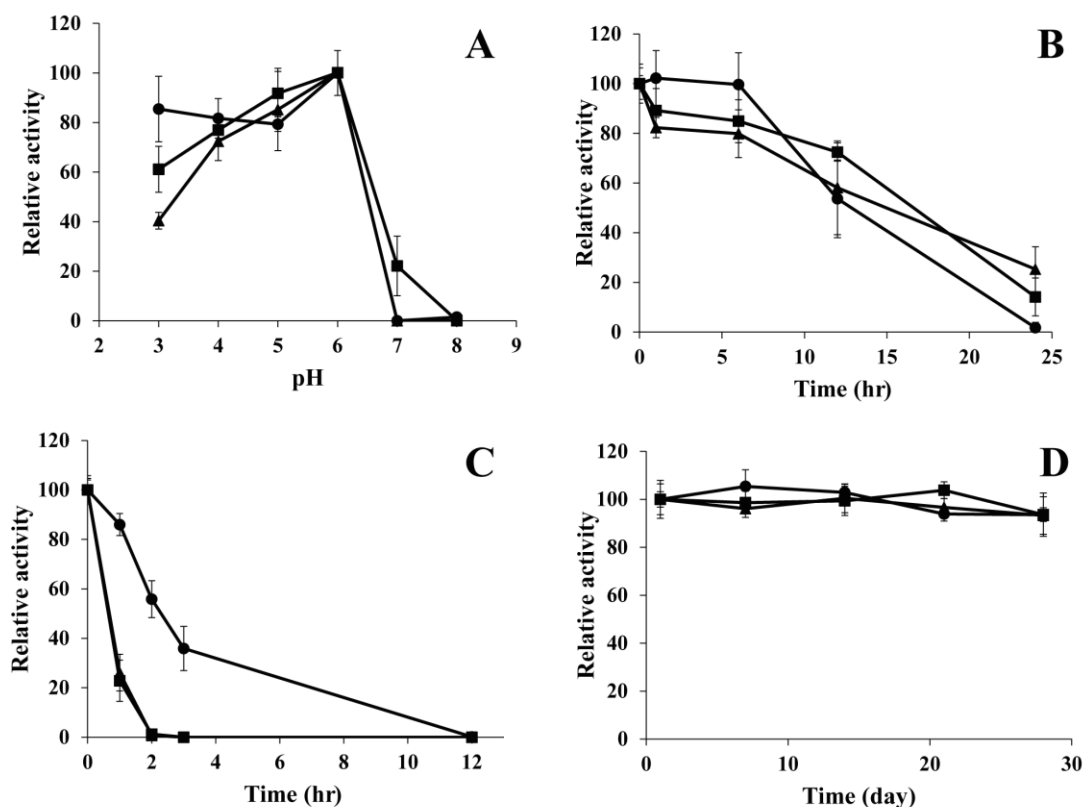


Figure 26 Determination of enzyme stability of WTALT, $\Delta 3$ SHALT and $\Delta 7$ SHALT in various conditions; (A) pH stability at 30 °C for 2 hr, (B) stability at pH 6, 30 °C for 0-24 hr, (C) stability in optimum pH at 37 °C for 0-12 hr, and (D) storage stability at pH 6.2, 4 °C for 0-30 d. (●), (■) and (▲) represent WTALT, $\Delta 3$ SHALT and $\Delta 7$ SHALT, respectively.

Table 7 The kinetic parameters of WTALT, $\Delta 3$ SHALT and $\Delta 7$ SHALT

Enzyme	Transglycosylation			Hydrolysis		
	K_m (mM)	k_{cat} (s ⁻¹)	k_{cat}/K_m (s ⁻¹ mM ⁻¹)	K_m (mM)	k_{cat} (s ⁻¹)	k_{cat}/K_m (s ⁻¹ mM ⁻¹)
WTALT	32.2 ± 3.2	290 ± 12	8.97	N/D	N/D	N/D
$\Delta 3$ SHALT	15.4 ± 1.1	59.0 ± 1.4	3.83	10.2 ± 2.3	2.9 ± 0.2	0.29
$\Delta 7$ SHALT	18.8 ± 2.0	110 ± 4.2	5.85	12.4 ± 2.0	8.54 ± 0.7	0.69

*N/D = not detectable

3.4 Product characterisation

3.4.1 Oligosaccharide characterisation

According to oligosaccharide production of WTALT, Δ 3SHALT and Δ 7SHALT, overall pattern of their products was not significantly different. However, the amount of oligosaccharides produced by Δ 3SHALT and Δ 7SHALT were significantly higher than that of WTALT as analysed by HPAEC-PAD (Fig. 27). After that, oligosaccharides produced by WTALT was chosen as a representative for characterisation. The WTALT oligosaccharides were analysed by GPC and DP2 to DP8 were observed as shown in Fig. 28. In addition, these DP2-8 harboured only glucose residues as confirmed by complete hydrolysis (Fig. 29) and also showed reducing property judged by DNS assay. Obviously, at least 3 isomers with identical mass of each DP were detected by HPAEC-PAD and MALDI-TOF MS (Fig. 30 and 31, respectively). Interestingly, we found that WTALT was able to hydrolyse its oligosaccharide products as confirmed by HPAEC-PAD and MALDI-TOF MS (Fig. 32 and 33, respectively).

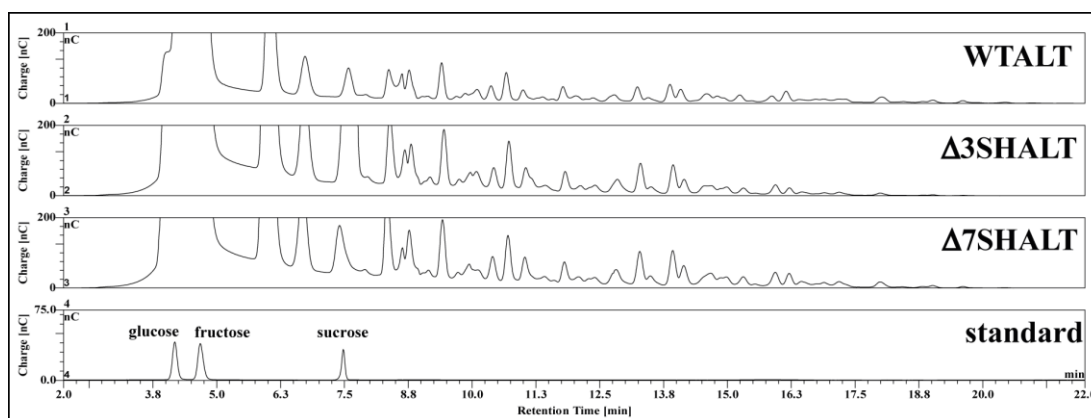


Figure 27 Comparison oligosaccharide pattern of WTALT, $\Delta 3$ SHALT and $\Delta 7$ SHALT by HPAEC-PAD, the 0.6 U/mL of WTALT, $\Delta 3$ SHALT and $\Delta 7$ SHALT were incubated at 37 °C for overnight in 50 mM sodium citrate buffer at optimum pH of each enzyme using 10 % (w/v) sucrose as substrate.

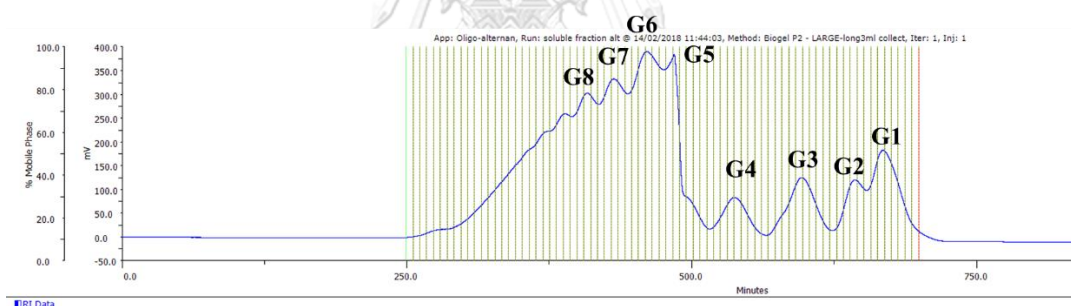


Figure 28 Separation of oligosaccharides by GPC, the overnight WTALT reaction were precipitated with acetone, the soluble phase was evaporated and dissolved in DI water before separating by GPC using Biogel-P2 column.

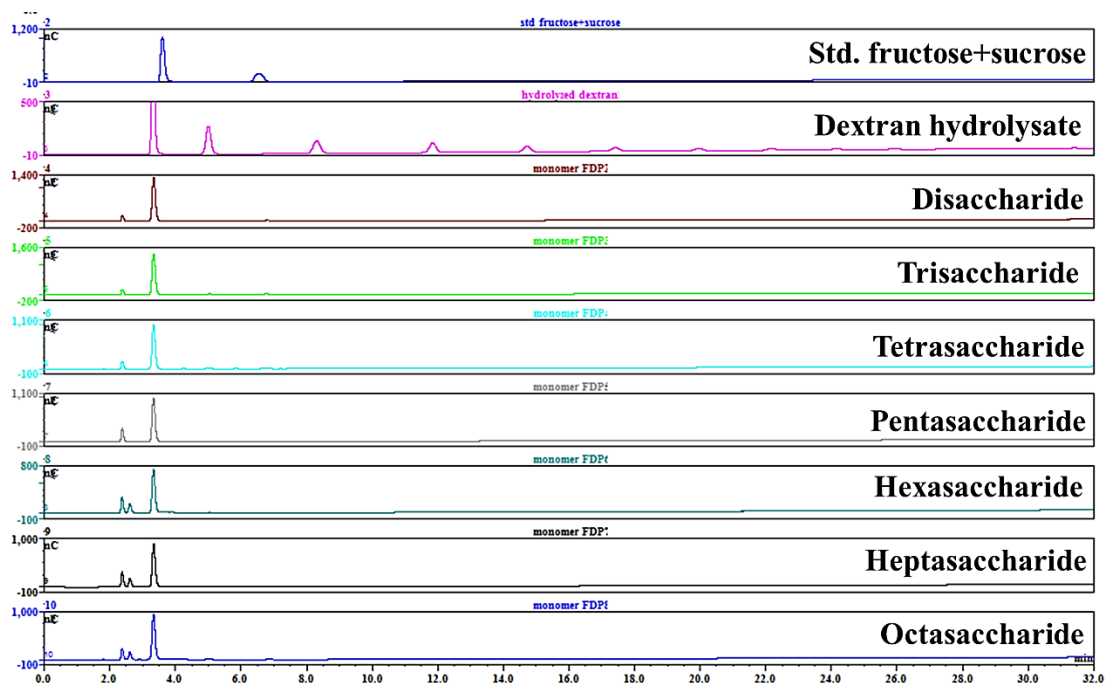


Figure 29 Complete hydrolysis of WTALT oligosaccharides, the each size of WTALT oligosaccharides were hydrolysed in 4 M TFA at 100 °C for 4 hr before analysed by HPAEC-PAD.

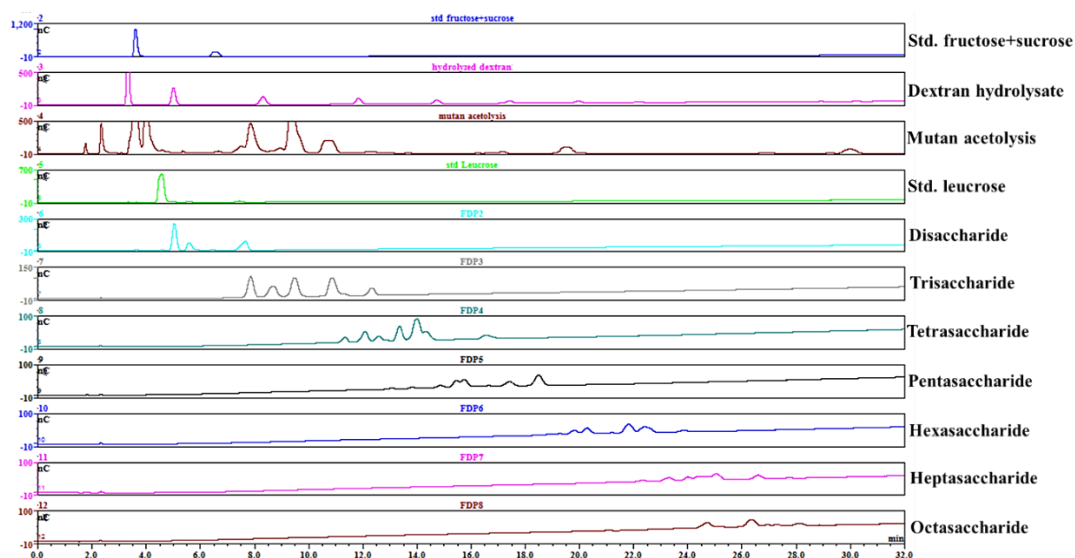


Figure 30 Oligosaccharides (DP2-8) pattern of WTALT, the oligosaccharide DP2- DP8 from WTALT reaction separated by GPC, were analysed by HPAEC-PAD

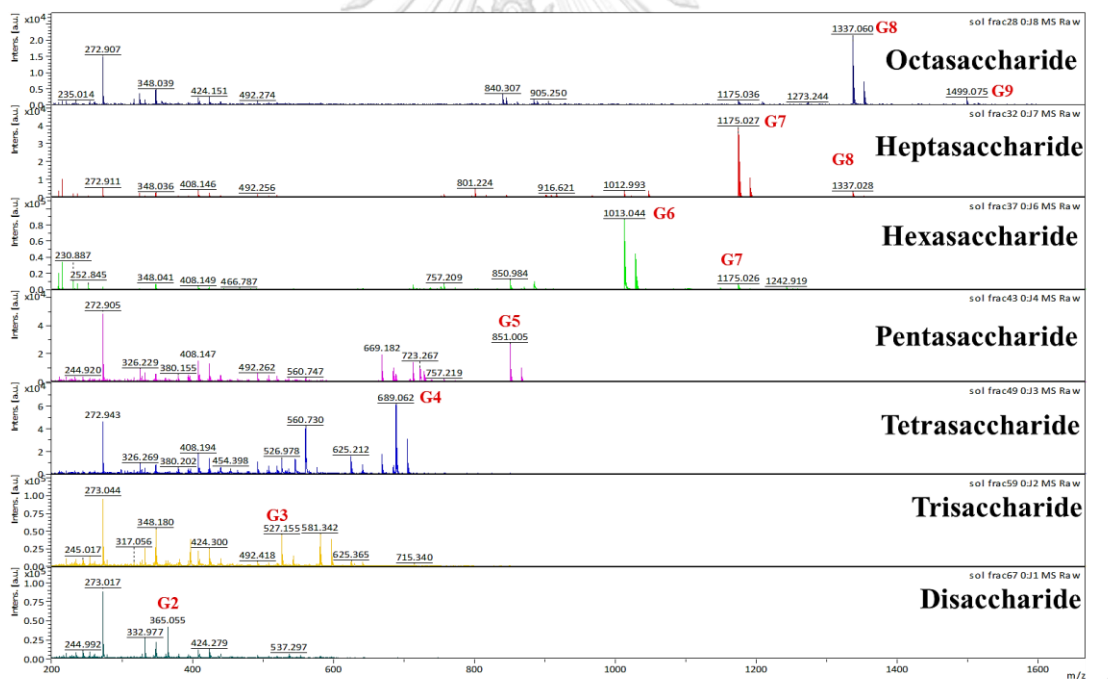


Figure 31 Mass analysis by MALDI-TOF MS, the oligosaccharide from WTALT reaction separated by GPC, fraction No. 28,32,37,43,49,59 and 67, corresponded with masses of oligosaccharide DP8-DP2, respectively.

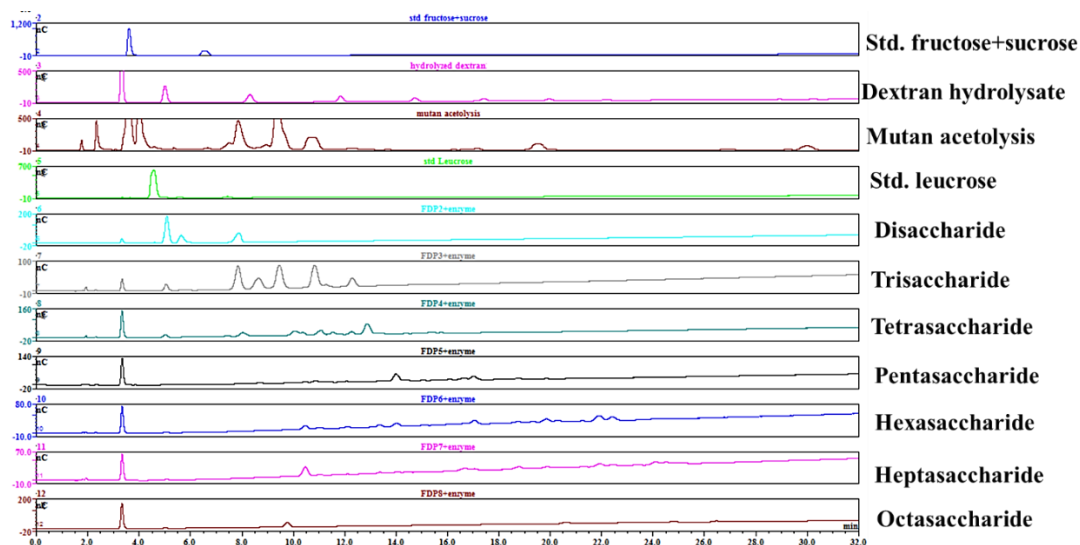


Figure 32 Hydrolysis of WTALT oligosaccharide by WTALT, each size of WTALT oligosaccharides was incubated with 1 U/mL of WTALT in 50 mM citrate buffer pH 4 at 37 °C for overnight. The results were analysed by HPAEC-PAD.

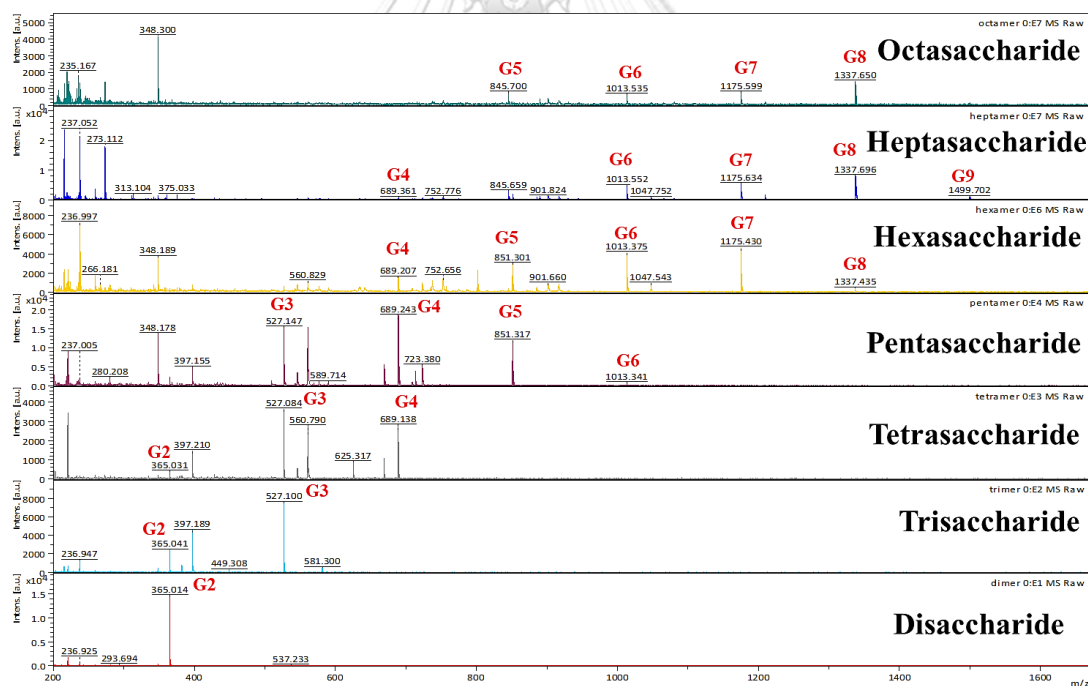
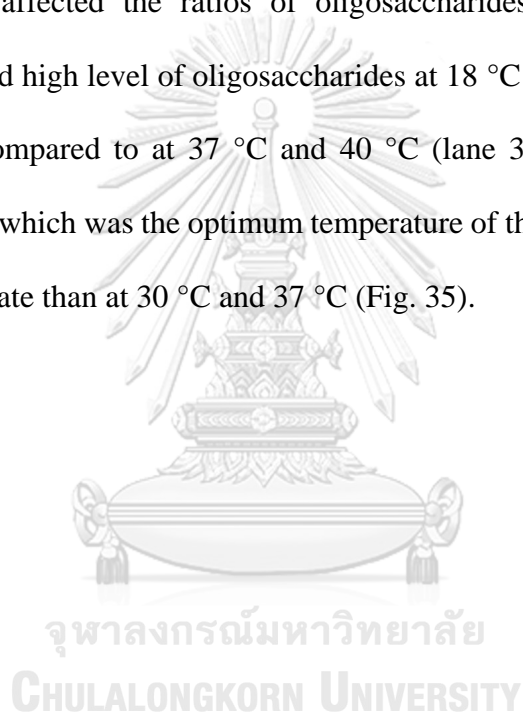


Figure 33 Product mass of WTALT oligosaccharide after incubating with WTALT, each size of WTALT oligosaccharides was incubated with 1 U/mL of WTALT in 50 mM citrate buffer pH 4 at 37 °C for overnight. The results were analysed by MALDI-TOF MS.

After that, effect of unit of enzyme on oligosaccharide production was considered by TLC. WTALT could completely converted sucrose substrate to oligosaccharide products with at least 4 units per gram of sucrose (as shown in lane 4, Fig. 34A), while $\Delta 3$ SHALT and $\Delta 7$ SHALT required more than 6 units of enzyme per gram of sucrose substrate (Fig. 34B and 34C, respectively). Noticeably, the more units of enzyme used, the longer oligosaccharide products obtained. Moreover, incubating temperature also affected the ratios of oligosaccharides (Fig. 35). All enzymes obviously produced high level of oligosaccharides at 18 °C and 30 °C (lane 1 and 2 of Fig. 35A-35C), compared to at 37 °C and 40 °C (lane 3 and 4 of Fig. 35A-35C). Notably, at 40 °C, which was the optimum temperature of these ALTs, they used much less sucrose substrate than at 30 °C and 37 °C (Fig. 35).



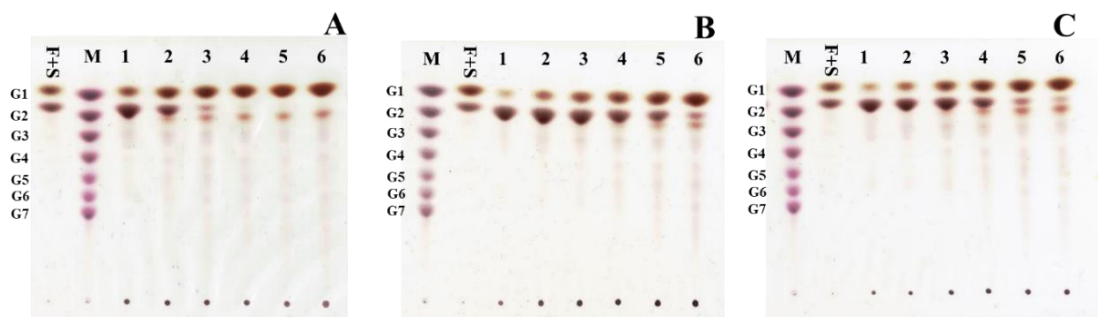


Figure 34 Effect of enzyme on product formation, A) WTALT, B) $\Delta 3$ SHALT and C) $\Delta 7$ SHALT, The various unit of enzyme were incubated with 10 % (w/v) sucrose in 50 mM citrate buffer at optimum pH, 37 °C for overnight. Then, the products pattern were investigated by TLC.

Lane F+S: std. fructose and sucrose

Lane M: std. maltooligosaccharide (G1-G7)

Lane 1: the reaction incubated with 1 unit/g of substrate

Lane 2: the reaction incubated with 2 unit/g of substrate

Lane 3: the reaction incubated with 3 unit/g of substrate

Lane 4: the reaction incubated with 4 unit/g of substrate

Lane 5: the reaction incubated with 5 unit/g of substrate

Lane 6: the reaction incubated with 6 unit/g of substrate

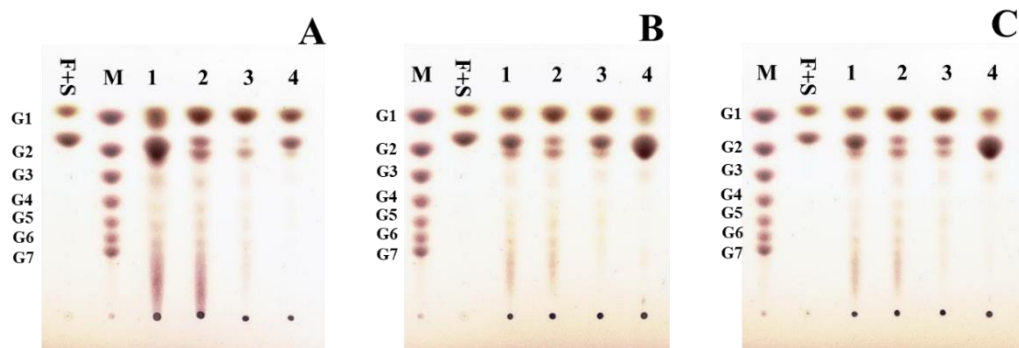


Figure 35 Effect of temperature on product formation, A) WTALT, B) Δ 3SHALT and C) Δ 7SHALT, 5 U of enzymes were incubated with 10 % (w/v) sucrose in 50 mM citrate buffer at optimum pH for overnight. Then, the products pattern were investigated by TLC.

Lane F+S: std. fructose and sucrose

Lane M: std. maltooligosaccharide (G1-G7)

Lane 1: the reaction incubated at 18 °C

Lane 2: the reaction incubated at 30 °C

Lane 3: the reaction incubated at 37 °C

Lane 4: the reaction incubated at 40 °C

3.4.2 Polymer characterisation

3.4.2.1 NMR analysis

^1H and ^{13}C NMR spectra of polymers produced by WTALT, $\Delta 3\text{SHALT}$ and $\Delta 7\text{SHALT}$ were analysed. ^1H NMR spectrum was analysed at 400 MHz in D_2O (Fig. 36). The anomeric protons of α -1,3 and α -1,6 linkages of WTALT polymer were identified as $\text{H1}'$ at δ 5.36 ppm and H1 at δ 5.01 ppm, respectively. The integration ratio of anomeric proton signals ($\text{H1}':\text{H1}$) was 1:1.54, representing around 1.5-fold higher level of α -1,6 linkage than α -1,3 linkage (Fig. 36A). ^{13}C NMR spectrum was analysed at 100 MHz in D_2O (Fig. 37). Chemical shift at anomeric carbon region contained at least four different types of anomeric carbon. Signals at δ 99.61 and 99.14 ppm corresponded to anomeric carbon $1'$ ($\text{C1}'$) of α -1,3 linkages whereas signals at δ 98.15 and 97.89 ppm corresponded to anomeric carbon 1 (C1) of α -1,6 linkages in WTALT polymer (Fig. 37A). Furthermore, ^1H and ^{13}C NMR spectra of $\Delta 3\text{SHALT}$ and $\Delta 7\text{SHALT}$ polymers were similar to those of WTALT polymer (Fig. 36B and C, and Fig. 37B and C, respectively).

After that, assignment of proton and carbon residues of WTALT polymer was further confirmed by 2D NMR experiments; COSY, multiplicity-edited HSQC and HMBC. Both H1 and $\text{H1}'$ were confirmed by COSY spectrum (Fig. 38). Anomeric proton H1 showed two strong coupling signals with H2 at δ 3.68 and 3.58 ppm.

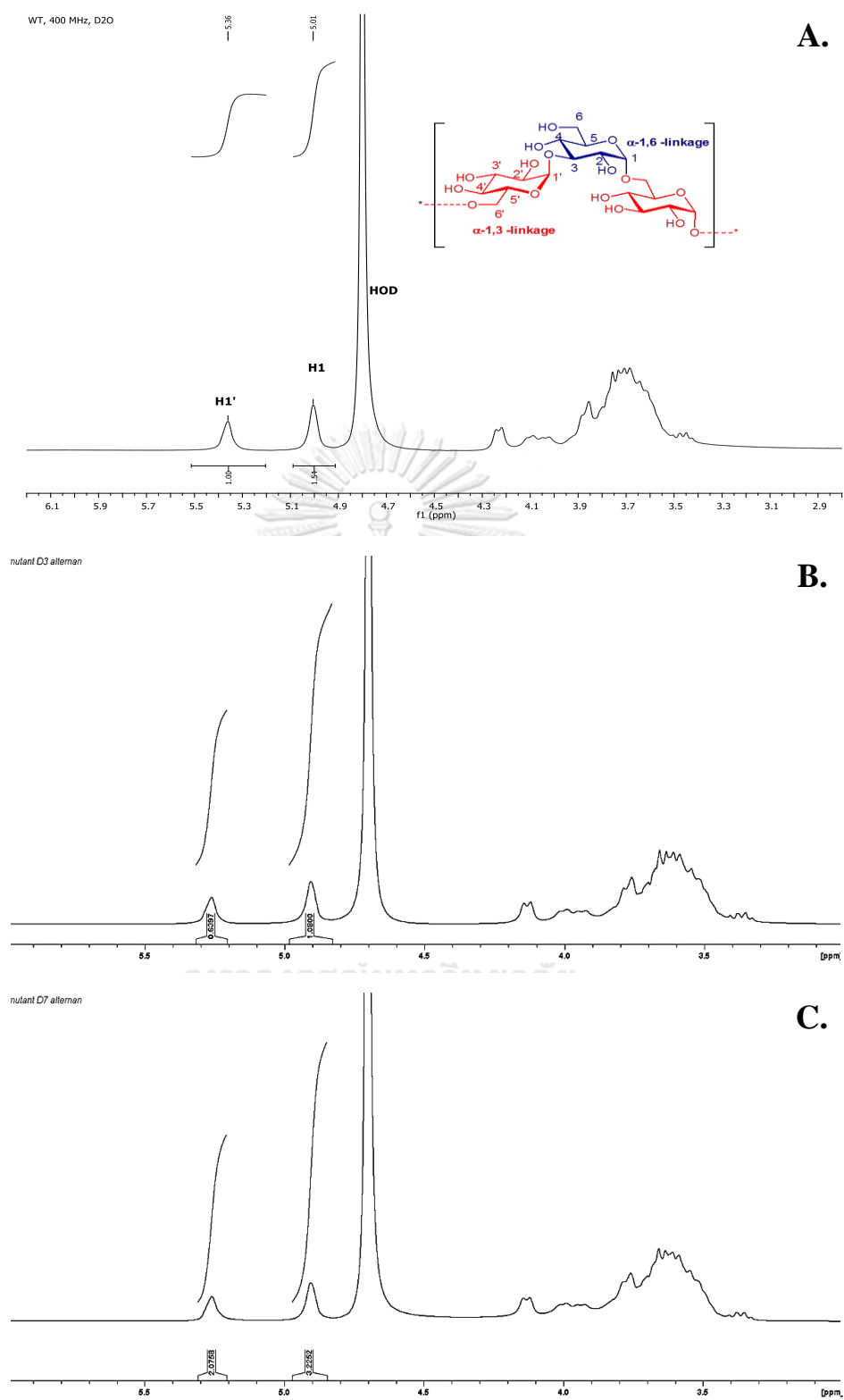


Figure 36 ^1H NMR spectrum of polymeric products obtained from (A) WTALTA (B) $\Delta 3\text{SHALTA}$ and (C) $\Delta 7\text{SHALTA}$ (400 MHz, D₂O)

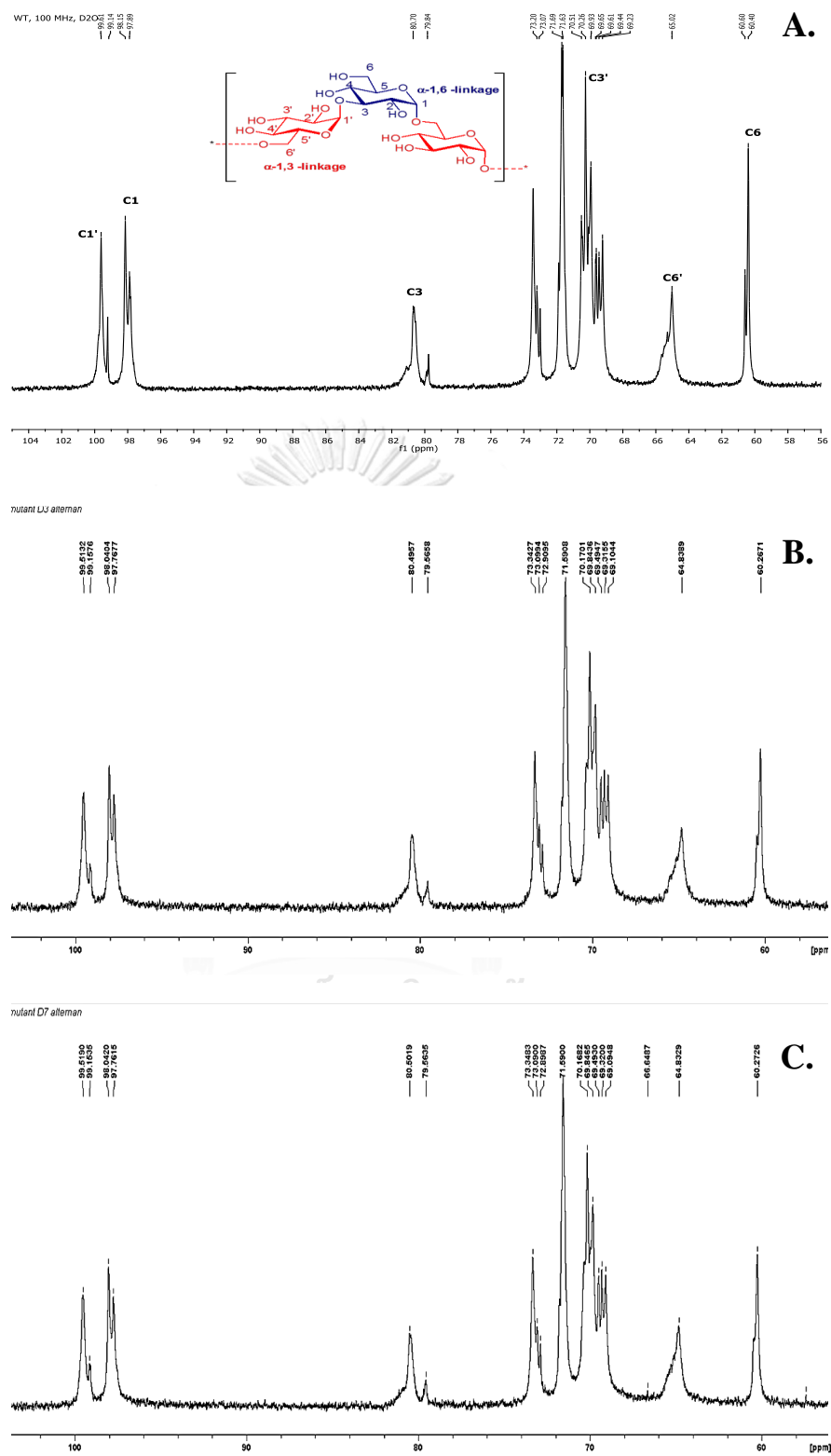


Figure 37 ^{13}C NMR spectrums of (A) WTALT, (B) $\Delta 3\text{SHALT}$ and (C) $\Delta 7\text{SHALT}$ polymers (100 MHz, D₂O)

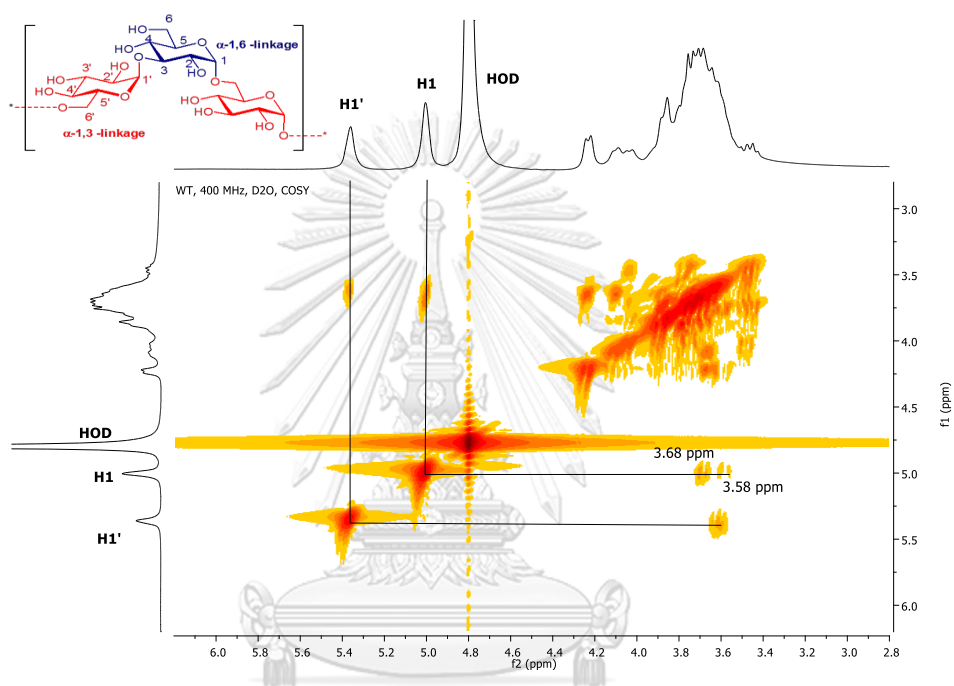


Figure 38 COSY spectrum of WTALT polymer (400 MHz, D₂O)

To understand insight into the chemical structure of WTALT polymer, ^1H and COSY experiments were performed in DMSO- d_6 containing small amount of a strong acid, trifluoroacetic acid (TFA), instead of D_2O ⁷⁹. Fortunately, H1 anomeric proton region (δ 4.88 – 4.60 ppm) analysed by ^1H NMR clearly showed four separated signals; δ 4.79, 4.76, 4.72, and 4.70 ppm (Fig. 39). Furthermore, COSY spectrum also revealed four strong coupling cross-peaks of four H2 protons (Fig. 40).

Multiplicity-edited HSQC experiment (Fig. 41) provided connectivity between protons and carbons on carbohydrate skeleton. The multiplicity-edited HSQC informed not only the connectivity but also multiplicity of carbon nuclei, due to its nature of phase-sensitive experiment. In this measurement set-up, the presence of CH_2 moieties appeared in blue cross-peaks while CH and CH_3 moieties were in red cross-peaks. Thus structural information of WTALT polymer was extracted and identified as $\text{C1}'$ (δ 99.58 ppm), C1 (δ 99.08 ppm), C3 (δ 80.39 ppm), $\text{C3}'$ (δ 70.47 ppm), $\text{C6}'$ (δ 65.21 ppm), and C6 (δ 60.49 ppm) for carbon skeleton. Proton nucleus were elucidated as $\text{H1}'$ (δ 5.36 ppm), H1 (δ 5.01 ppm), $\text{H3}'$ (δ 4.22 ppm), $\text{H6}'$ (2 protons; δ 4.07, 3.69 ppm), H3 (δ 3.87 ppm), and H6 (δ 3.81 ppm). Additionally, HMBC spectrum (Fig. 42) gave information of long-range connectivity between carbon and proton nucleus. $\text{H1}'$ signal at δ 5.36 ppm showed strong couplings with $\text{C3}'$ (δ 70.47 ppm) and interlinkage coupling with C3 (δ 80.39 ppm). For another glucose residue, H1 signal at δ 5.01 ppm also coupled with C3 (δ 80.39 ppm) and interlinkage coupling with $\text{C6}'$ (δ 65.21 ppm), thus it confirmed the previous assignments of the 1,3- and 1,6-linkages. However, several cross-peaks within anomeric proton regions of both $\text{H1}'$ (3 cross-peaks) and H1 (2 cross-peaks) were observed.

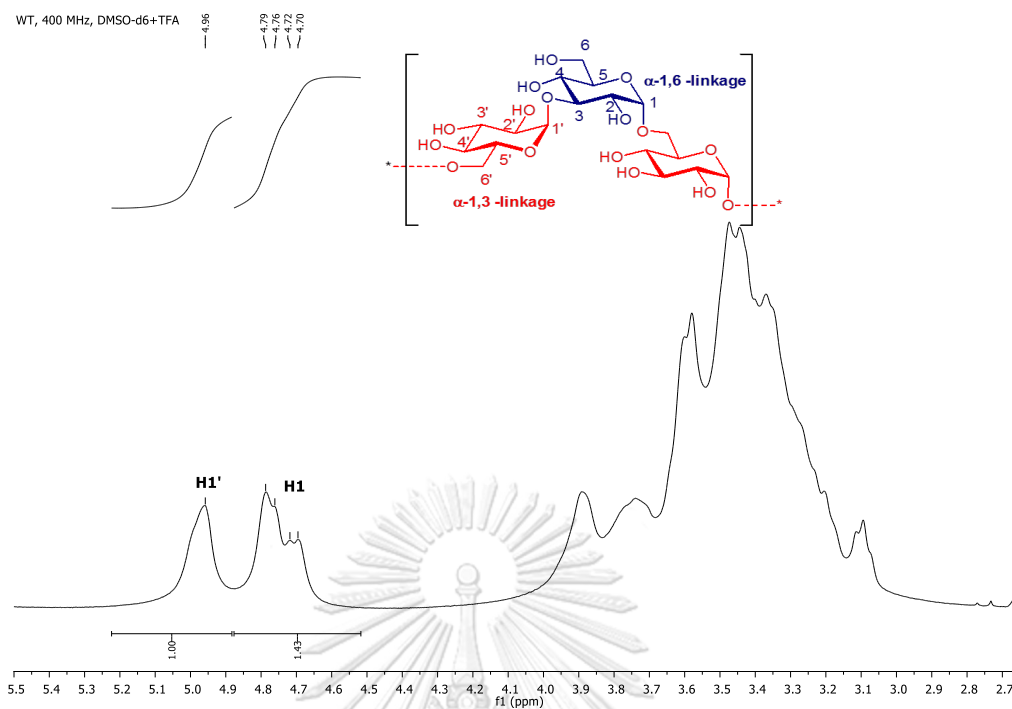


Figure 39 ¹H NMR spectrum of WTALT polymer (400 MHz, DMSO-d₆+TFA)

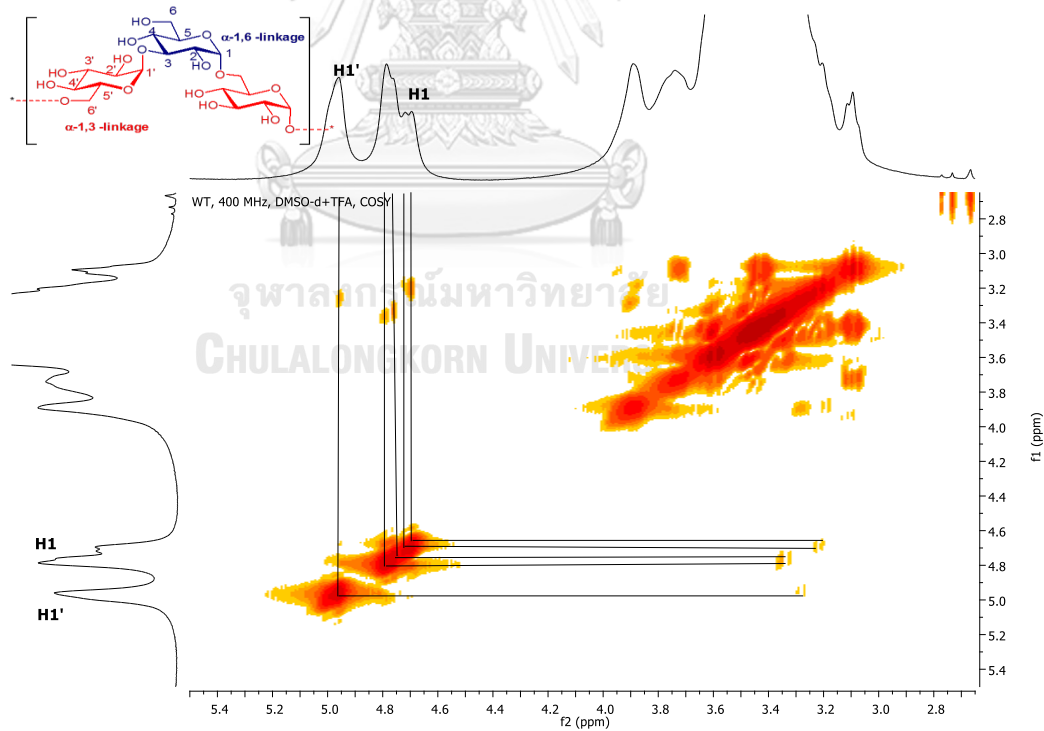


Figure 40 COSY spectrum of WTALT polymer (400 MHz, DMSO-d₆+TFA)

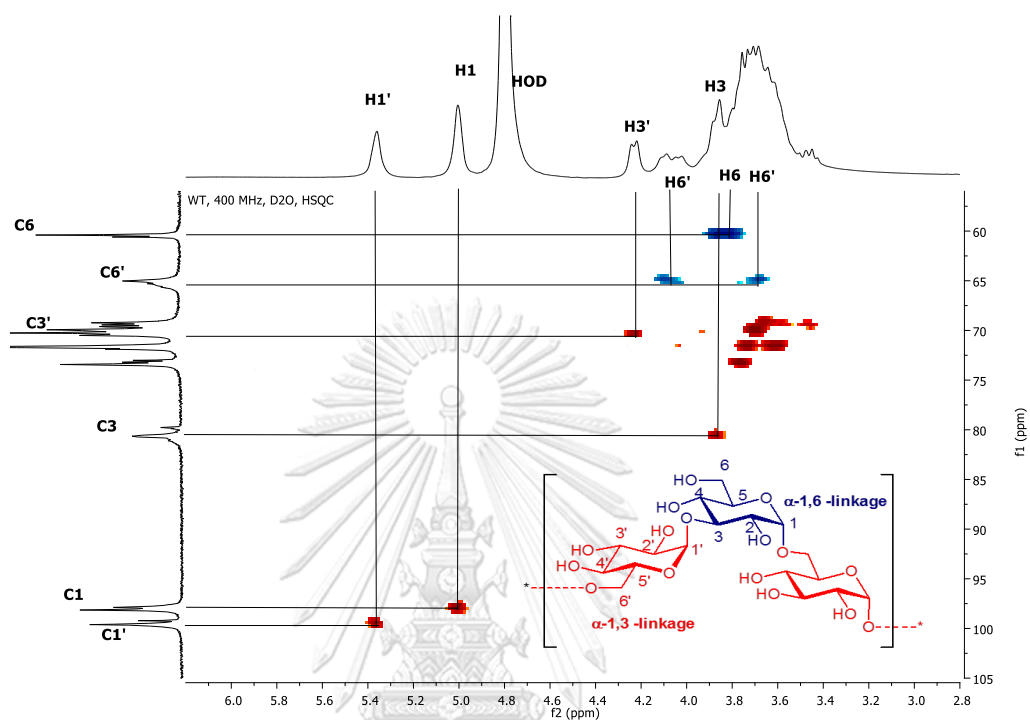


Figure 41 Multiplicity-edited HSQC spectrum of WTALT polymer (400 MHz, D₂O).

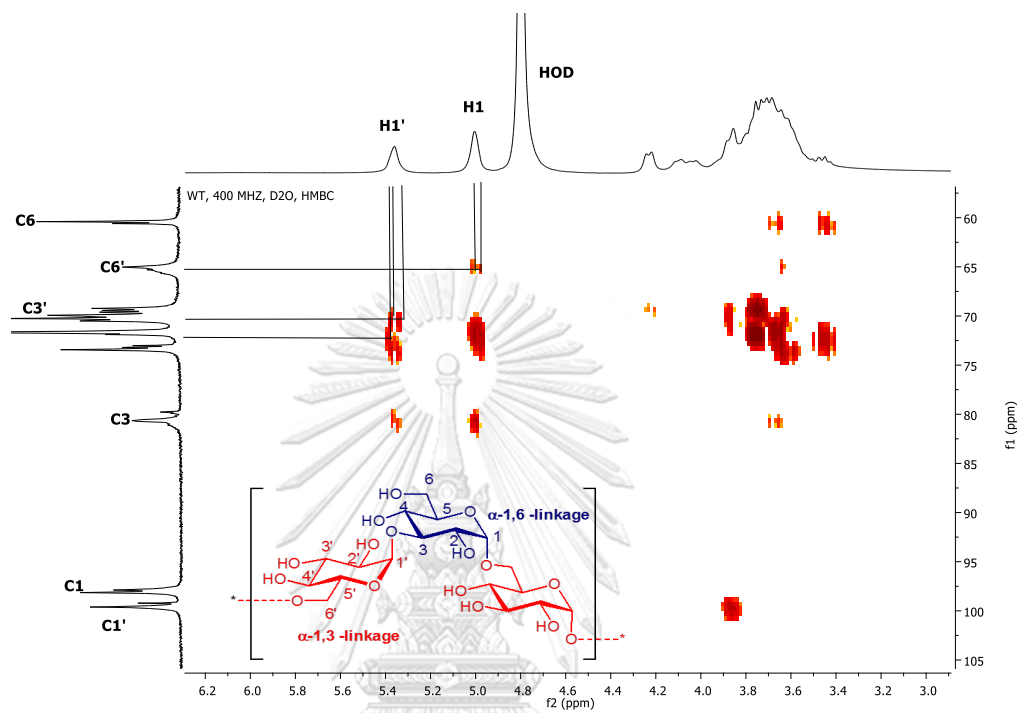


Figure 42 HMBC spectrum of WTALT polymer (400 MHz, D₂O).

3.4.2.2 Linkage analysis by methylation experiment

Since alternan is an insoluble polymer, methylation was performed twice for complete methylation. On the other hand, alternan polymer was also sonicated prior to methylation. The % methylated glucopyranose of polymers of WTALT, WTALT (sonicated form), Δ 3SHALT and Δ 7SHALT were not significantly different and consistent (Table 3.5). In addition to NMR results, C3 and C6 substitution also showed the presence of α -1,3 and α -1,6 linkages in core structure of WTALT polymer. Additionally, the branching structure was also revealed clearer by observation of methylated C3/C6 (Table 8).

3.4.2.3 Polymer analysis by partial hydrolysis

To further investigate the structure of polymer, WTALT polymer were primarily partially hydrolysed by 1 M HCl and then separated by BioGel P-2 column (Fig. 43). The products from BioGel P-2 column, were primarily analysed by TLC (Fig. 44). Each fraction of separated oligosaccharides was then further analysed by MALDI-TOF MS and HPAEC-PAD. Single mass of each fraction was detected (Fig. 45A). However, at least 3 isomers were appeared (Fig. 45B). Interestingly, one of the isomers of tri- to heptasaccharide (G3-G7) was present at the same retention time with dextran hydrolysate (α -1,6 linked) but not mutan hydrolysate (α -1,3 linked) (Fig. 45).

Table 8 Mole percentage of methylated glucoses in hydrolysates of glucans

Glucansucrase source	Glucopyranose methylation (%)					Reference	
	terminal	3- substituted	6- substituted	3,6- substituted	2- substituted		3,4- substituted
WTALT	16	26	47	11	N/A	N/A	This work
WTALT (sonicated polymer)	12	27	50	10	N/A	N/A	This work
Δ3SHALT	14	28	48	10	N/A	N/A	This work
Δ7SHALT	13	27	48	12	N/A	N/A	This work
<i>L. mesenteroides</i> NRRL-B1355	13	35	40	11	N/A	N/A	⁵⁰
<i>L. citreum</i> SK24.002	16	33	41	8	2	N/A	⁸⁰
<i>L. mesenteroides</i> NRRL-B1118	15	44	29	9	N/A	4	⁸¹
<i>L. reuteri</i> 180	12	24	52	12	N/A	N/A	⁴⁹
<i>L. brevis</i> E25	19	19	54	8	N/A	N/A	⁵⁰

*N/A = not available

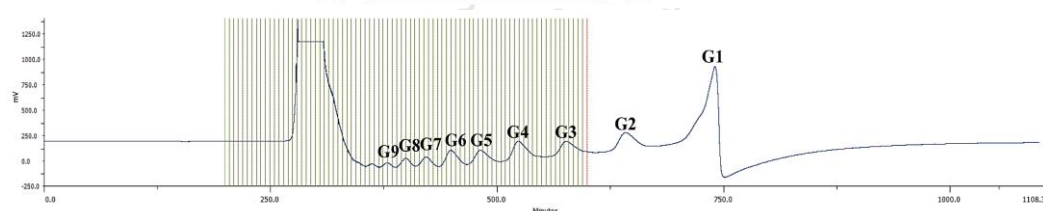


Figure 43 Separation of partially hydrolysed product by size exclusion. The partially hydrolyzed WTALT polymer polymers were separated using BioGel P-2 column at 50 °C, flow rate 0.5 ml/min. Blue line showed signal detected by RI detector. The 2.5-ml fraction size was collected between 200 – 600 min.

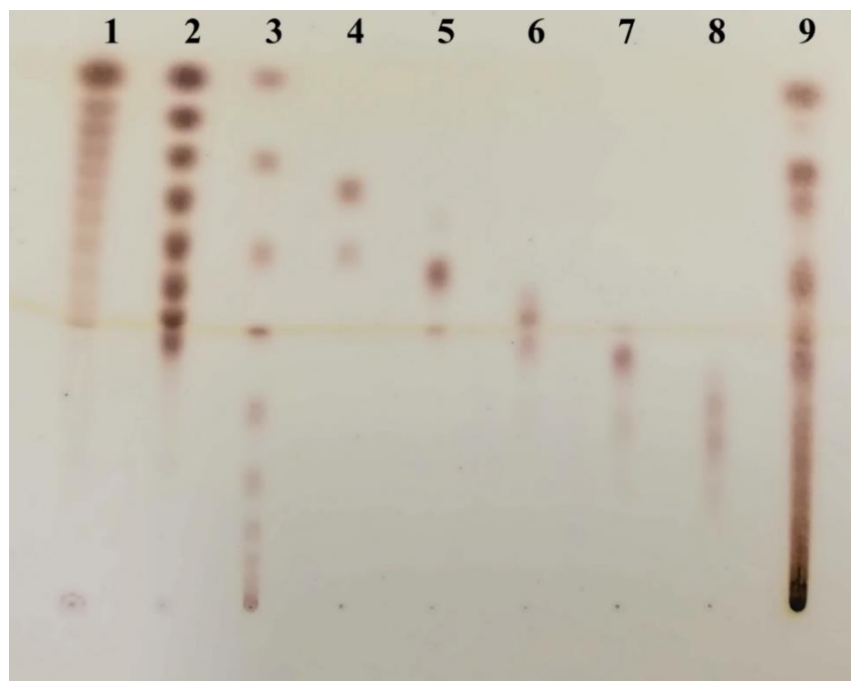


Figure 44 TLC analysis of partially hydrolysed WTALT polymer separated by BioGel P-2 column. Lane 1; partially hydrolysed mutant polymer of *S. sobrinus* MFe28 (obtained from acetolysis), lane 2; std. maltooligosaccharide (G1 - G8), and lane 3; partially hydrolysed dextran polymer of *Leuconostoc* spp. (Sigma). Lane 4 – 8 are products from fraction No. 77, 66, 58, 52 and 46 (G3 – G7, respectively). Lane 9; partially hydrolysed WTALT polymer. The TLC was run for 2 ascents in mobile phase, Acetonitrile:Ethyl acetate:1-propanol:Water (85:20:50:60).

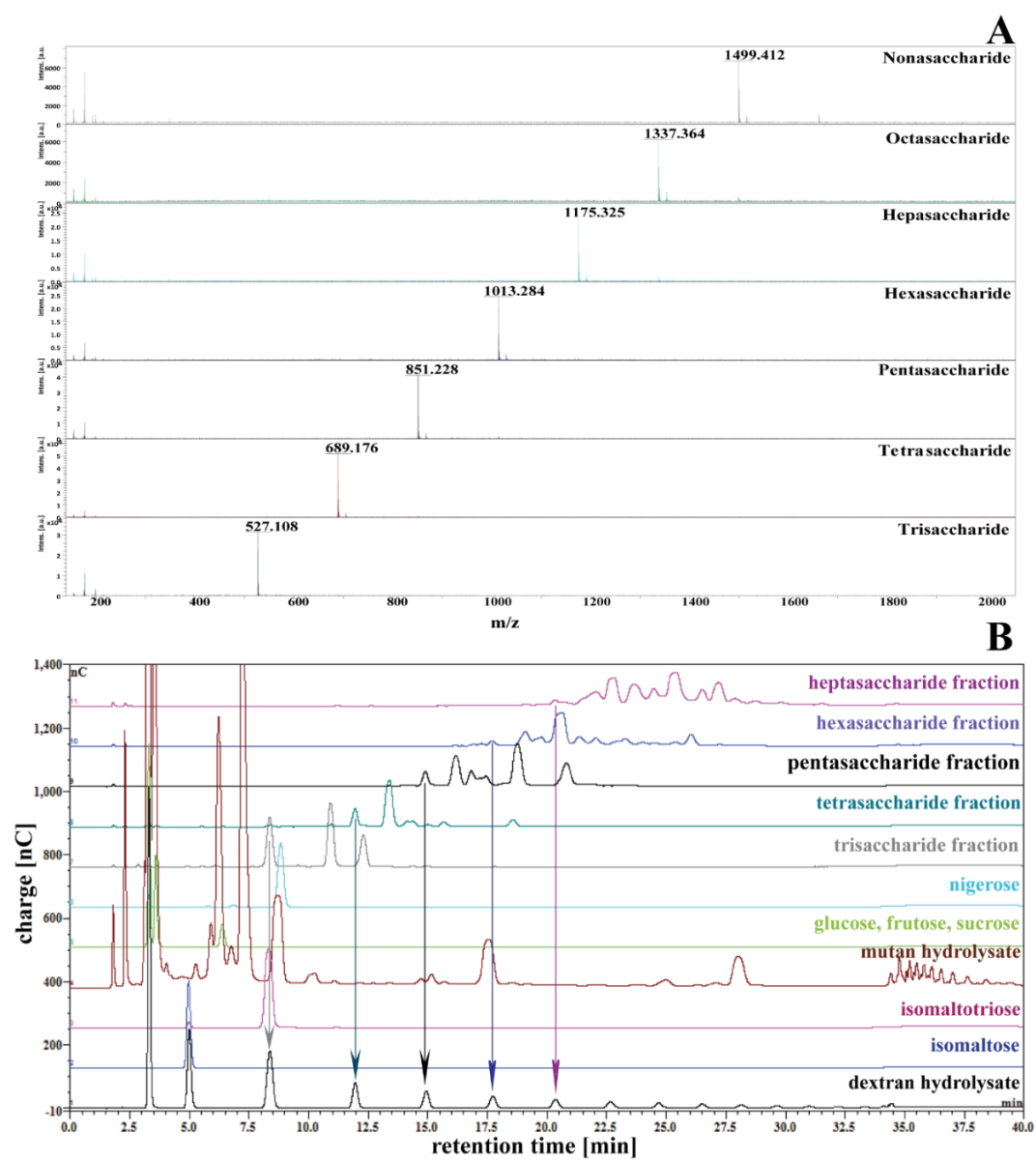


Figure 45 Analysis of partially hydrolysed WTALT polymer. (A) Mass analysis by MALDI-TOF and (B) product pattern analysis by HPAEC-PAD.

3.4.2.4 Solubility of polymer

At low concentration (less than 10 % (w/v)), WTALT, Δ 3SHALT and Δ 7SHALT polymers formed fine colloid particles in water solution. On the contrary, mutan polymer which is mainly linked by α -1,3 linkages was precipitated while dextran (mainly linked by α -1,6 linkages) was completely dissolved (Fig. 46). The size of WTALT colloid particle was 90 nm in average hydrodynamic diameter whereas Δ 3SHALT's and Δ 7SHALT's were 80 nm. Noticeably, sizes of these nanoparticles were unaffected by lyophilisation process (Fig. 47). Obviously, viscosity of these polymers was greatly increased when the concentration was higher than 10 % (w/v). At 15 % (w/v), WTALT and Δ 3SHALT polymers formed gel-like (Fig. 48A and 48B, respectively) with the maximum viscosity value, approximately 10,000 mPa·s (as shown in Fig. 49), that was able to be detected by viscosity meter. Nonetheless, gel-forming property could not be observed in Δ 7SHALT polymer at this concentration although it was present as high viscous solution with 5,650 mPa·s viscosity value (Fig. 49). However, Δ 7SHALT polymer could be transformed into gel-like material when dissolved at 20 % (w/v) (Fig. 48C). Moreover, WTALT polymer could not be dissolved in H₂O at 1 % (w/v) solution (Tube 2, Fig. 50A) but its solubility was partially dissolved in DMSO and in 50 % (w/v) NaOH (Tubes 10 and 13, Fig. 50A). Noticeably, 20 % (w/v) of WTALT polymer in DMSO formed clear gel but opaque gel was present when it was dissolved in water or in 50 % (w/v) NaOH (Tubes 11, 7 and 14, respectively, Fig. 50A). Interestingly, WTALT, Δ 3SHALT and Δ 7SHALT polymers exhibited changeable physical state among nanoparticle, gel-like material and transparent film once the concentration was changed as shown in Fig. 50B. Nevertheless, none of

nanoparticle could be observed in WTALT, $\Delta 3$ SHALT and $\Delta 7$ SHALT polymers under transmission electron microscopy (TEM) (Fig. 51).



Figure 46 Comparison of solubility of three glucan polymers in water. Tube 1; 1% (w/v) of dextran polymer of *Leuconostoc* spp. (Sigma), tube 2; 1% (w/v) of WTALT polymer, and tube 3; 1% (w/v) of insoluble mutan polymer of *S. sorbinus*. The polymers were suspended in water and stood still for 15 min.

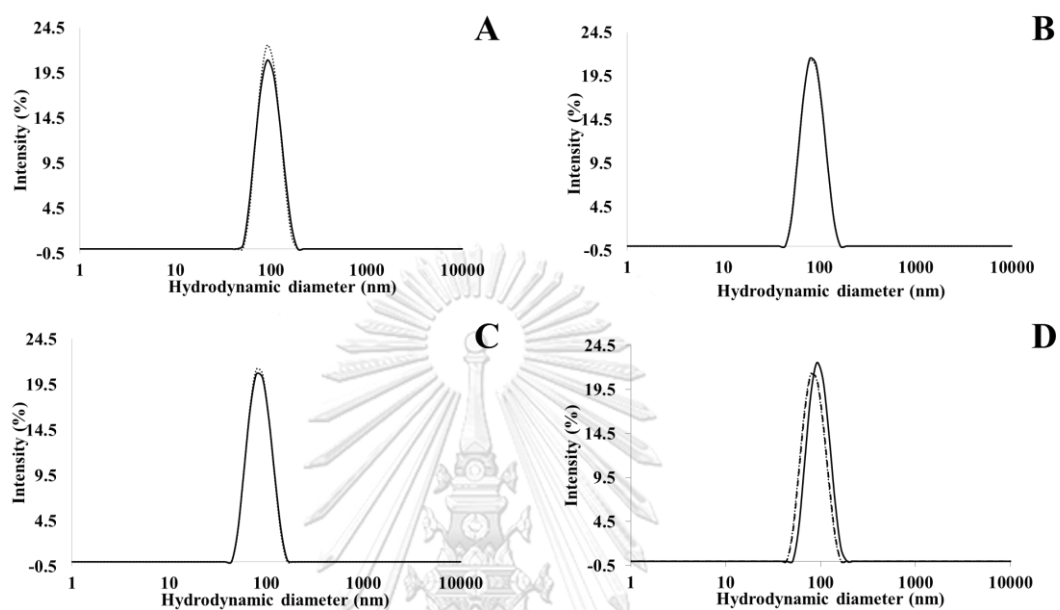


Figure 47 Determination of sizes of WTALT, Δ 3SHALT and Δ 7SHALT nanoparticles in average diameter. (A), (B) and (C) showed the sizes in diameter of pre- (solid line) and post- (dash line) lyophilised WTALT, Δ 3SHALT and Δ 7SHALT, respectively. (D) Comparison of sizes of three lyophilised polymers: WTALT (solid line), Δ 3SHALT (dot line) and Δ 7SHALT (dash line).



Figure 48 Comparison of solubility of WTALT (A), Δ 3SHALT (B) and Δ 7SHALT (C) polymers. Tubes no. 1-7 represent polymer in concentrations of 1, 2.5, 5, 10, 15, 20 and 25 % (w/v), respectively.

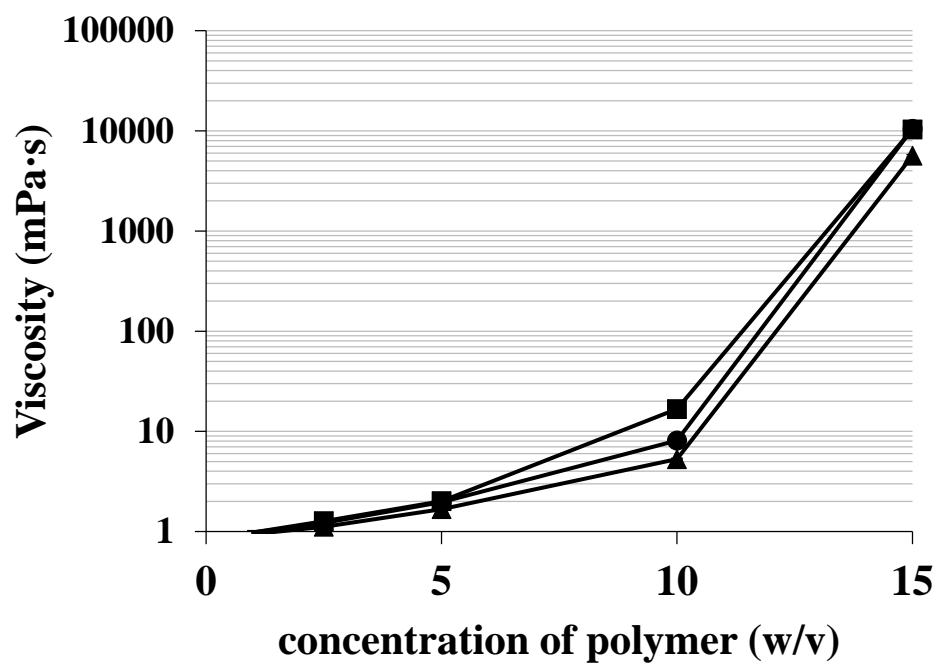


Figure 49 Comparison of viscosity of WTALT (●), Δ3SHALT (■) and Δ7SHALT (▲) polymers. The viscosity was measured by viscosity meter at 25 - 27 °C.

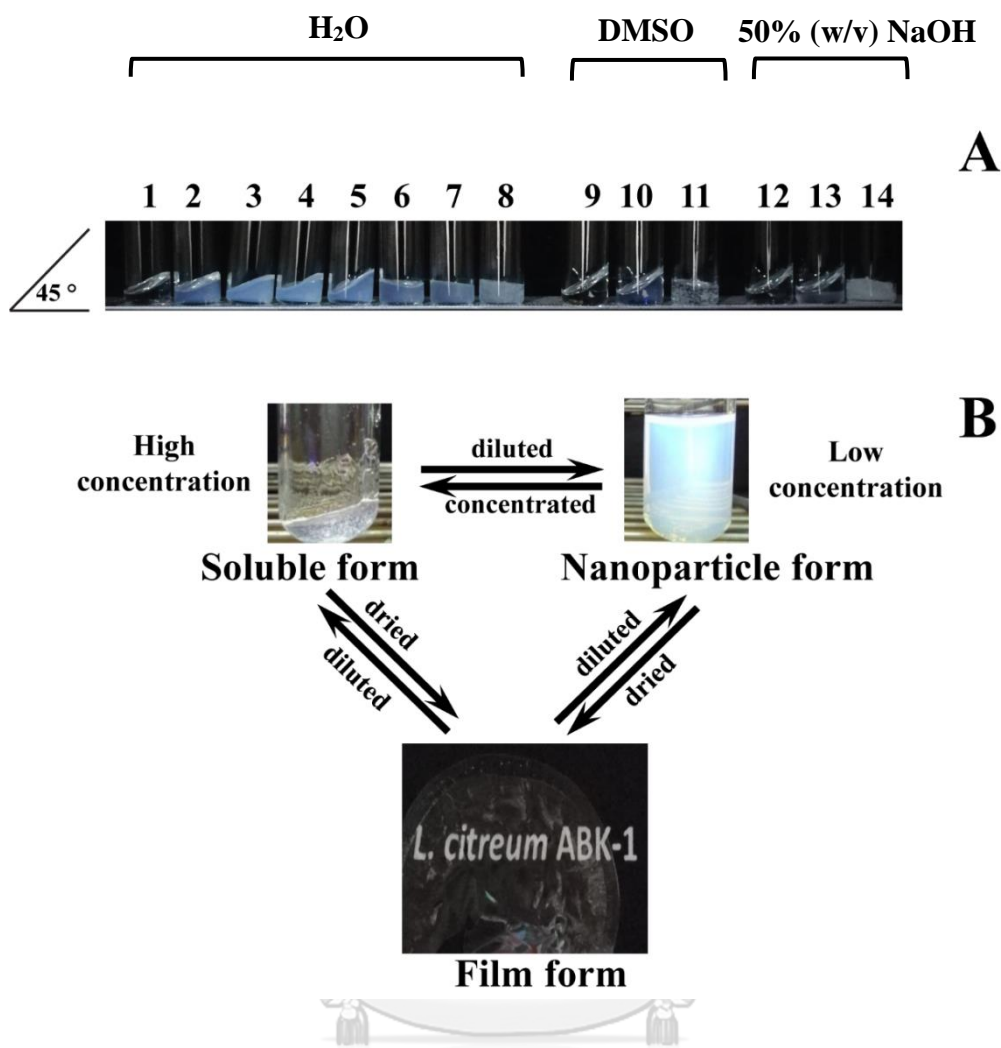


Figure 50 Solubility, nanoparticle and film formation properties of WTALT polymer.

(A) Tubes 1 - 8 present 0, 1, 2.5, 5, 10, 15, 20 and 25 % (w/v) WTALT polymer in water, tubes 9 - 11 present 0, 1 and 20 % (w/v) WTALT polymer in DMSO, and tubes 12 - 14 showed 0, 1 and 20 % (w/v) WTALT polymer in 50 % (w/v) NaOH, respectively. The tubes were set at a 45-degree angle. (B) Interconversion of WTALT polymer among its three physical forms: aqueous solution, nanoparticles and film.

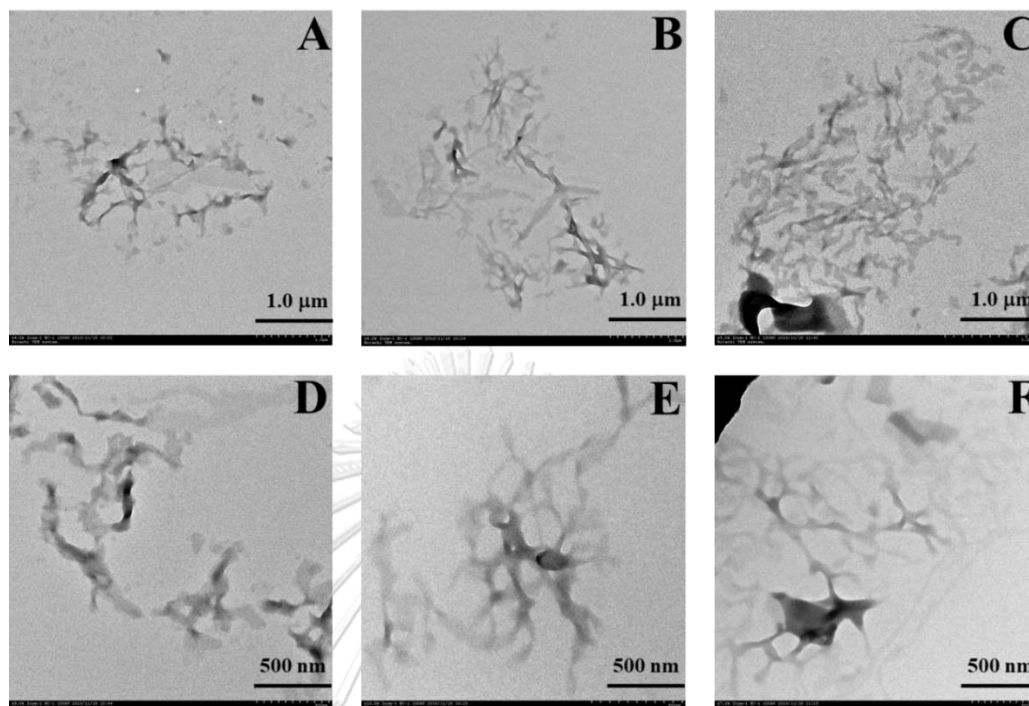


Figure 51 TEM images of WTALT, Δ 3SHALT and Δ 7SHALT polymers. (A), (B) and (C) were WTALT, Δ 3SHALT and Δ 7SHALT polymers at 1.0 μ m of magnification. (D), (E) and (F) represent WTALT, Δ 3SHALT and Δ 7SHALT polymers at 500 nm of magnification.

In addition, the size of WTALT polymer was also determined. Various sizes of WTALT polymer were obtained from GPC (Fig. 52) and then analysed by MALDI-TOF MS. Noticeably, masses corresponded to cyclic oligosaccharide structures were observed in non-methylated polymer (Fig. 53A). While, masses corresponded to linear glucans were detected in permethylated version (Fig. 53B). Nevertheless, analysis of mass of WTALT polymer was confirmed by High resolution ESI-TOF MS. Figure 54 showed that no masses of either linear or cyclic oligosaccharides were present.

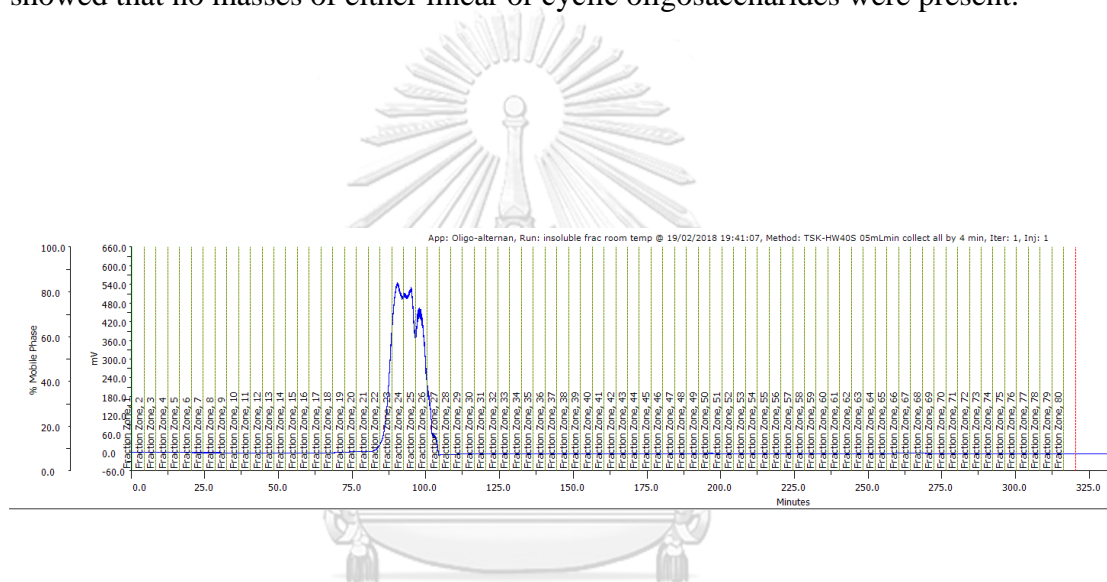


Figure 52 Purification of WTALT polymer by GPC. WTALT obtained from the overnight reaction was precipitated with acetone. Insoluble phase was suspended in DI water followed by acetone precipitation (repeat 3 times). The solubilised polymer was then purified by Toyopearl HW-40S column.

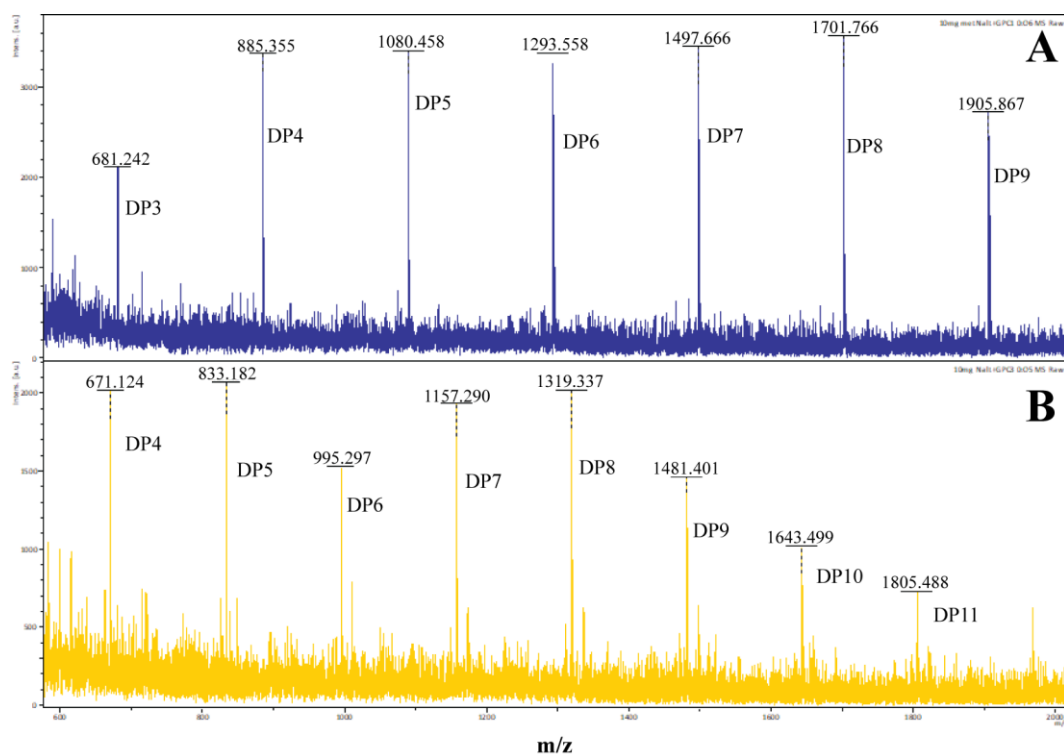


Figure 53 MALDI-TOF MS analysis of purified WTALT polymer. Masses of WTALT polymer without methylation (A), and permethylated WTALT polymer (B) were detected. The dihydroxybenzoic acid (DHB) was used as matrices.

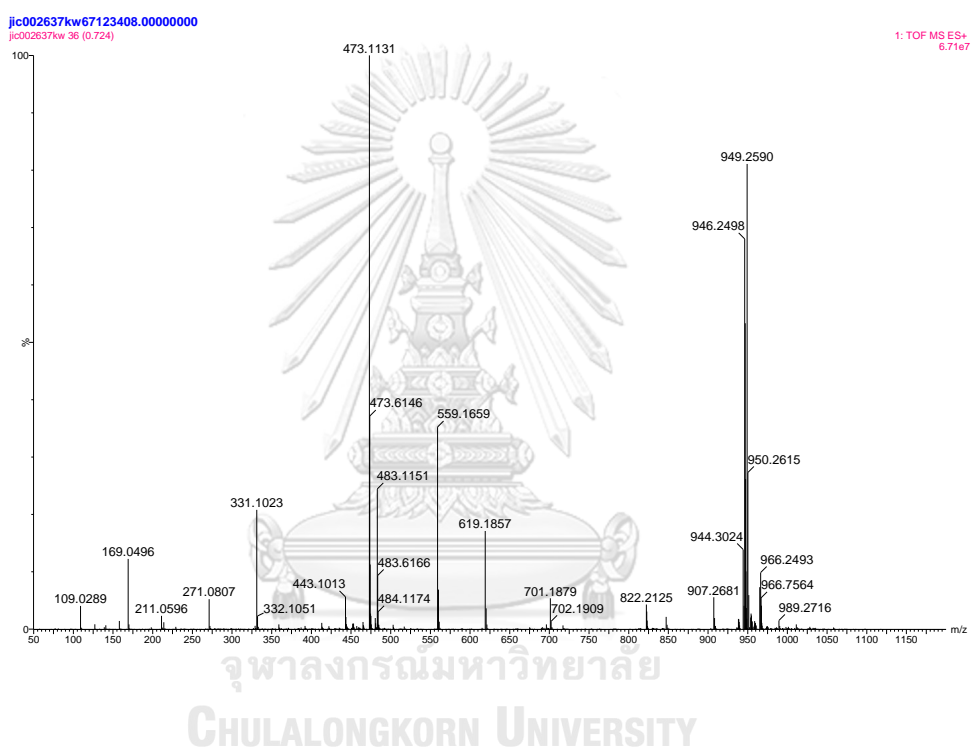


Figure 54 Analysis of the purified WTALT polymer by high resolution ESI-TOF MS.

3.5 Mutagenesis of *alt* gene

Due to the lacking of crystal structure of alternansucrase in database, $\Delta 7$ SHALT was chosen for constructing a homology model as shown in Fig. 55, based on crystal structure of N-terminally truncated glucansucrase GTFA of *Lactobacillus reuteri* 121 (PDB code: 4amc)⁸² as a template which showed 54.48 % identity with $\Delta 7$ SHALT sequence. Moreover, the model was considered by Ramachandran plot that 91.4 %, 6.2 %, and 2.4 % of residues were found in favoured region, allowed region, and outlier region, respectively (Fig. 56). Thirteen residues of aromatic amino acids (shown in yellow), possibly involved in binding of substrate or product, which located around catalytic residues (shown in green) were considered. These aromatic residues were changed to alanine, so-called alanine scanning method, consisting of F538A, W543A, W675A, Y695A, F701A, W716A, Y717A, Y768A, F802A, F813A, Y816A, Y1110A and Y1124A using PCR driven overlapping extension method. All mutants were successfully constructed where gene expression and protein purification conditions were similar to that of $\Delta 7$ SHALT. The proteins produced by all mutants were purified by DEAE and Phenyl Toyopearl 650M column and shown as a single band protein with similar size on SDS gel (Fig. 57).

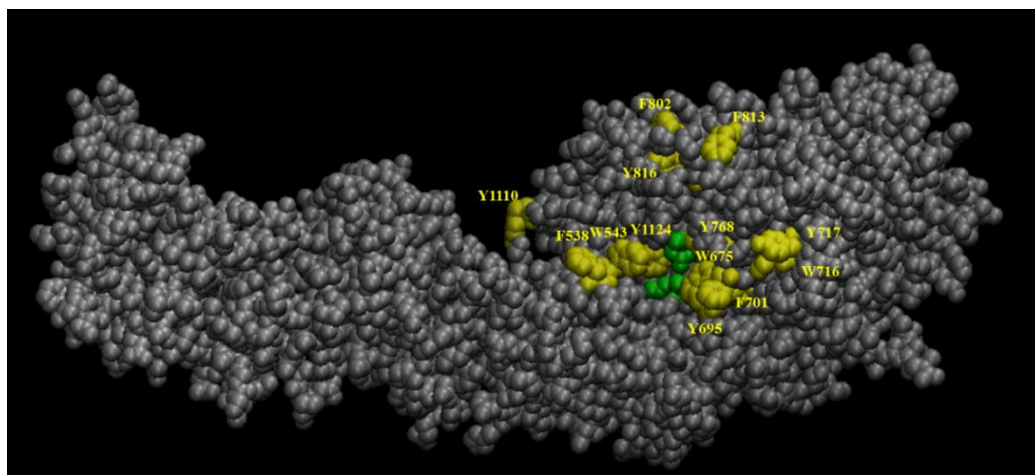


Figure 55 Homology model of $\Delta 7$ SHALT. Three catalytic residues were shown in green and yellow residues represent 13 aromatic residues of interest (F538A, W543, W675, Y695, F701, W716, Y717, Y768, F802, F813, Y816, Y1110 and Y1124). The homology modelling was built by SWISS-MODEL server using 4amc as template.

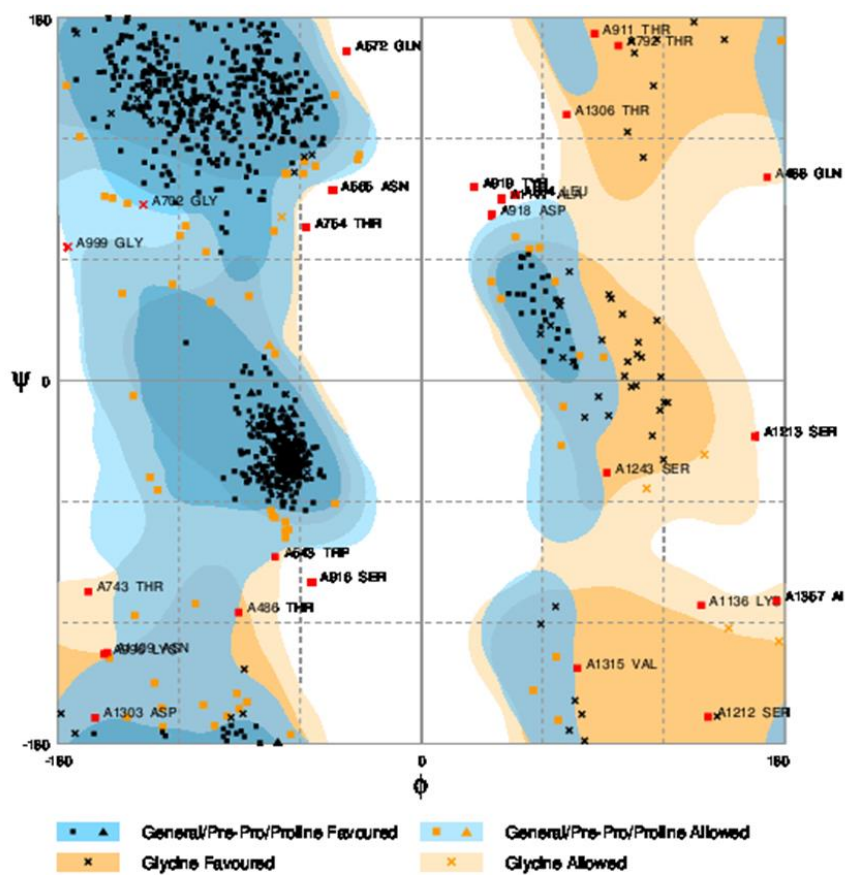


Figure 56 Ramachandran plot of $\Delta 7$ SHALT homology model. The model was analysed by RAMPAGE server.

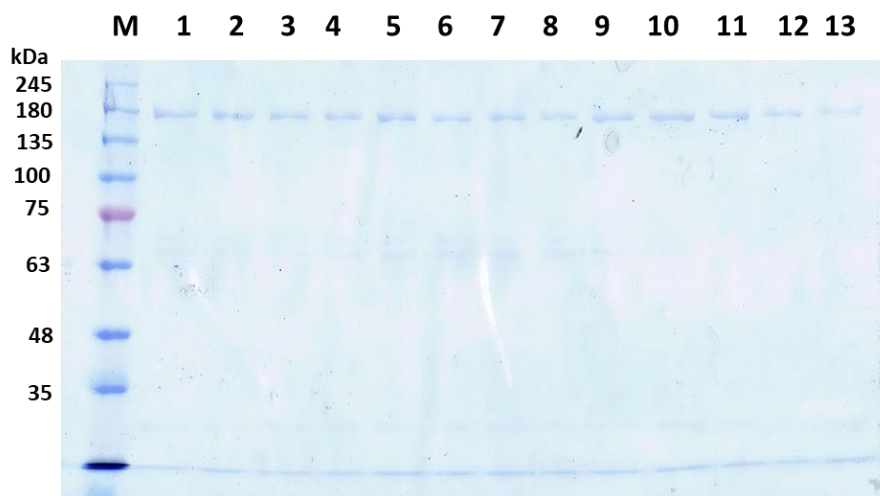


Figure 57 SDS-PAGE analysis of purified ALTs produced by alanine scanning mutants. Proteins of each mutant were purified by DEAE and Phenyl Toyopearl 650M columns, respectively.

Lane M: protein molecular weight marker

Lane 1: F538A

Lane 2: W543A

Lane 3: W675A

Lane 4: Y695A

Lane 5: F701A

Lane 6: W716A

Lane 7: Y717A

Lane 8: Y768A

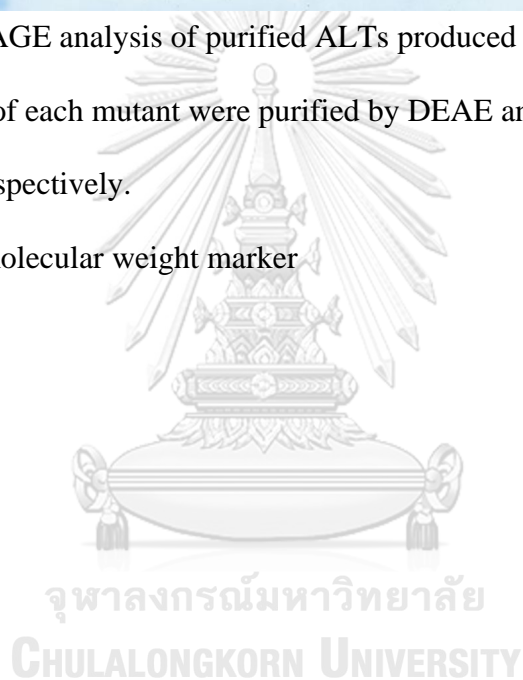
Lane 9: F802A

Lane 10: F813A

Lane 11: Y816A

Lane 12: Y1110A

Lane 13: Y1124A



After that, effect of mutation was compared with wide-type enzyme ($\Delta 7$ SHALT) the patterns of product were primarily observed by TLC technique. Obviously, W675A and Y1124A (Lanes 5 and 15, respectively, Fig. 58) mainly produced shorter chain oligosaccharides (up to around G7) with less intense spot of polymers at their spotting sites compared to the others. However, sucrose substrate apparently remained in Y1124A in much higher level than in W675A. Interestingly, W675A oligosaccharide pattern analysed by TLC (Fig. 58) and HPAEC-PAD (Fig. 59) was clearly different from $\Delta 7$ SHALT's and also those of all other mutants. Furthermore, mass analysis from MALDI-TOF MS (Figure 60) showed that the longest products of W675A was heptasaccharide.

Importantly, sequence alignments of bacterial glucansucrases from different sources showed that W675 located in conserved II region and were absolutely conserved in all species as shown in box in Fig. 61. So, saturation mutagenesis at this position was then performed. W675A, W675D, W675F, W675H, W675I, W675L, W675N, W675S and W675Y were successfully generated by PCR driven overlapping extension method using $\Delta 7$ SHALT as template. $\Delta 7$ SHALT and all mutated ALTs were produced, purified by DEAE and Phenyl toyopearl 650M column, and analysed on SDS gel (Fig. 62). According to the analysis of products of mutants, W675F and especially W675Y (Lanes 3 and 4, respectively, Fig. 63) still produced high level of polymer present as dark spots at their spotting sites whereas slightly low level of polymer was produced by W675H and W675D (Lanes 8 and 9, Fig. 63). On the other hand, short chain oligosaccharides could be observed in W675A, W675L, W675I, W675N, and W675S (Fig. 63). Notably, TLC together with HPAEC-PAD (Fig. 64) analyses showed

that patterns of product obtained from some saturated mutants at W675 position were apparently different from $\Delta 7$ SHALT's.

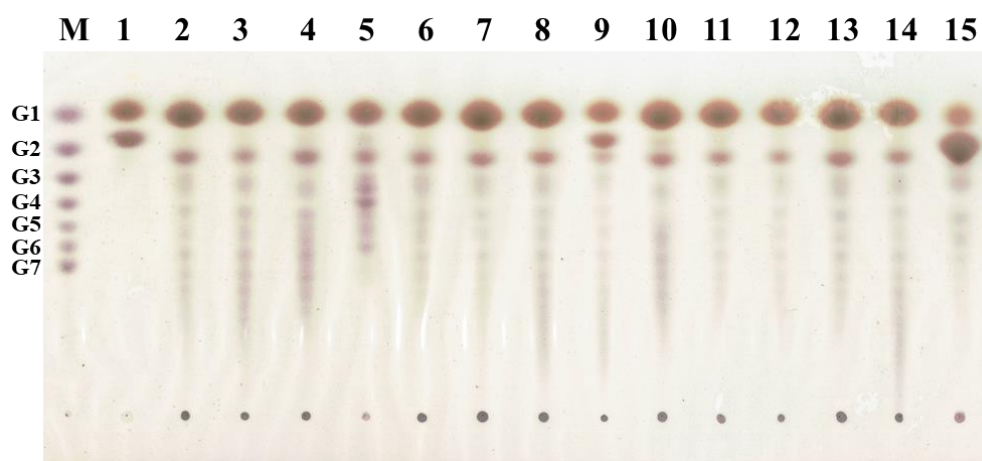


Figure 58 TLC analysis of glucan products produced by alanine scanning mutants.

Lane M: std. maltooligosaccharides, lane 1: std. fructose and sucrose, and lanes 2 - 15 were products of $\Delta 7$ SHALT, F538A, W543A, W675A, Y695A, F701A, W716A, Y717A, Y768A, F802A, F813A, Y816A, Y1110A and Y1124A, respectively. Enzymatic reactions were carried out in 50 mM citrate buffer pH 4.0 at 37 °C using 10 % (w/v) sucrose as substrate.

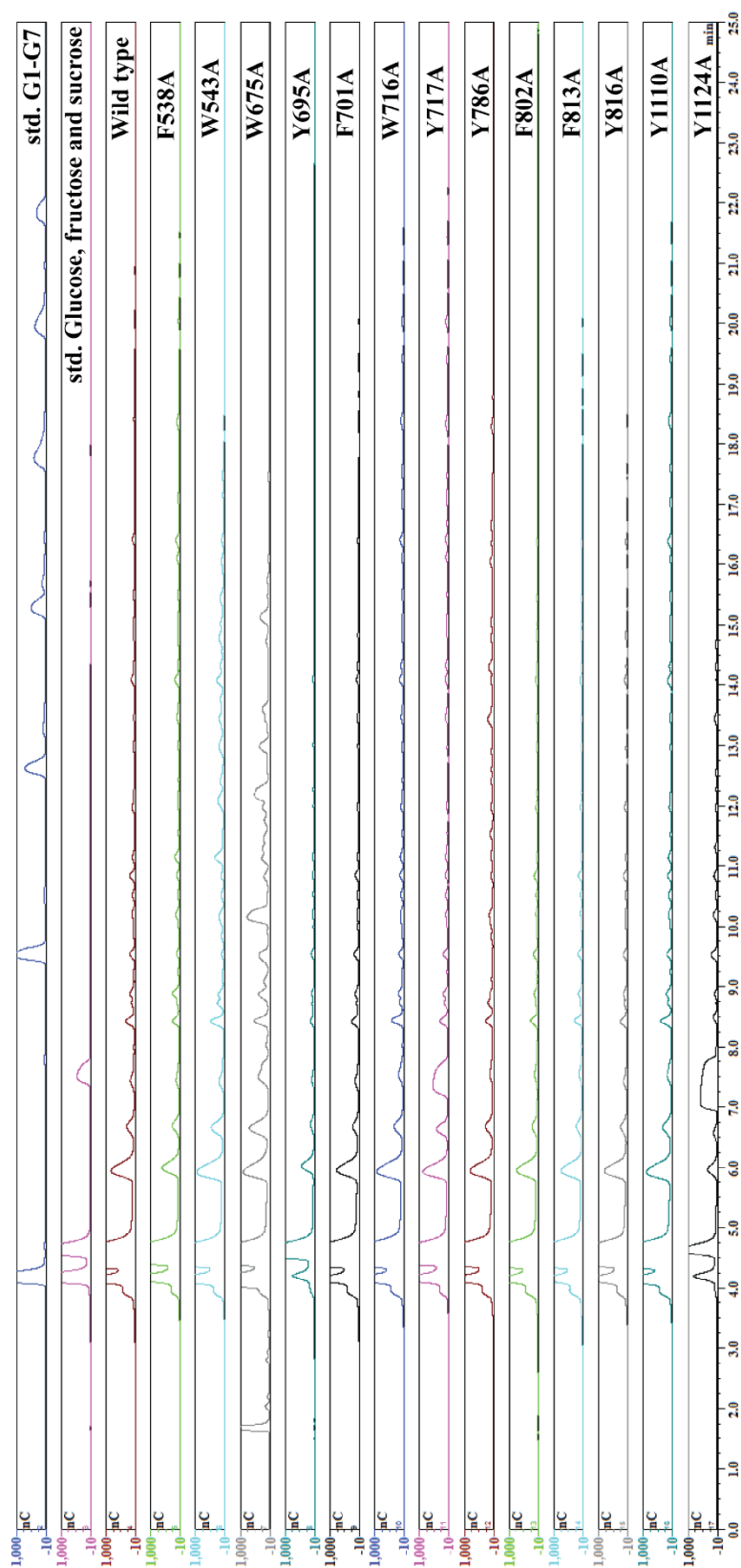


Figure 59 Comparison of oligosaccharide patterns of alanine scanning mutants. WT, F538A, W543A, W675A, Y695A, F701A, W716A, Y717A, Y786A, F802A, F813A, Y816A, Y1110A and Y1124A (0.6 U/ml) were incubated with 10 % (w/v) sucrose and various concentrations of maltose in 50 mM citrate buffer pH 4.0 at 37 °C for overnight and then analysed by HPAEC-PAD.

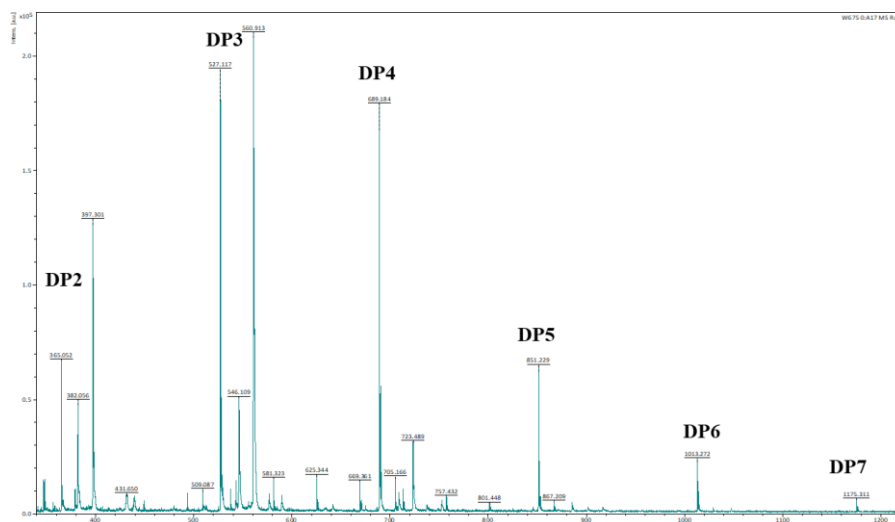


Figure 60 Determination of masses of oligosaccharide products of W675A by MALDI-TOF MS

Bacterial strain	conserved I	conserved II	conserved III	Accession No.
<i>L. citreum</i> ABK-1	627 ANFDGIRVD <u>AV</u> DNVDADLLKI	668 <u>HL</u> SILE <u>W</u> NGKDPQY	760 YSFIRAH <u>D</u> YDAQDPI	This work
<i>L. mesenteroides</i> NRRL B-1355	627 ANFDGIRVD <u>AV</u> DNVDADLLKI	668 <u>HL</u> SILE <u>W</u> NGKDPQY	760 YSFVRAH <u>D</u> YDAQDPI	CAB65910.2
<i>L. citreum</i> B/110-1-2	547 ANFDSIRVD <u>AV</u> DNVDADLLDI	588 <u>HIS</u> I <u>LE</u> W <u>S</u> GLDPNE	658 YSFVRAH <u>D</u> SEVQGII	ACY92456.2
<i>S. sobrinus</i> OMZ176	439 ANFDSIRVD <u>AV</u> DNVDADLLQI	480 <u>HVS</u> I <u>VE</u> W <u>S</u> DNDTPY	551 YSFARAH <u>D</u> SEVQDII	BAA02976.1
<i>L. mesenteroides</i> NRRL B-1299	519 ANFDGYRVD <u>AV</u> DNVDADLLQI	560 <u>HIS</u> I <u>LE</u> W <u>DN</u> ND SAY	631 YAFIRAH <u>D</u> SEVQTVI	CAD22883.1
<i>L. mesenteroides</i> NRRL B-512F	543 ANFDGIRVD <u>AV</u> DNVDADLLQI	584 <u>HL</u> SILE <u>W</u> SHNDPLY	655 YSFVRAH <u>D</u> SEVQTVI	AAD10952.1
<i>L. reuteri</i> 121	1016 ANFDSVRVD <u>AP</u> DNIDADLMNI	1056 <u>HIN</u> I <u>LE</u> W <u>N</u> HADPEY	1126 YSFVRAH <u>D</u> NNSQDQI	OJH11530.1
<i>S. mutans</i> GS-5	457 ANFDGVRVD <u>AV</u> DNVNADLLQI	498 <u>HL</u> SILE <u>W</u> SDNDPQY	577 YIFIRAH <u>D</u> SEVQTVI	AAA26895.1
<i>L. reuteri</i> 180	1017 ANFDGIRVD <u>AV</u> DNVDVLLSI	1058 <u>HIN</u> I <u>LE</u> W <u>G</u> WDDPAY	1129 YNFVRAH <u>D</u> SNAQDQI	AAU08001.1
	****, **** *: : . *: . *	*: . *: * *	* * **** : * *	

Figure 61 Comparison of three conserved sequence motifs of various glucansucrases. Catalytic triad were underlined and conserved tryptophan residues at the same position of W675 of *L. citreum* ABK-1 alternansucrase were shown in the box.

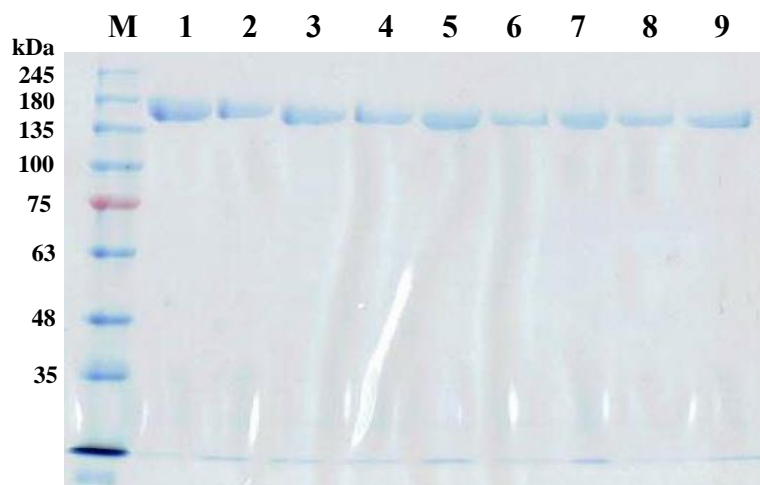


Figure 62 SDS-PAGE analysis of purified ALTs produced by alanine scanning mutants. The mutated enzymes were purified by DEAE and Phenyl Toyopearl 650M columns.

Lane M: protein molecular weight marker

Lane 1: W675F

Lane 2: W675Y

Lane 3: W675A

Lane 4: W675L

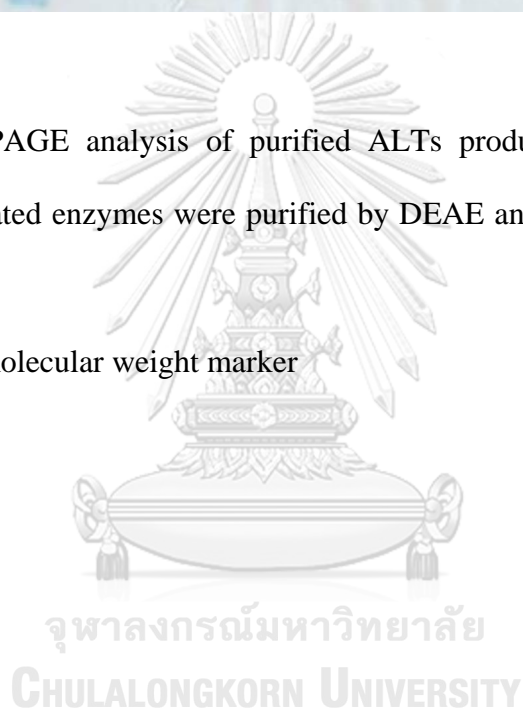
Lane 5: W675I

Lane 6: W675H

Lane 7: W675D

Lane 8: W675N

Lane 9: F802S



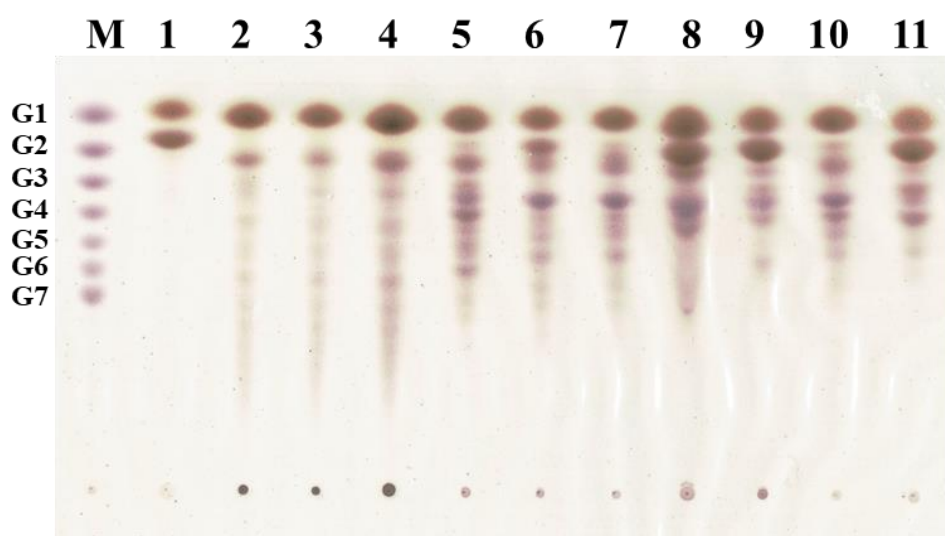


Figure 63 TLC analysis of glucan products produced by alanine scanning mutants.

Lane M: std. maltooligosaccharides, lane 1: std. fructose and sucrose, and lanes 2-15 were products from $\Delta 7$ SHALT, W675F, W675Y, W675A, W675L, W675I, W675H, W675D, W675N and W675S, respectively. Enzymatic reactions were performed in 50 mM citrate buffer pH 4.0 at 37 °C using 10 % (w/v) as substrate.

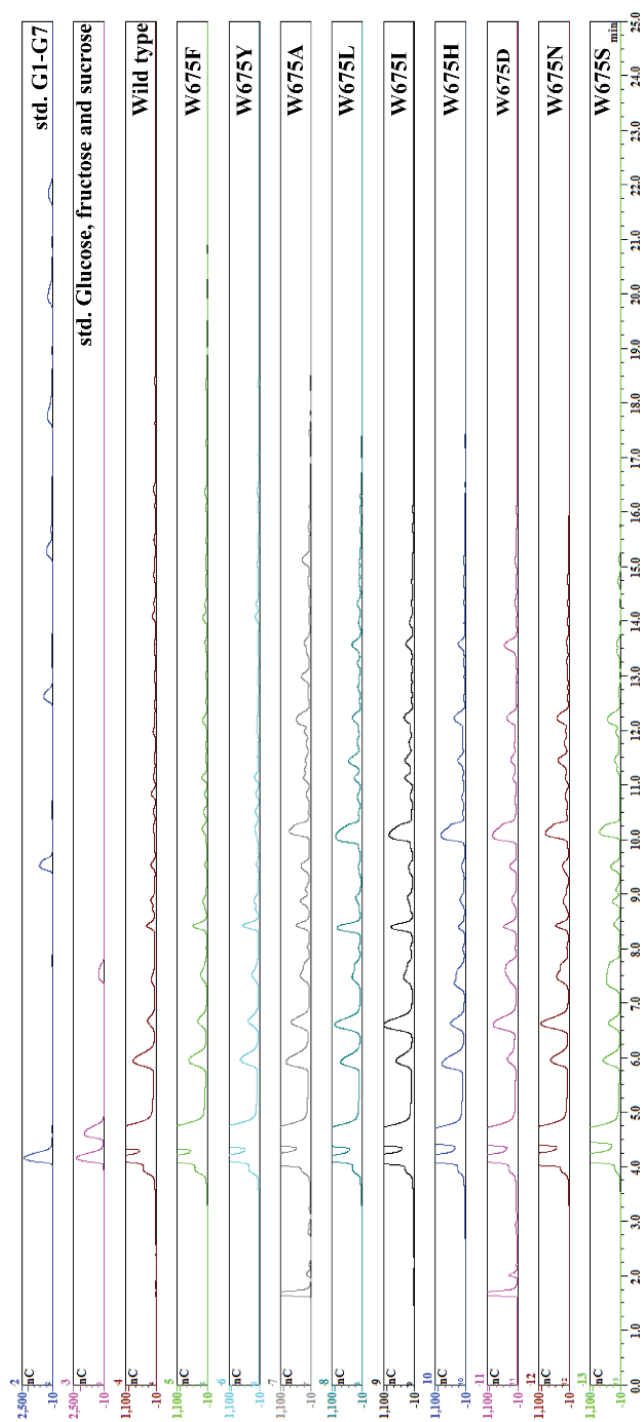


Figure 64 Comparison of oligosaccharide patterns of saturation mutagenesis at W675. WT, W675F, W675Y, W675A, W675L, W675I, W675H, W675D, W675N and W675S (0.6 U/ml) were incubated with 10 % (w/v) sucrose and various concentrations of maltose in 50 mM citrate buffer pH 4.0 at 37 °C for overnight and then analysed by HPAEC-PAD.

3.6 Characterisation of W675A

Since W675A mutant mainly produced short oligosaccharides (up to G7) as described above, it was chosen as a model for characterisation of mutated alternansucrase compared to the $\Delta 7$ SHALT. The optimum temperature of W675A was at 40 °C (Fig. 65A) similar to that of $\Delta 7$ SHALT however the optimum pH of W675A was at pH 5.0 (Fig. 65B) while $\Delta 7$ SHALT's was at pH 4.0. In terms of the kinetic study of W675A mutant, K_m value of hydrolysis activity was 13.1 ± 0 mM but the transglycosylation activity apparently exhibited linear relationship with sucrose concentration as shown in Fig. 66.

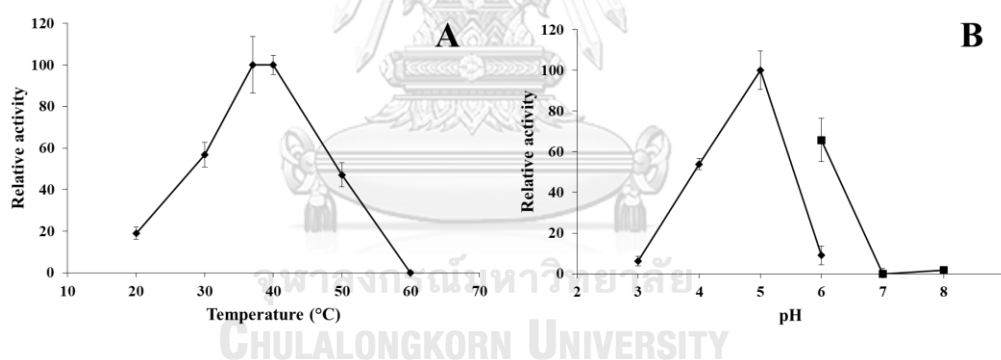


Figure 65 Optimum temperature (A) and optimum pH (B) of W675A mutant. The optimum temperature was performed in 20% (w/v) sucrose in 50 mM citrate buffer pH 4.0 at various temperature. The optimum pH were assayed at 40 °C in 50 mM citrate buffer pH 3-6 and phosphate pH6-8 using 20% (w/v) sucrose as substrate.

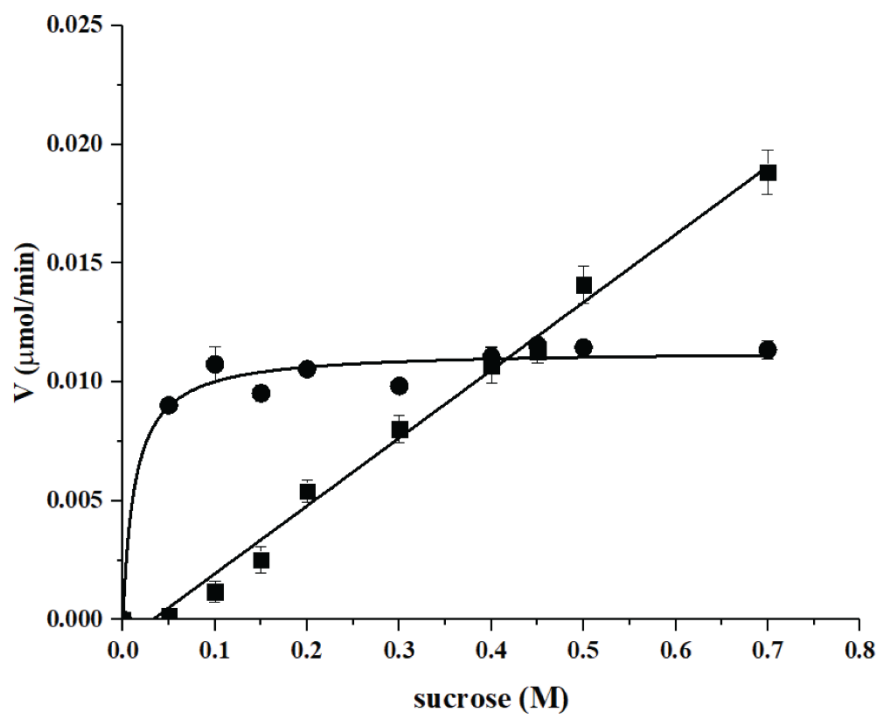


Figure 66 Kinetic study of W675A. (●) represent hydrolysis activity, while transglycosylation was represented by (■).

Importantly, products of W675A was clearly different from $\Delta 7$ SHALT by showing the production of much more species of oligosaccharides without polymer analysed by HPAEC-PAD (Fig. 67). Figure 68 showed the separation of W675A products; two peaks of G2 and single peaks of G3 - G6, by using BioGel P-2 column and their molecular masses corresponded to G2 – G6 were confirmed by MALDI-TOF MS (Fig. 69). Further analyses of these purified oligosaccharides by using TLC and HPAEC techniques revealed the presence of isomeric forms of all oligosaccharide species, which were shown as more than one separated bands detected in each lane of purified products on TLC plate (Fig. 70) and several peaks of products were observed in HPAEC chromatograms (Fig. 71).

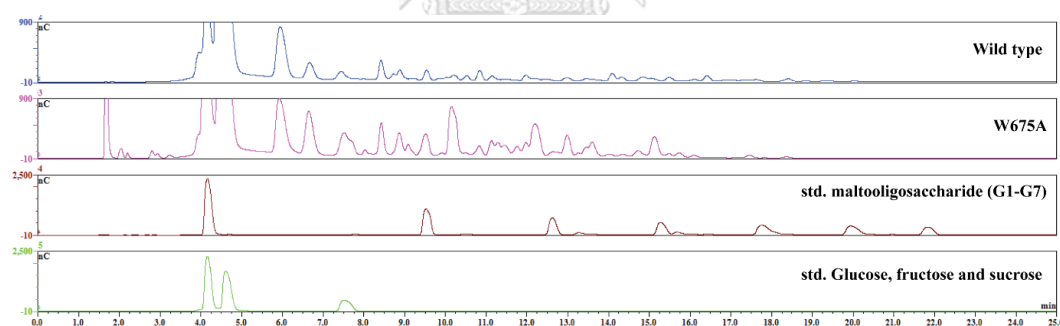


Figure 67 Comparison of oligosaccharide patterns of $\Delta 7$ SHALT and W675A.

$\Delta 7$ SHALT and W675A (0.6 U/ml) were incubated with 10% (w/v) sucrose in 50 mM citrate buffer pH 4.0 (pH 5.0 for W675A) at 37 °C for overnight and then analysed by HPAEC-PAD.

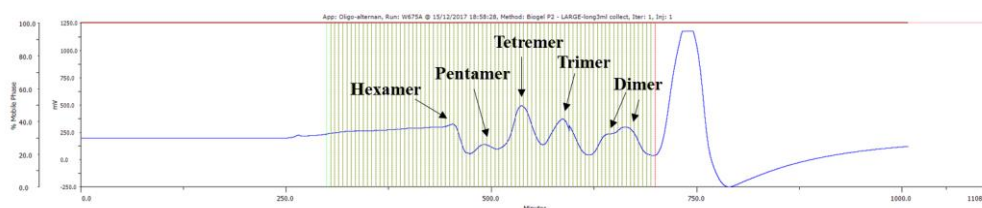


Figure 68 Separation of W675A products by GPC column. Ten percent (w/v) of sucrose was incubated with 1 U/mL of W675A in 50 mM citrate buffer pH 5.0 at 37 °C for overnight, and then separated by BioGel P-2 column.

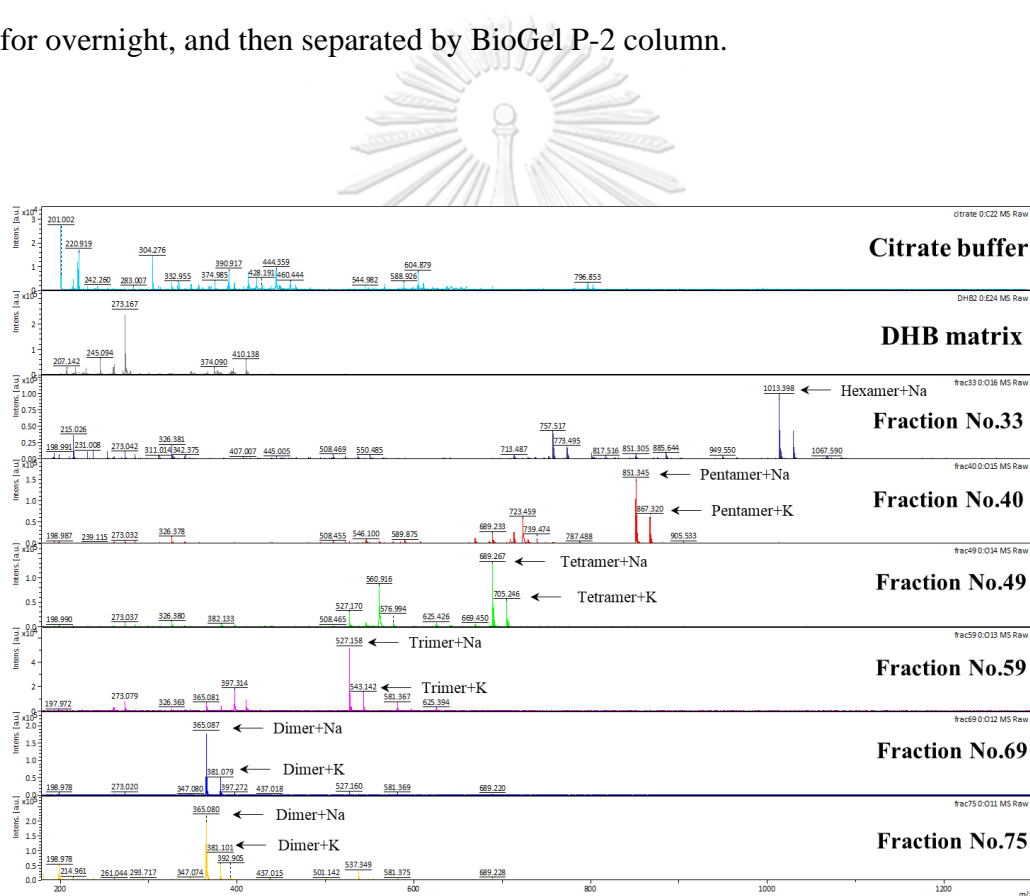


Figure 69 Analysis of masses of W675A products by MALDI-TOF MS

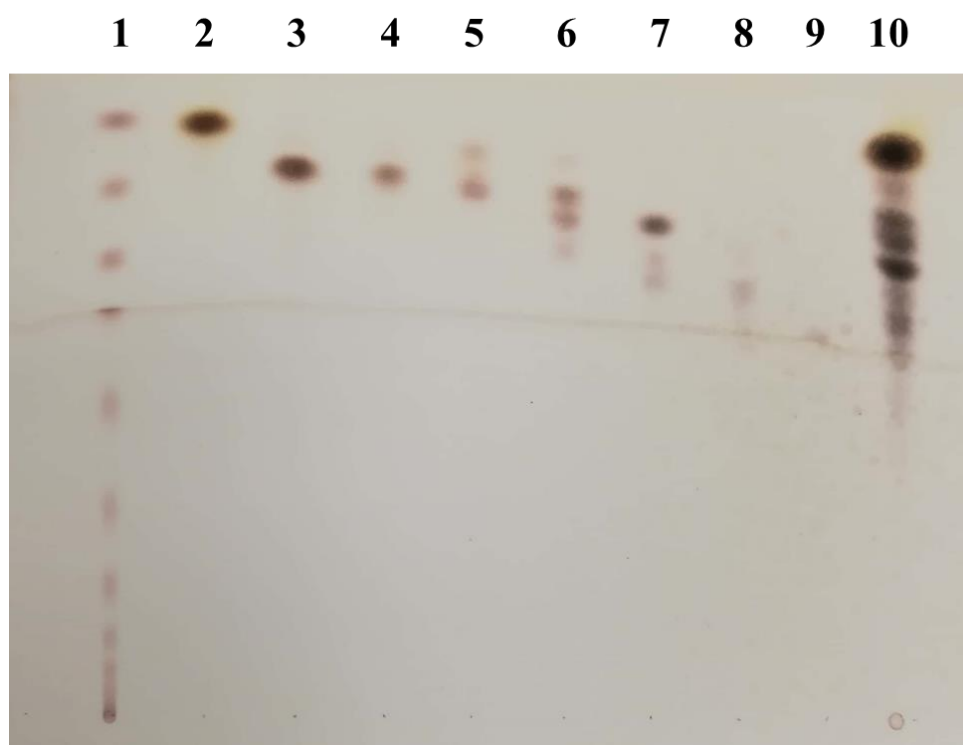


Figure 70 TLC analysis of W675A products after purified by BioGel P-2 column

Lane 1: dextran hydrolysate

Lane 2: std. fructose and sucrose

Lane 3: std. leucrose

Lane 4: fraction 75

Lane 5: fraction 69

Lane 6: fraction 59

Lane 7: fraction 49

Lane 8: fraction 40

Lane 9: fraction 33

Lane 10: crude mixture

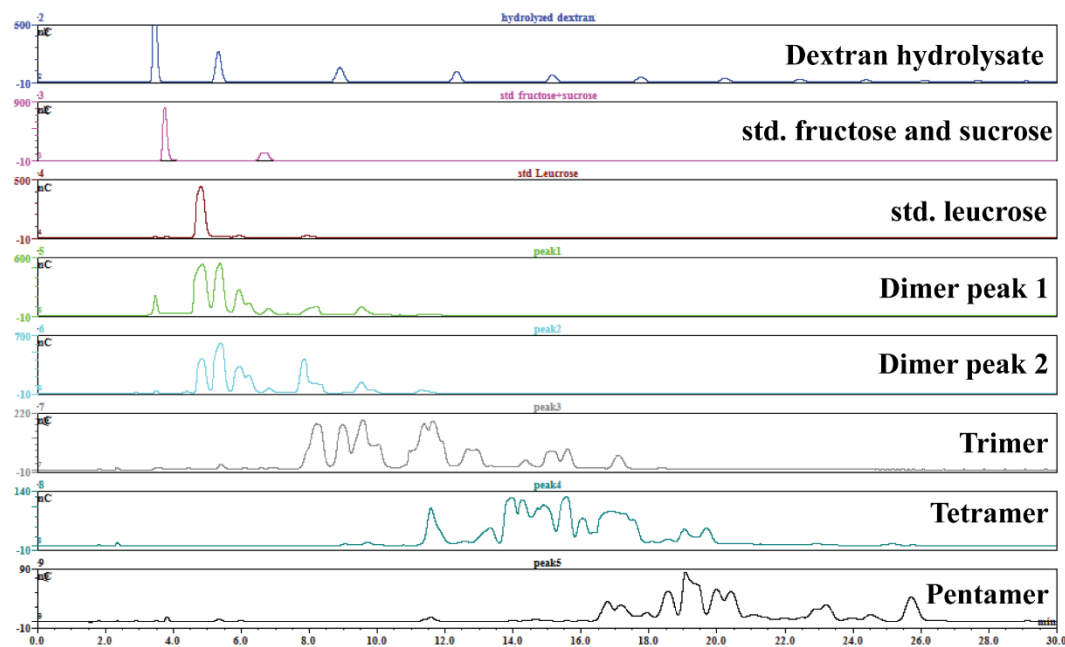


Figure 71 HPAEC-PAD analysis of W675A products after purified by BioGel P-2 column

To confirm the involvement of W675 residue in substrate binding, comparison of product patterns between $\Delta 7$ SHALT and W675A via acceptor reaction was performed using various acceptor molecules. Patterns of products produced by WT ($\Delta 7$ SHALT) and W675A using the similar acceptor were compared (Lanes 4 and 6, lanes 8 and 10, lanes 12 and 14, lanes 16 and 18, and lanes 20 and 22, Fig. 72) which the changing of oligosaccharide production patterns was apparently observed in the mutant. According to being as such an effective acceptor and easily available molecule, maltose was selected for further study. In addition, sucrose itself can act as both donor and acceptor making quantitative measurement of products difficult (Fig. 73). Interestingly, higher levels of glucose and fructose were found in W675A reaction compared with that of WT ($\Delta 7$ SHALT) which mainly produced fructose with small amount of glucose (Fig. 74-76). In addition to different product pattern, consumption of acceptor molecule of each enzyme was also significantly dissimilar. The WT could consume maltose molecule finishing although the maltose concentration was elevated up to 100 mM. In contrast, the maltose consumption of W675A was around 80 % quantitated by HPAEC-PAD (Fig. 77). Moreover, length of maltose acceptor product from WT, trended to depend on maltose concentration while W675A totally lost this ability (Fig. 73-75).

The molecular docking of maltose into active site of WT ($\Delta 7$ SHALT) and W675A, were preliminary performed (Fig. 78). Unlike WT, maltose molecule could not move inside to active site of W675A. Moreover, W675A active site also harboured wider empty space compared to WT. Importantly, orientation of maltose in active site of W675A differed from that of WT and also showed longer distance between maltose molecule and W675 residue.

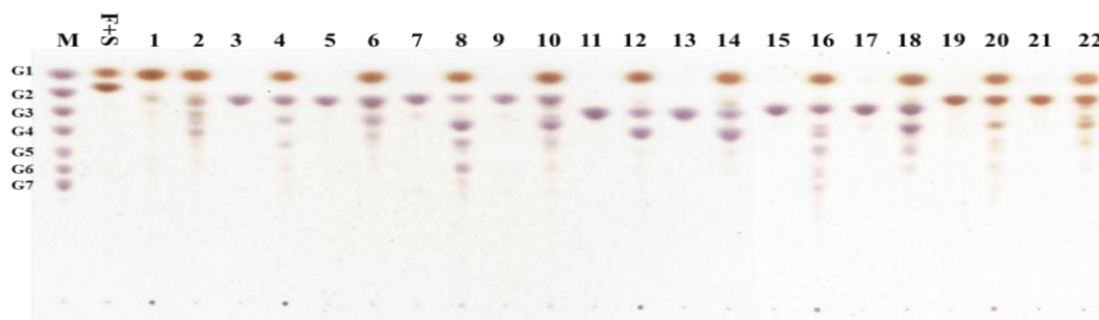


Figure 72 Analysis of acceptor reaction between WT and W675A on TLC. Enzymes (1.5 U/ml) were incubated with 100 mM sucrose and 100 mM of various acceptor molecules in 50 mM citrate buffer pH 4.0 (pH 5.0 for W675A) at 37 °C for overnight.

Lane M: std. maltooligosaccharides (G1-G7)

Lane F+S: std. fructose and sucrose

Lane 1: WT with 100 mM sucrose

Lane 2: W675A with 100 mM sucrose

Lane 3: WT with 100 mM cellobiose

Lane 4: WT with 100 mM cellobiose and 100 mM sucrose

Lane 5: W675A with 100 mM cellobiose

Lane 6: W675A with 100 mM cellobiose and 100 mM sucrose

Lane 7: WT with 100 mM maltose

Lane 8: WT with 100 mM maltose and 100 mM sucrose

Lane 9: W675A with 100 mM maltose

Lane 10: W675A with 100 mM maltose and 100 mM sucrose

Lane 11: WT with 100 mM melibiose

Lane 12: WT with 100 mM melibiose and 100 mM sucrose

Lane 13: W675A with 100 mM melibiose

Lane 14: W675A with 100 mM melibiose and 100 mM sucrose

Lane 15: WT with 100 mM isomaltose

Lane 16: WT with 100 mM isomaltose and 100 mM sucrose

Lane 17: W675A with 100 mM isomaltose

Lane 18: W675A with 100 mM isomaltose and 100 mM sucrose

Lane 19: WT with 100 mM palatinose

Lane 20: WT with 100 mM palatinose and 100 mM sucrose

Lane 21: W675A with 100 mM palatinose

Lane 22: W675A with 100 mM palatinose and 100 mM sucrose

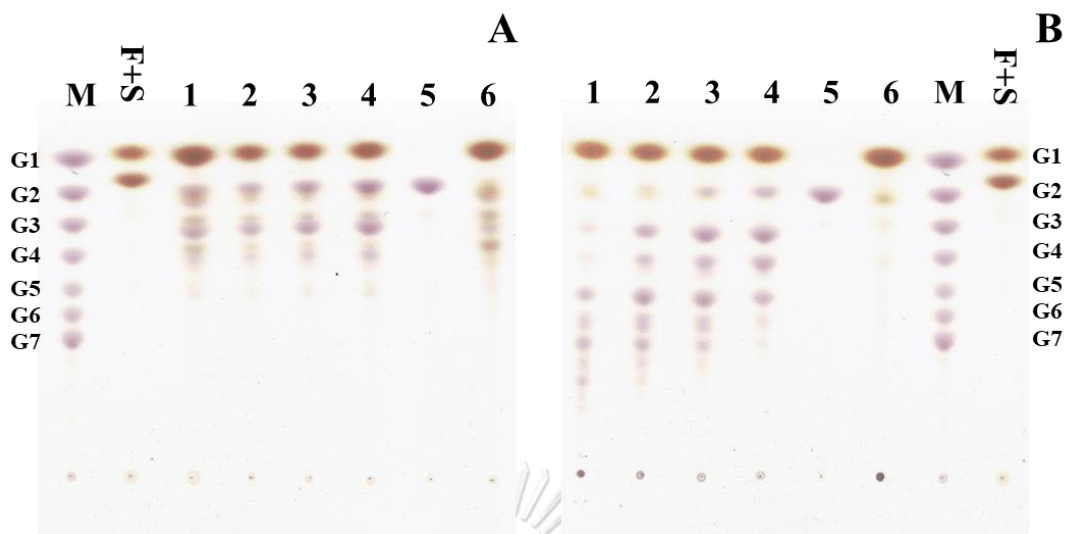


Figure 73 Comparison of products from maltose acceptor reaction of W675A (A) and WT (B). Enzymes (1.5 U/ml) were incubated with 100 mM sucrose and various concentrations of maltose in 50 mM citrate buffer pH 4.0 (pH 5.0 for W675A) at 37 °C for overnight.

Lane M: std. maltooligosaccharide (G1-G7)

Lane F+S: std. fructose and sucrose

Lane 1: reaction with 100 mM sucrose and 25 mM maltose

Lane 2: reaction with 100 mM sucrose and 50 mM maltose

Lane 3: reaction with 100 mM sucrose and 75 mM maltose

Lane 4: reaction with 100 mM sucrose and 100 mM maltose

Lane 5: reaction with 100 mM maltose

Lane 6: reaction with 100 mM sucrose

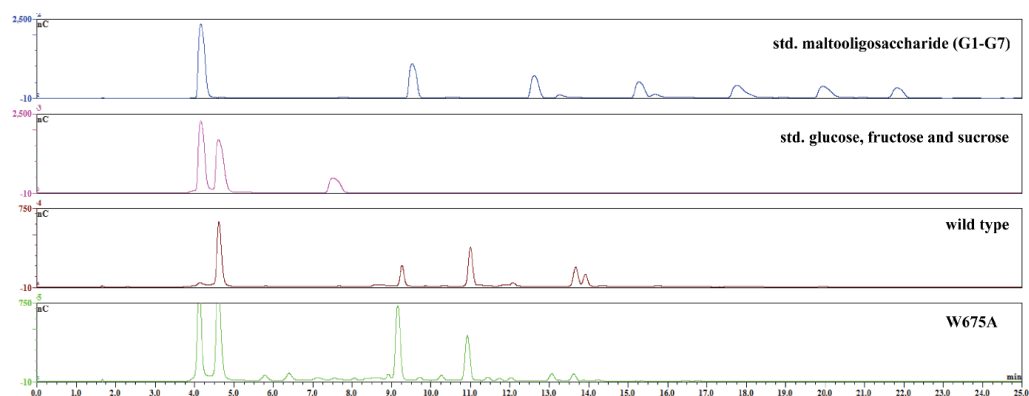


Figure 74 Comparison of oligosaccharide patterns produced by maltose acceptor reactions of WT and W675A. Enzymes (1.5U/ml) were incubated with 100 mM sucrose and 100 mM maltose in 50 mM citrate buffer pH 4.0 (pH 5.0 for W675A) at 37 °C for overnight and then analysed by HPAEC-PAD.

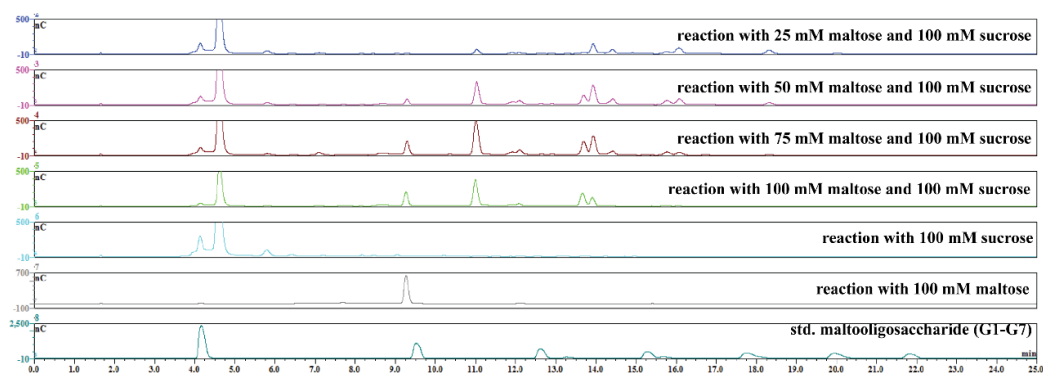


Figure 75 Effect of maltose concentration on WT products. Enzyme (1.5 U/ml) was incubated with 100 mM of sucrose and 25, 50, 75 and 100 mM of maltose in 50 mM citrate buffer pH 4.0 at 37 °C for overnight, and analysed by HPAEC-PAD.

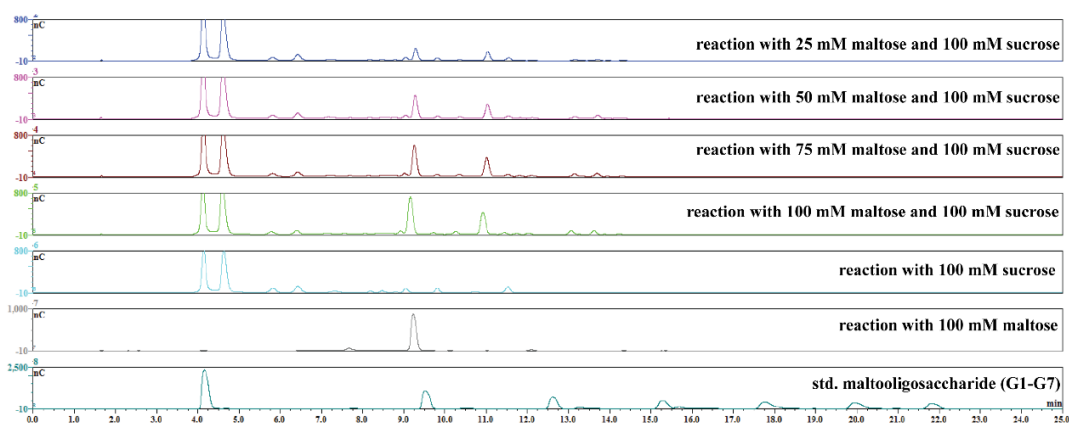


Figure 76 Effect of concentration of maltose acceptor on W675A products. Enzyme (1.5U/ml) was incubated with 100 mM sucrose and 25, 50, 75 and 100 mM maltose in 50 mM citrate buffer pH 4.0 at 37 °C for overnight and then analysed by HPAEC-PAD.

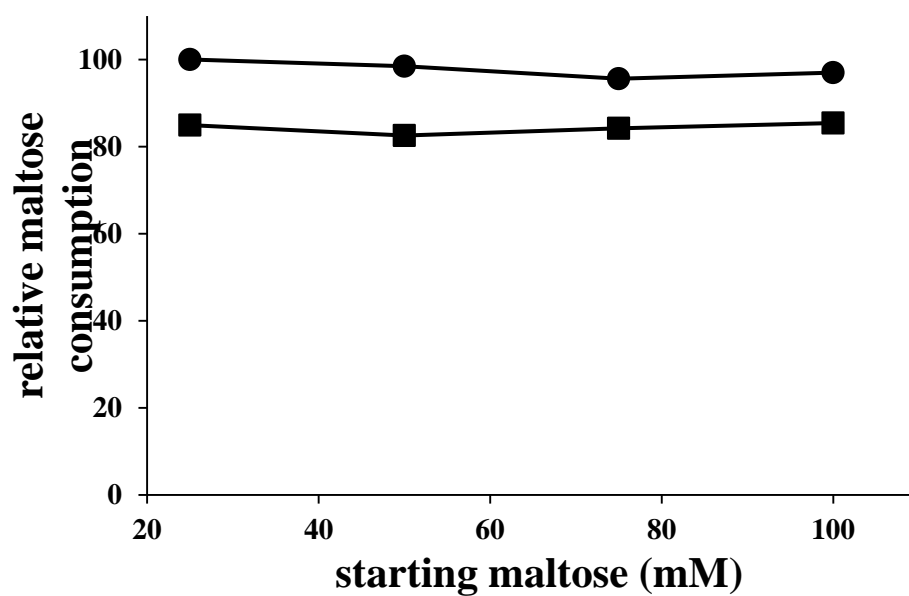


Figure 77 Comparison of maltose consumption between WT (●) and W675A (■) quantitated by HPAEC-PAD.

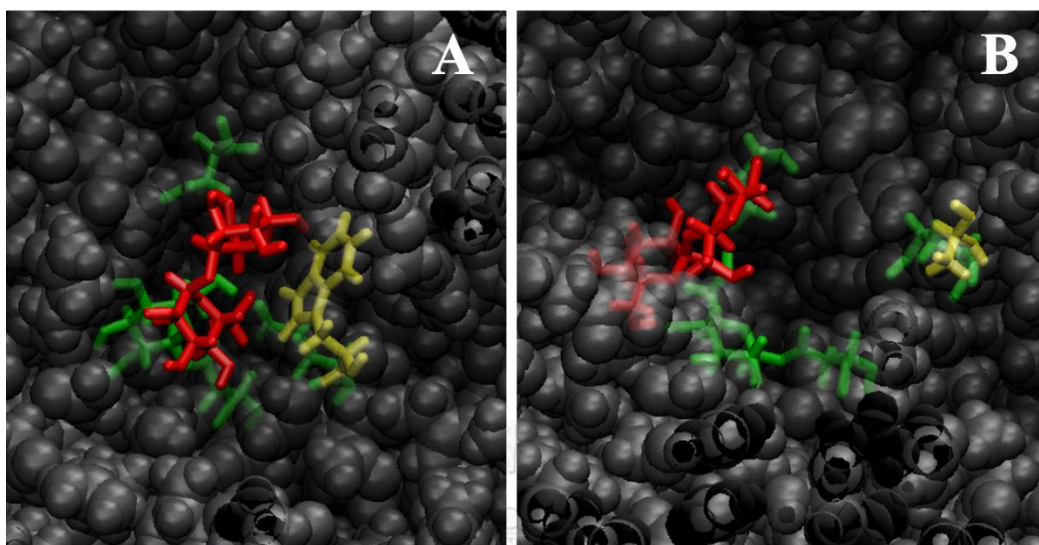


Figure 78 Preliminary of molecular docking. Maltose was docked into WT ($\Delta 7$ SHALT) (Panel A) and W675A (Panel B) active sites using AutoDock Vina. Maltose molecule was shown in red, 675 residue was shown in yellow, and catalytic triad with glucosyl-intermediate was in green.

CHAPTER IV

DISCUSSION

Glucansucrase consisted of various types of enzymes such as dextransucrase, reuteransucrase and alternansucrase and so on depend on their products. They catalyse transferring of glucose unit from sucrose substrate to produce different types of glucan products. Several glucansucrases and their products have been extensively characterised which their properties of the products depended on source of enzyme. Interestingly, glucan products derived from various strains of either *L. citreum* or *L. mesenteroides* greatly showed the diverse properties. However, only an alternansucrase (ALT) from *L. mesenteroides* NRRL-B1335 was cloned and fully characterised in contrast with many dextransucrases which have already been studied. Our work aims to biochemically and chemically characterise both *L. citreum* ABK-1 alternansucrase isolated from Khow-tom-mud and its products and investigate role of 7 tandem repeated SH3-like domain in C-terminus. Moreover, we also observed role of surface aromatic residues on its product size.

4.1 Cloning of *WTalt*, $\Delta 3SHalt$ and $\Delta 7SHalt$ genes

Nucleotide sequence of *Lcalt* or *WTalt* shares rather high percent identity, 99 % and 97 %, with those of *L. citreum* KM20 [DQ489736.1] and *L. mesenteroides* NRRL-B1335 [AJ250173.2], respectively. Noticeably, since *alt* genes are such a very long gene, only low level of dissimilarity of nucleotide sequence resulted in changing of several numbers of nucleotide, possibly causing several amino acid replacement. *WTALT* contained 45 of substituted amino acids compared to that of *LmALT*, which

especially 32 residues located in catalytic domain and I763V was in conserved sequence motif III (Fig. 10 and 11, respectively)^{17,26}. On the other hand, 7 tandem repeat sequences of SH3-like domain were also present in other glucosyltransferases and fructosyltransferases: GSC11-3 of *L. citreum* LBAE-C11, GSE16-5 and GSE16-4 of *L. citreum* LBAE-E16⁶⁴, IslA of *L. citreum* CW28⁶⁶ and *LmALT* of *L. mesenteroides* NRRL-B1335⁴¹, while 2 tandem repeat sequences of SH3-like domain were found in DSR-F of *L. citreum* B/110-1-2⁶⁵.

4.2 Expression of WTalt, Δ 3SHalt and Δ 7SHalt genes

WTALT was mainly produced as an insoluble protein. However, solubility of WTALT protein could be enhanced by growing cells at low temperature (16 °C) with slightly low IPTG induction (0.4 mM). Additionally, we found that activity of WTALT could be increased by adding of a non-ionic detergent, 0.1 % (v/v) Triton X-100, to lysis buffer. This suggested that native WTALT might be present together with its insoluble form which probably led to the protein aggregation and consequently decreased enzyme activity. Interestingly, no protein degradation of WTALT was observed, unlike *LmALT*⁴¹, which might be resulted from increasing stability of protein of interest via production at low temperature. Besides, total amount production of Δ 3SHALT and Δ 7SHALT were 1.7 and 2-fold higher than WTALT, respectively, under the same conditions. Nevertheless, the ratios of soluble to insoluble protein of WTALT, Δ 3SHALT and Δ 7SHALT were not significant as observed on SDS-PAGE. This suggested that protein aggregation of ALTs was independent of the tandem repeat SH3-like domains at C-terminus. Conversely, some other proteins harboured SH3 domains such as PI3-SH3⁸³, Fyn-SH3⁸⁴, c-Src-SH3⁸⁵, c-Yes-SH3⁸⁶ and Abl-SH3⁸⁷

aggregated as amyloid fibril. In addition, $\Delta 3$ SHALT and $\Delta 7$ SHALT could not bind to hydrophobic Phenyl Toyopearl 650M column under the same condition used for WTALT. This result showed that SH3-like domain apparently affected on overall hydrophobicity of ALT. On the other hand, SH3b domain of ALE-1, a peptidoglycan hydrolase, was shown as a cell wall-targeting protein by binding to pentaglycine inter-peptide bridge of *S. aureus* cell wall⁵⁸ but cell wall binding ability of SH3-like domain has not been reported. This evidence was in agreement with the presence of cloned WTALT, $\Delta 3$ SHALT and $\Delta 7$ SHALT mainly in intracellular fraction with up to 97 % of total protein. In addition, full length ALT was produced as an extracellular enzyme by its natural hosts: *L. messenteroides* NRRL B-1355^{47,88}. Obviously, localisation of native and heterologous ALTs was different probably resulted from the incompatibility of the secretory signal sequence between two different types of bacteria: gram positive *Leuconostoc* species and gram negative *E. coli*.

4.3 Characterisation of WTALT, $\Delta 3$ SHALT and $\Delta 7$ SHALT

Optimum temperature and pH of WTALT were at 40 °C pH 5.0, correlated to that of previously reported *LmALT*⁸⁸. While, optimum temperatures and pHs of $\Delta 3$ SHALT and $\Delta 7$ SHALT were at 40 °C pH 4.0. The activities of WTALT, $\Delta 3$ SHALT and $\Delta 7$ SHALT were obviously promoted by Mn^{2+} . However, activities of other glucansucrases were strongly dependent on Ca^{2+} ^{26,89,90}. Nevertheless, different metal ions effect on ALTs' activities with different degrees. SH3-like domain of diphtheria toxin repressor (DtxR) from *Corynebacterium diphtheriae* could bind to Co^{2+} and Mn^{2+} ^{62,91}. Therefore, SH3-like domains of ALTs might be able to bind to some metal ions. According to the effect of metal ions, the results showed that activity of $\Delta 7$ SHALT

was apparently responded by metal ions less than WTALT, whereas remaining SH3-like domains in Δ 3SHALT possibly made it more effectively responded to metal ions than WTALT.

On the other hand, WTALT greatly exhibited transglycosylation activity without detectable hydrolysis activity observed in kinetic study. This result related to determination of enzyme activity of *Lm*ALT, which showed very low level of hydrolytic activity (less than 5%⁴¹). The K_m value of WTALT was approximately 10-fold higher than those of other glucansucrases such as reuteransucrase²⁶ and dextransucrase⁹², as 4.6 mM and 3 mM, respectively. Nonetheless, hydrolytic ability was slightly observed in Δ 3SHALT and Δ 7SHALT but their k_{cat} values of transglycosylation activity were significantly decreased 4.9 and 2.6-times, respectively, compared to WTALT. Additionally, K_m values of Δ 3SHALT and Δ 7SHALT were also reduced 2.1 and 1.7-fold, respectively. Decreased K_m with around 1.5-fold was observed in fully truncated SH3-like domain of inulosucrase (IsIA). However k_{cat} and ratio of transglycosylation per hydrolysis were not significantly affected compared to wild type⁹³. Moreover, Δ 3SHALT and Δ 7SHALT produced higher amount of total oligosaccharides than WTALT with approximately 2-fold. Furthermore, size of polymer produced by Δ 7SHALT was relatively smaller than WTALT and Δ 3SHALT judged by viscosity analysis.

For stability testing of ALTs after stored at 30 °C pH 6.0 and at 37 °C in optimum pH, WTALT obviously showed higher stability compared to Δ 3SHALT and Δ 7SHALT (Fig. 26B and 26C). This evidence was in agreement with the results of incubation of various units of enzyme at 37 °C in optimum pH for overnight. Only 0.4 U of WTALT could completely convert 10 % (w/v) sucrose to products, while more

than 0.6 units of both $\Delta 3$ SHALT and $\Delta 7$ SHALT were required as shown in Fig. 34. In addition, half-life of IsIA was apparently decreased when its SH3-like domains were removed⁶⁶. On the contrary, deletion of C-terminal domain (7 tandem repeat SH3-like domains and 2 tandem repeat CW-like domains) of *Lm*ALT has been reported to not affect enzyme stability⁴¹. Nevertheless, WTALT, $\Delta 3$ SHALT and $\Delta 7$ SHALT were able to retain almost activity when they were kept at 4 °C at least a month.

On the other hand, to explain the effect of 7 tandem repeat SH3-like domains on activity of ALT is much complicated due to the lacking of 3D structure of this enzyme in all databases. However, crystal structures of several glucansucrases exhibited U shape-like protein folding and formation of 5 domains: A, B, C, IV and V. Based on the crystal structures of glucansucrase GTF180 from *Lactobacillus reuteri* 180 and DSR-M dextransucrase from *Leuconostoc citreum* NRRL B-1299, Pijning et al. (2014)²⁹ and Claverie et al. (2017)³⁰ clearly revealed that domains IV and V were flexible and could lead to the formation of horse shoe-like structure protein after domain V was folded, which these two domains was proposed to serve as helper domains for holding of glucan chain products during glucan polymerisation³⁰. Moreover, domain V was connected to 7 tandem repeat SH3-like domains at its C-terminus. Hence, these data and our findings may imply that after horse shoe-like structure was formed, 7 tandem repeat SH3-like domain will also located closely to active site of ALT (proposed model was shown in Fig. 79). This possibly provided hydrophobic environment at the active site resulted in reduction of water molecule accessibility and enhancement of possessivity of enzyme-polymer complex. When SH3-like domains were removed, the active site will then be easily attacked by water molecule, a competitive acceptor, that could interfered the elongation of polymers led to the

production of oligosaccharides by the truncated ALTs. Moreover, affinity analysis on native gel suggested that tandem repeat SH3-like domains participated in glucan binding. The different running patterns on native gel with or without dextran substrate together with relative mobility (R_f values) of each protein suggested that substrate binding abilities of WTALT, $\Delta 3$ SHALT and $\Delta 7$ SHALT were dissimilar, which WTALT most strongly bound to dextran followed by $\Delta 3$ SHALT and $\Delta 7$ SHALT, respectively (Fig. 22 and 23). Even though dextran itself is such a high molecular weight polymer, it does not interfere the protein movement in the gel since R_f value of bovine serum albumin used as a protein standard was not changed despite the increased concentration of dextran. However, two bands with similar size of both $\Delta 3$ SHALT and $\Delta 7$ SHALT were present on native gel whereas only single protein bands of each ALT were shown on SDS gel. This evidence might be the reasons of either (1) the presence of 2 forms of native-like folding $\Delta 3$ SHALT and $\Delta 7$ SHALT or (2) the fragmentation of $\Delta 3$ SHALT and $\Delta 7$ SHALT during running on native gel.

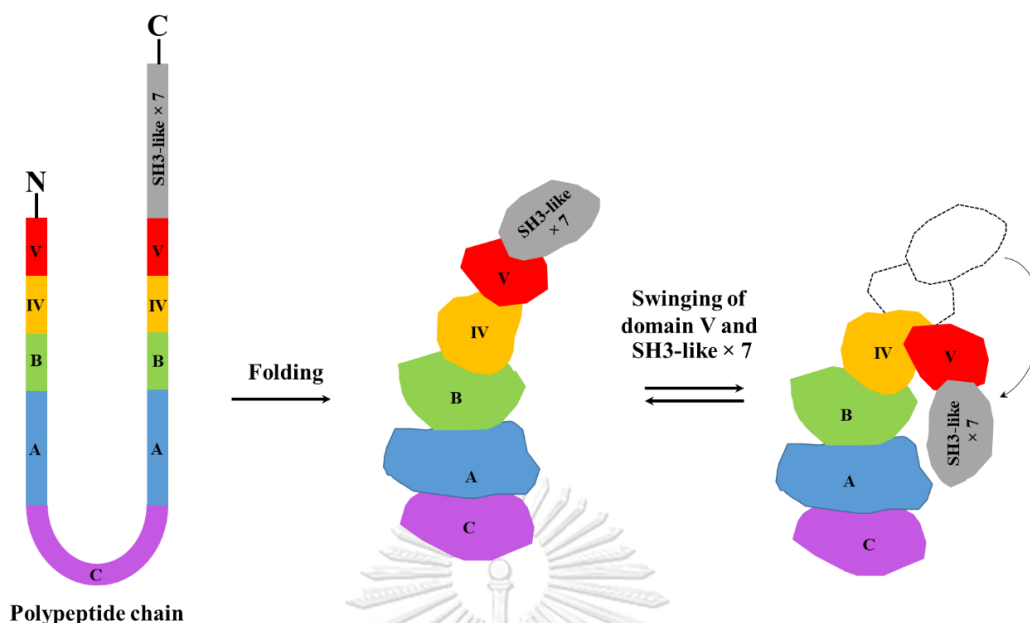


Figure 79 Schematic model of proposed conformation of ALT. Domain A harbouring catalytic triad was shown in blue. Domains B and C were shown in green and purple, respectively. Domains IV and V were represented in yellow and red, while grey colour represents 7 tandem repeat SH3-like domains.

4.4 Characterisation of ALT products

Since the patterns of products of WTALT, $\Delta 3$ SHALT and $\Delta 7$ SHALT were slightly similar, the products of WTALT were chosen as a representative for further characterisation.

4.4.1 Oligosaccharide characterisation

Generally, oligosaccharide products of some glucanase made up of fructose connected with chain of glucoses (Fru-Glc_(n)) with various types of linkages such as in D-Glucosyltransferase (GTF-S3)⁹⁴ and glucosyltransferase I⁹⁵ from *Streptococcus sobrinus*. On the contrary, no detectable fructose molecule present at the end of oligosaccharide chains produced by WTALT as confirmed by reducing property of products. A proposed mechanism explained that fructose of sucrose acceptor was

eliminated during reaction³⁹. To the best of our knowledge, we also proposed that oligosaccharide products were hydrolysed by the WTALT resulted in removal of fructose from the product chains although hydrolysis activity of glucansucrases on their own products has not been reported so far. Hence, this could be an alternative reaction of glucansucrase catalysis mechanisms^{7,17} as shown in Fig. 80. Noticeably, the self-cleaved products could possibly act as an acceptor molecule again.

Furthermore, effect of reaction temperature (18 - 30 °C) was also observed. Notably, shorter products were produced when incubated at lower temperature. This phenomenon was very difficult to explain since the longer chain of products were normally obtained after incubated at lower temperature due to the reduction of hydrolysis rate such as the production of longer chains of levan products produced by levansucrase from *Zymomonas mobilis*⁹⁶.

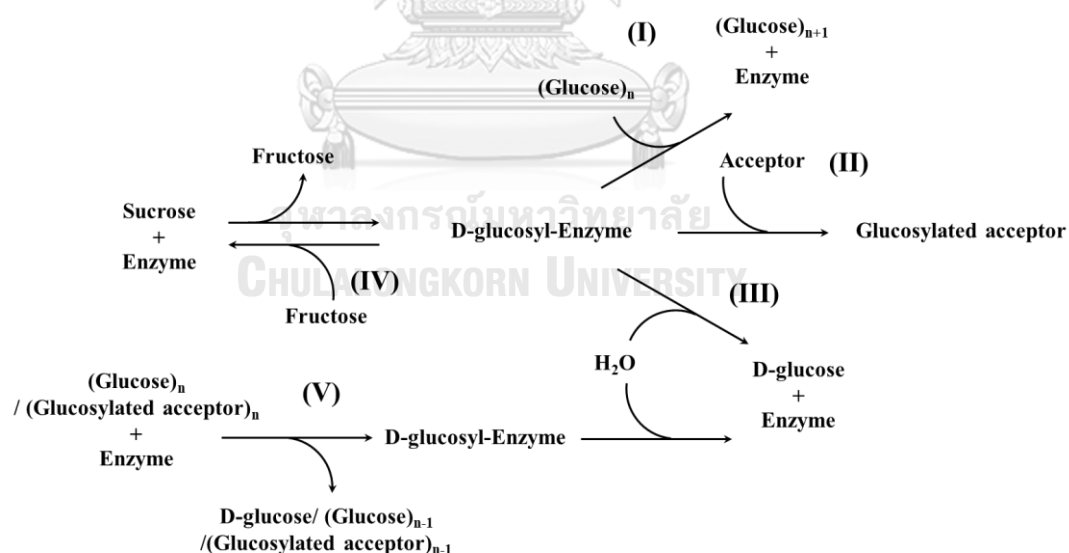


Figure 80 The novel proposed reactions catalysed by glucansucrases. (I) glucan synthesis by transferring of glucosyl units; (II) oligosaccharide synthesis by acceptor reaction; (III) sucrose hydrolysis; (IV) isotopic exchange by reverse reaction of glucosyl-enzyme complex formation and (V) glucanase activity.

4.4.2 Polymer characterisation

Considering the linkage analysis, the polymer was subjected to NMR. However, at high concentration (more than 15 % (w/v)) of polymer, it presents as gel-like material with very high viscosity, which could interfere the NMR signals. To avoid the chemical bias of α -1,3 and α -1,6 linkages, the polymer was sonicated prior to NMR to reduce the viscosity. The ^{13}C anomeric spectra of α -1,3 and α -1,6 linkages were indicated. However, each anomeric peak was split into at least 2 peaks indicated heterogeneous environments as same as the ^1H and COSY spectra with the presence of small amount of TFA that could efficiently separate α -1,6 linkage anomeric peak into 4 strong coupling signal peaks. This evidence clearly indicated the distribution of α -1,3 and α -1,6 linkages in WTALT polymer with irregular alternating pattern.

Because the original WTALT polymer was rarely dissolved, the polymer was then sonicated and the methylation analysis was therefore performed twice for ensuring complete reaction. Then, the methylations of both original and sonicated WTALT polymers were conducted in parallel under the same condition. The percent methylation of glucopyranose at different positions in original and sonicated forms was significantly similar as shown in Table 3.8 (Section 3.4.2.2), suggested that the methylation was complete. Obviously, the overall ratios of methylated glucose of WTALT polymer were similar to that of *L. reuteri* 180 (EPS180)⁴⁹ although they shared only 50 % identity of their amino acid sequences³². In addition, the patterns of linkage of polymers produced by the two truncated ALTs, Δ 3SHALT and Δ 7SHALT, were also similar to that of WTALT polymer confirmed by ^{13}C , ^1H NMR and linkage analysis, indicated that SH3-like domains did not participate in defining of linkage of products which corresponded to the previous result of *LmALT*⁴¹.

Considering the investigation of linkage pattern of the polymers by HPAEC-PAD, the purified tri- to heptasaccharides from partial acid hydrolysis of WTALT polymer were compared with two linear oligosaccharides, dextran and mutan hydrolysates, which were linked by α -1,6 and α -1,3 linkages, respectively. Apparently, one of the fragments corresponded to tri- to heptasaccharides found in mixture of each species of oligosaccharide only linked by α -1,6 continuously without α -1,3 linkage, indicated that the core structure of the polymer should harbour the partial sequences of alternating between α -1,6 and α -1,3 linkages which randomly inserted within α -1,6-linked backbone. Our proposed structure was similar to that of the glucans produced by *L. reuteri* 180⁴⁹ and *L. brevis* E2538⁵⁰ rather than the alternan product of *L. messenteroides* NRRL-B1355 (*Lm*-alternan)^{48,97}. Nevertheless, some patterns of oligosaccharide might be disappeared during acid hydrolysis because the acid itself probably preferentially acts on some particular linkages⁹⁸.

4.4.3 Solubility properties of the polymer

The solubility of WTALT polymer depended on the concentration. At low concentration (less than 10 % (w/v) in H₂O), the polymer was not dissolved but it self-assembled to nanoparticle with average size of 90 nm. This fine colloid was generally dispersed in solution but not precipitated like mutan polymer⁶⁹ which is mainly α -1,3 linkage glucan (Fig. 46). Moreover, when the concentration was increased more than 10 % (w/v), the WTALT polymer become more soluble with high viscosity. Obviously, an opaque gel-like material could be obtained at the concentration of at least 15 % (w/v). The concentration-dependent manner have also been observed in alternan produced from *L. messenteroides* NRRL-B1335⁵² and *L. citreum* SK24.0024⁹⁹. On the other hand, if the concentration of WTALT polymer is increased up to 20 % (w/v) in DMSO, the

WTALT polymer will form clear solution with high viscosity. Interestingly, drying of WTALT polymer caused formation of a transparent film and this film was readily reformed to gel-like materials at high concentration solution or nanoparticle at low concentration solution as well. Nonetheless, the improvement of flexibility of transparent film is still required since it is slightly fragile.

Surprisingly, the reversible physical state of WTALT polymer definitely differed from other well-known carbohydrate polymers such as starch and dextran which are completely dissolved at low concentration. Nonetheless, the WTALT nanoparticles cannot be observed under TEM since these particles were only present in solution not in solid phase provided by this technique. In addition, all properties of WTALT polymer were also found in Δ 3SHALT and Δ 7SHALT polymers except only the molecular weight, which was relatively smaller than WTALT's.

Though other polymers such as dextran^{100,101}, chitosan¹⁰² and cellulose¹⁰³ have been reported to be able to form nanoparticles and have been applied as encapsulation agents with success, additional processes such as chemical modification or solvent exchange were needed. The properties of WTALT, Δ 3SHALT and Δ 7SHALT polymers and their ability to shift into different forms, simply by changing its concentration make these polymer a very promising candidate for encapsulation applications or concentration-dependent sensor materials.

The nanoparticle and solubility properties of the polymer in water might be occurred from the overall structure of its polymer backbone, promoting strong intramolecular interactions and packaging of the polymer chains. These interactions could be a result of the insertion of α -1,3 glycosidic linkages into backbone, as dextran containing mainly α -1,6 linkages is known to be freely soluble in aqueous solution²⁵.

Furthermore, glucans containing high ratio of α -1,3 linkage were reported to be insoluble, such as glucans from *L. messenteroides* NRRL-B1355⁴⁷, *S. mutans*¹⁰⁴, *S. sorbinus*^{69,105} and *L. messenteroides* NRRL B-1118⁸¹. Nevertheless, the sonicated WTALT, Δ 3SHALT and Δ 7SHALT polymers were lost the original properties of polymer and freely dissolved in low concentration. This suggested nanoparticle packing was also depended on length⁵² of polymer.

The various sizes of WTALT polymers were purified by GPC and analysed by MALDI-TOF. The masses corresponded to the sizes of linear structure of permethylated polymers were observed (as shown in Fig. 53A). Noticeably, MALDI-TOF results of unmodified polymers showed the acquired m/z corresponded to cyclic structures (Fig. 53B). These evidences suggested that the cyclisation is an artefact of MALDI-TOF ionisation (probably catalysed by dihydroxybenzoic acid (DHB) used as a matrix). Conversely, no masses of oligosaccharide fragments were detected by another technique for mass detection, ESI-MS, which exhibited milder condition than MALDI-TOF. This suggested that the ESI could not make polymer fragmentation which was a false positive result obtained from MALDI-TOF.

4.5 Mutagenesis of ALT by alanine scanning

Considering the results of truncated SH3-like domains, no significant change in product pattern was observed. Moreover, because *Lcalt* is such a very long gene, to reduce error rate from gene amplification, the mutation was performed based on the sequence of shortest truncated *Lcalt*, Δ 7Shalt, standing for 'wild type' in this experiment. The alanine scanning mutagenesis of candidate aromatic residues surrounded active site was conducted. W675A and Y1124A produced oligosaccharide products without detectable polymers. Nevertheless, almost activity of Y1124A was

obviously lost. This is possible that Y1124 located very closely to and under the catalytic triad residues as shown in homology model (Fig. 55), which directly impacted on its catalytic ability. Noticeably, W675A produced only desirable products or short chain glucans (G2 – G7) confirmed by MALDI-TOF MS. After that, W675 was further characterised by saturated mutation. We found that substitution with aromatic residues (W675F and W675Y) resulted in polymer production. However, replacement at W675 position by different types of amino acids led to production of different patterns of glucans as demonstrated by TLC and HPAEC-PAD. Finally, W675A was the mutant of interest due to its short glucan chain products (G2 – G7) as described above.

4.6 Characterisation of W675A

Then, W675A was biochemically characterised. The optimum pH was shifted from pH 4.0 to pH 5.0 whereas the optimum temperature was not changed (40 °C). In addition, the hydrolytic activity corresponded to Michaelis–Menten kinetic which its K_m value was similar to that of WT ($\Delta 7SHALT$). On the contrary, linear relationship between transglycosylation activity and sucrose concentration was shown. These evidence suggested that W675 residue might participate in acceptor binding. To confirm the involvement of W675 in substrate binding, five disaccharides (maltose, isomaltose, cellobiose, melibiose, palatinose) were used as acceptor molecules. Interestingly, the product patterns from acceptor reactions of WT and W675A were apparently different in terms of species and amount of products. On the other hand, consumption of maltose between WT and W675A was also different. Approximately 20 % of free maltose could be detected in W675A reaction, but no detectable maltose was observed in reaction of WT. These results reinforced that W675 was the acceptor binding residue which located at +1 subsite of alternansucrase. This was similar to

W1065 in glucansucrase from *L. reuteri* 180 that was an important residue in acceptor molecule binding. Furthermore, branching of glucan catalyzed by sucrose branching enzyme¹⁰⁶ was also predicted to be present at +1 acceptor binding subsite.

Besides, the experiments were supported by the molecular docking of WT and W675A with maltose acceptor molecule. The orientation of maltose molecule in the active sites of WT and W675A was different. In WT, maltose interacted with W675 residue via hydrophobic interaction and was fit nicely in the active site. In contrast, alanine residue of W675A was located quite far away from maltose molecule. Moreover, non-reducing glucosyl residue (C6) of maltose was located closely to glucosyl donor intermediate in catalytic site. The orientation of maltose in catalytic sites of WT and glucansucrase 180 complex crystal structure (PDB code: 3KLL)³⁴ was similar. Additionally, this was also found in maltose acceptor reaction of *LmALT*, which produced panose trisaccharide (α -D-Glcp-(1,6)- α -D-Glcp-(1,4)-D-Glc) product¹⁰⁷. Obviously, unlike WT, maltose molecule could not move inside the active site of W675A. Hence, the space of the active site was increased led to less hydrophobicity environment, so water molecule could enter easily. This was consistent with the high rate of hydrolysis observed in kinetic study together with acceptor reaction analysed by HPAEC-PAD (Fig. 74-76). Therefore, high hydrolysis rate and loss of acceptor binding ability made the enzyme lost polymer elongation capability. Similarly, amino acid substitution of levansucrase from *Bacillus megaterium* (Y421F) at +1 subsite¹⁰⁸ made more hydrophobicity and reduced water accessibility into active site, and transglycosylation activity was enhanced about 3 times. Furthermore, according to the improperly positioning of maltose molecule in active site of W675A, glucosyl unit might be randomly transferred to hydroxyl groups of maltose molecule

not to the C6's position as present in WT. Thus, various products with isomeric forms were obtained by the activity of W675A. So, mutation at W675 affected the acceptor site and product pattern, which could also be observed in glucansucrase from *L. reuteri* 180¹⁰⁶.



CHAPTER V

CONCLUSION

Alternansucrase (ALT) is one of the glucansucrase enzymes. In this research, the full length alternansucrase gene from *Leuconostoc citreum* ABK-1 was successfully cloned, expressed in *E. coli* BL21 (DE3), and biochemically characterised. Our work provides varieties of glucansucrases found in lactic acid bacteria. We also confirmed the glucanase activity present in some glucansucrases since we found that ALT was able to hydrolyse its products.

The function of 7 tandem repeated SH3-like domains function in ALT were investigated using partially and fully truncated enzymes (Δ 3SHALT and Δ 7SHALT, respectively). The results showed that these domains are involved in rate of hydrolysis, enzyme stability, and amount and size of oligosaccharide and polymer products. To support the function analysis of these domains, more information based on 3D structure is still required. Moreover, we found that the stability of enzyme is not relied on the size of protein.

The relationship between carbohydrate structures and their product properties was also demonstrated. Some properties of polymer produced ALTs such as nanoparticle forming and gel-like property make it a promising carbohydrate polymer, which may be applied for nanotechnology, encapsulation and control released technology, as well as the food and pharmaceutical industries.

The mutation at acceptor binding residue (W675), located in +1 subsite, causes higher hydrolysis rate whereas apparently lower transglycosylation activity however increased diversities of products were present. The acceptor binding site mutation might

be one methodology and opportunity to extend variety of enzymatically carbohydrate synthesis.



REFERENCES

- 1 Kamerling, J. P. & Boons, G.-J. *Comprehensive glycoscience: from chemistry to systems biology*. (Elsevier, 2007).
- 2 Ajit, V. *et al.* Essentials of glycobiology. *Cold Spring Harbor Laboratory Press, New York* (2009).
- 3 Fialho, A. M. *et al.* Occurrence, production, and applications of gellan: current state and perspectives. *Applied microbiology and biotechnology* **79**, 889 (2008).
- 4 Rehm, B. H. in *Alginates: Biology and Applications* 55-71 (Springer, 2009).
- 5 Freitas, F., Alves, V. D. & Reis, M. A. Advances in bacterial exopolysaccharides: from production to biotechnological applications. *Trends in biotechnology* **29**, 388-398 (2011).
- 6 Bielecki, S., Krystynowicz, A., Turkiewicz, M. & Kalinowska, H. Bacterial cellulose. *Biopolymers online* (2005).
- 7 Leemhuis, H. *et al.* Glucansucrases: three-dimensional structures, reactions, mechanism, α -glucan analysis and their implications in biotechnology and food applications. *Journal of biotechnology* **163**, 250-272 (2013).
- 8 Patel, S., Majumder, A. & Goyal, A. Potentials of exopolysaccharides from lactic acid bacteria. *Indian journal of microbiology* **52**, 3-12 (2012).
- 9 Ogier, J.-C., Casalta, E., Farrokh, C. & Saihi, A. Safety assessment of dairy microorganisms: the *Leuconostoc* genus. *International journal of food microbiology* **126**, 286-290 (2008).
- 10 Badel, S., Bernardi, T. & Michaud, P. New perspectives for *Lactobacilli* exopolysaccharides. *Biotechnology advances* **29**, 54-66 (2011).
- 11 Prajapati, J. B., Nathani, N. M., Patel, A. K., Senan, S. & Joshi, C. G. Genomic analysis of dairy starter culture *Streptococcus thermophilus* MTCC 5461. *J. Microbiol. Biotechnol* **23**, 459-466 (2013).
- 12 Riedl, C. R. *et al.* Bacterial colonization of ureteral stents. *European urology* **36**, 53-59 (1999).
- 13 Cerning, J. Exocellular polysaccharides produced by lactic acid bacteria. *FEMS microbiology reviews* **7**, 113-130 (1990).
- 14 Trevors, J., Barkay, T. & Bourquin, A. Gene transfer among bacteria in soil and aquatic environments: a review. *Canadian Journal of Microbiology* **33**, 191-198 (1987).
- 15 De Vuyst, L. & Degeest, B. Heteropolysaccharides from lactic acid bacteria. *FEMS microbiology reviews* **23**, 153-177 (1999).
- 16 van Hijum, S. A., Kralj, S., Ozimek, L. K., Dijkhuizen, L. & van Geel-Schutten, I. G. Structure-function relationships of glucansucrase and fructansucrase enzymes from lactic acid bacteria. *Microbiology and Molecular Biology Reviews* **70**, 157-176 (2006).
- 17 Monchois, V., Willemot, R.-M. & Monsan, P. Glucansucrases: mechanism of action and structure-function relationships. *FEMS Microbiology Reviews* **23**, 131-151 (1999).
- 18 Naessens, M., Cerdobbel, A., Soetaert, W. & Vandamme, E. J. *Leuconostoc* dextranase and dextran: production, properties and applications. *Journal of Chemical Technology and Biotechnology* **80**, 845-860 (2005).

- 19 Bounaix, M.-S. *et al.* Biodiversity of exopolysaccharides produced from sucrose by sourdough lactic acid bacteria. *Journal of Agricultural and Food Chemistry* **57**, 10889-10897 (2009).
- 20 Tewari, Y. B. & Goldberg, R. N. Thermodynamics of hydrolysis of disaccharides: lactulose, α -d-melibiose, palatinose, d-trehalose, d-turanose and 3-o- β -d-galactopyranosyl-d-arabinose. *Biophysical chemistry* **40**, 59-67 (1991).
- 21 Kralj, S., Buchholz, K., Dijkhuizen, L. & Seibel, J. Fructansucrase enzymes and sucrose analogues: a new approach for the synthesis of unique fructo-oligosaccharides. *Biocatalysis and Biotransformation* **26**, 32-41 (2008).
- 22 Lombard, V., Golaconda Ramulu, H., Drula, E., Coutinho, P. M. & Henrissat, B. The carbohydrate-active enzymes database (CAZy) in 2013. *Nucleic acids research* **42**, D490-D495 (2013).
- 23 Moulis, C., André, I. & Remaud-Simeon, M. GH13 amylosucrases and GH70 branching sucrases, atypical enzymes in their respective families. *Cellular and molecular life sciences* **73**, 2661-2679 (2016).
- 24 Gangoiti, J., Pijning, T. & Dijkhuizen, L. Biotechnological potential of novel glycoside hydrolase family 70 enzymes synthesizing α -glucans from starch and sucrose. *Biotechnology advances* (2017).
- 25 Jeanes, A. *et al.* Characterization and classification of dextrans from ninety-six strains of bacteria 1b. *Journal of the American Chemical Society* **76**, 5041-5052 (1954).
- 26 Kralj, S., van Geel-Schutten, G., Van Der Maarel, M. & Dijkhuizen, L. Biochemical and molecular characterization of *Lactobacillus reuteri* 121 reuteransucrase. *Microbiology* **150**, 2099-2112 (2004).
- 27 Kralj, S., Stripling, E., Sanders, P., van Geel-Schutten, G. & Dijkhuizen, L. Highly hydrolytic reuteransucrase from probiotic *Lactobacillus reuteri* strain ATCC 55730. *Applied and environmental microbiology* **71**, 3942-3950 (2005).
- 28 Ito, K. *et al.* Crystal structure of glucansucrase from the dental caries pathogen *Streptococcus mutans*. *Journal of molecular biology* **408**, 177-186 (2011).
- 29 Pijning, T., Vujičić-Žagar, A., Kralj, S., Dijkhuizen, L. & Dijkstra, B. W. Flexibility of truncated and full-length glucansucrase GTF180 enzymes from *Lactobacillus reuteri* 180. *The FEBS journal* **281**, 2159-2171 (2014).
- 30 Claverie, M. *et al.* Investigations on the Determinants Responsible for Low Molar Mass Dextran Formation by DSR-M Dextransucrase. *ACS Catalysis* **7**, 7106-7119 (2017).
- 31 Kingston, K. B., Allen, D. M. & Jacques, N. A. Role of the C-terminal YG repeats of the primer-dependent streptococcal glucosyltransferase, GtfJ, in binding to dextran and mutan. *Microbiology* **148**, 549-558 (2002).
- 32 Kralj, S. *et al.* Glucan synthesis in the genus *Lactobacillus*: isolation and characterization of glucansucrase genes, enzymes and glucan products from six different strains. *Microbiology* **150**, 3681-3690 (2004).
- 33 Shah, D. S., Joucla, G., Remaud-Simeon, M. & Russell, R. R. Conserved repeat motifs and glucan binding by glucansucrases of oral streptococci and *Leuconostoc mesenteroides*. *Journal of bacteriology* **186**, 8301-8308 (2004).

- 34 Vujičić-Žagar, A. *et al.* Crystal structure of a 117 kDa glucansucrase fragment provides insight into evolution and product specificity of GH70 enzymes. *Proceedings of the National Academy of Sciences* **107**, 21406-21411 (2010).
- 35 Jensen, M. H. *et al.* Crystal structure of the covalent intermediate of amylosucrase from *Neisseria polysaccharea*. *Biochemistry* **43**, 3104-3110 (2004).
- 36 Parnaik, V. K., Luzio, G. A., Grahame, D. A., Ditson, S. L. & Mayer, R. M. A D-glucosylated form of dextransucrase: preparation and characteristics. *Carbohydrate research* **121**, 257-268 (1983).
- 37 Robyt, J. F. & Walseth, T. F. The mechanism of acceptor reactions of *Leuconostoc mesenteroides* B-512F dextransucrase. *Carbohydrate research* **61**, 433-445 (1978).
- 38 Robyt, J. F. & Taniguchi, H. The mechanism of dextransucrase action: biosynthesis of branch linkages by acceptor reactions with dextran. *Archives of biochemistry and biophysics* **174**, 129-135 (1976).
- 39 Robyt, J. F., Yoon, S.-H. & Mukerjee, R. Dextransucrase and the mechanism for dextran biosynthesis. *Carbohydrate research* **343**, 3039-3048 (2008).
- 40 Argüello-Morales, M. A. *et al.* Sequence analysis of the gene encoding alternansucrase, a sucrose glucosyltransferase from *Leuconostoc mesenteroides* NRRL B-1355. *FEMS microbiology letters* **182**, 81-85 (2000).
- 41 Joucla, G., Pizzut, S., Monsan, P. & Remaud-Simeon, M. Construction of a fully active truncated alternansucrase partially deleted of its carboxy-terminal domain. *FEBS letters* **580**, 763-768 (2006).
- 42 Côté, G. L., Holt, S. M. & Miller-Fosmore, C. (ACS Publications, 2003).
- 43 Côté, G. L. & Robyt, J. F. Acceptor reactions of alternansucrase from *Leuconostoc mesenteroides* NRRL B-1355. *Carbohydrate Research* **111**, 127-142 (1982).
- 44 Morales, M. A. A., Remaud-Simeon, M., Willemot, R.-M., Vignon, M. R. & Monsan, P. Novel oligosaccharides synthesized from sucrose donor and cellobiose acceptor by alternansucrase. *Carbohydrate research* **331**, 403-411 (2001).
- 45 Richard, G., Morel, S., Willemot, R.-M., Monsan, P. & Remaud-Simeon, M. Glucosylation of α -butyl- and α -octyl-D-glucopyranosides by dextransucrase and alternansucrase from *Leuconostoc mesenteroides*. *Carbohydrate research* **338**, 855-864 (2003).
- 46 Holt, S., Miller-Fosmore, C. & Côté, G. Growth of various intestinal bacteria on alternansucrase-derived oligosaccharides. *Letters in applied microbiology* **40**, 385-390 (2005).
- 47 CÔTÉ, G. L. & Robyt, J. F. Isolation and partial characterization of an extracellular glucansucrase from *Leuconostoc mesenteroides* NRRL B-1355 that synthesizes an alternating (1 \rightarrow 6),(1 \rightarrow 3)- α -D-glucan. *Carbohydrate Research* **101**, 57-74 (1982).
- 48 Seymour, F. K., Knapp, R. D., Chen, E. C., Bishop, S. H. & Jeanes, A. Structural analysis of *Leuconostoc* dextrans containing 3-O- α -D-glucosylated α -D-glucosyl residues in both linear-chain and branch-point positions, or only in branch-point positions, by methylation and by ¹³C-NMR spectroscopy. *Carbohydrate Research* **74**, 41-62 (1979).

- 49 van Leeuwen, S. S. *et al.* Structural analysis of the α -D-glucan (EPS180) produced by the *Lactobacillus reuteri* strain 180 glucansucrase GTF180 enzyme. *Carbohydrate research* **343**, 1237-1250 (2008).
- 50 Dertli, E., Colquhoun, I. J., Côté, G. L., Le Gall, G. & Narbad, A. Structural analysis of the α -D-glucan produced by the sourdough isolate *Lactobacillus brevis* E25. *Food chemistry* **242**, 45-52 (2018).
- 51 Cote, G. L. Low-viscosity α -d-glucan fractions derived from sucrose which are resistant to enzymatic digestion. *Carbohydrate polymers* **19**, 249-252 (1992).
- 52 Leathers, T. D., Nunnally, M. S., Ahlgren, J. A. & Côté, G. L. Characterization of a novel modified alternan. *Carbohydrate polymers* **54**, 107-113 (2003).
- 53 Saksela, K. & Permi, P. SH3 domain ligand binding: What's the consensus and where's the specificity? *FEBS letters* **586**, 2609-2614 (2012).
- 54 McPherson, P. S. Regulatory role of SH3 domain-mediated protein-protein interactions in synaptic vesicle endocytosis. *Cellular signalling* **11**, 229-238 (1999).
- 55 Kurochkina, N. *Sh Domains: Structure, Mechanisms and Applications*. (Springer, 2015).
- 56 Xu, Q. *et al.* Structural basis of murein peptide specificity of a γ -D-glutamyl-L-diamino acid endopeptidase. *Structure* **17**, 303-313 (2009).
- 57 Xu, Q. *et al.* Structure of the γ -D-glutamyl-L-diamino acid endopeptidase YkfC from *Bacillus cereus* in complex with L-Ala- γ -D-Glu: insights into substrate recognition by NlpC/P60 cysteine peptidases. *Acta Crystallographica Section F: Structural Biology and Crystallization Communications* **66**, 1354-1364 (2010).
- 58 Lu, J. Z., Fujiwara, T., Komatsuzawa, H., Sugai, M. & Sakon, J. Cell wall-targeting domain of glycyglycine endopeptidase distinguishes among peptidoglycan cross-bridges. *Journal of Biological Chemistry* **281**, 549-558 (2006).
- 59 Jonquieres, R., Bierne, H., Fiedler, F., Gounon, P. & Cossart, P. Interaction between the protein InlB of *Listeria monocytogenes* and lipoteichoic acid: a novel mechanism of protein association at the surface of gram-positive bacteria. *Molecular microbiology* **34**, 902-914 (1999).
- 60 Jonquieres, R., Pizarro-Cerdá, J. & Cossart, P. Synergy between the N- and C-terminal domains of InlB for efficient invasion of non-phagocytic cells by *Listeria monocytogenes*. *Molecular microbiology* **42**, 955-965 (2001).
- 61 Braun, L., Ghebrehiwet, B. & Cossart, P. gC1q-R/p32, a C1q-binding protein, is a receptor for the InlB invasion protein of *Listeria monocytogenes*. *The EMBO journal* **19**, 1458-1466 (2000).
- 62 Pohl, E., Holmes, R. K. & Hol, W. G. Crystal structure of a cobalt-activated diphtheria toxin repressor-DNA complex reveals a metal-binding SH3-like domain. *Journal of molecular biology* **292**, 653-667 (1999).
- 63 Su, Y.-C. *et al.* Structure of *Stenotrophomonas maltophilia* FeoA complexed with zinc: a unique prokaryotic SH3-domain protein that possibly acts as a bacterial ferrous iron-transport activating factor. *Acta Crystallographica*

- Section F: Structural Biology and Crystallization Communications* **66**, 636-642 (2010).
- 64 Amari, M. *et al.* Overview of the glucansucrase equipment of *Leuconostoc citreum* LBAE-E16 and LBAE-C11, two strains isolated from sourdough. *FEMS microbiology letters* **362**, 1-8 (2015).
- 65 Fraga Vidal, R., Moulis, C., Escalier, P., Remaud-Siméon, M. & Monsan, P. Isolation of a gene from *Leuconostoc citreum* B/110-1-2 encoding a novel dextranucrase enzyme. *Current microbiology* **62**, 1260-1266 (2011).
- 66 Olivares-Illana, V., López-Munguía, A. & Olvera, C. Molecular characterization of inulosucrase from *Leuconostoc citreum*: a fructosyltransferase within a glucosyltransferase. *Journal of bacteriology* **185**, 3606-3612 (2003).
- 67 van der Veen, B. A. *et al.* Hydrophobic amino acid residues in the acceptor binding site are main determinants for reaction mechanism and specificity of cyclodextrin-glycosyltransferase. *Journal of Biological Chemistry* **276**, 44557-44562 (2001).
- 68 Kuttiyawong, K., Nakapong, S. & Pichyangkura, R. The dual exo/endo-type mode and the effect of ionic strength on the mode of catalysis of chitinase 60 (CHI60) from *Serratia* sp. TU09 and its mutants. *Carbohydrate research* **343**, 2754-2762 (2008).
- 69 Sato, S. *et al.* DNA sequence of the glucosyltransferase gene of serotype d *Streptococcus sobrinus*. *DNA Sequence* **4**, 19-27 (1993).
- 70 Sambrook, J., Fritsch, E. F. & Maniatis, T. *Molecular cloning: a laboratory manual*. (Cold spring harbor laboratory press, 1989).
- 71 Heckman, K. L. & Pease, L. R. Gene splicing and mutagenesis by PCR-driven overlap extension. *Nature protocols* **2**, 924 (2007).
- 72 Bollag, D., Rozycki, M. & Edelstein, S. Protein methods. 2nd eds. *Viley-Liss Press, USA. 414s* (1996).
- 73 Ghosh, A. *et al.* Deciphering ligand specificity of a *Clostridium thermocellum* family 35 carbohydrate binding module (CtCBM35) for gluco- and galacto-substituted mannans and its calcium induced stability. *PloS one* **8**, e80415 (2013).
- 74 Miller, G. L. Use of dinitrosalicylic acid reagent for determination of reducing sugar. *Analytical chemistry* **31**, 426-428 (1959).
- 75 Bradford, M. M. A rapid and sensitive method for the quantitation of microgram quantities of protein utilizing the principle of protein-dye binding. *Analytical biochemistry* **72**, 248-254 (1976).
- 76 Wangpaiboon, K. *et al.* An α -1, 6- and α -1, 3-linked glucan produced by *Leuconostoc citreum* ABK-1 alternansucrase with nanoparticle and film-forming properties. *Scientific reports* **8**, 8340 (2018).
- 77 Robyt, J. Thin-layer (planar) chromatography. *Encyclopedia of separation science. Academic, New York*, 2235-2244 (2000).
- 78 Oxley, D., Currie, G. & Bacic, A. Linkage analysis using the NaOH methylation method. *Cold Spring Harbor Protocols* **2006**, pdb. prot4249 (2006).
- 79 Tizzotti, M. J., Sweedman, M. C., Tang, D., Schaefer, C. & Gilbert, R. G. New ¹H NMR procedure for the characterization of native and modified food-

- grade starches. *Journal of agricultural and food chemistry* **59**, 6913-6919 (2011).
- 80 Miao, M. *et al.* Characterisation of a novel water-soluble polysaccharide from
Leuconostoc citreum SK24. 002. *Food hydrocolloids* **36**, 265-272 (2014).
- 81 Côté, G. L. & Skory, C. D. Cloning, expression, and characterization of an
insoluble glucan-producing glucansucrase from Leuconostoc mesenteroides
NRRL B-1118. *Applied microbiology and biotechnology* **93**, 2387-2394
(2012).
- 82 Pijning, T., Vujičić-Žagar, A., Kralj, S., Dijkhuizen, L. & Dijkstra, B. W.
Structure of the α -1, 6/ α -1, 4-specific glucansucrase GTFA from Lactobacillus
reuteri 121. *Acta Crystallographica Section F: Structural Biology and
Crystallization Communications* **68**, 1448-1454 (2012).
- 83 Zurdo, J., Gujjarro, J., Jiménez, J. L., Saibil, H. R. & Dobson, C. M.
Dependence on solution conditions of aggregation and amyloid formation by
an SH3 domain1. *Journal of molecular biology* **311**, 325-340 (2001).
- 84 Neudecker, P. *et al.* Structure of an intermediate state in protein folding and
aggregation. *Science* **336**, 362-366 (2012).
- 85 Cámara-Artigas, A., Martín-García, J. M., Morel, B., Ruiz-Sanz, J. & Luque,
I. Intertwined dimeric structure for the SH3 domain of the c-Src tyrosine
kinase induced by polyethylene glycol binding. *FEBS letters* **583**, 749-753
(2009).
- 86 Martín-García, J. M., Luque, I., Mateo, P. L., Ruiz-Sanz, J. & Cámara-Artigas,
A. Crystallographic structure of the SH3 domain of the human c-Yes tyrosine
kinase: Loop flexibility and amyloid aggregation. *FEBS letters* **581**, 1701-
1706 (2007).
- 87 Lapidus, D. *et al.* Multiple β -sheet molecular dynamics of amyloid formation
from two ABL-SH3 domain peptides. *Peptide Science* **98**, 557-566 (2012).
- 88 Lopez-Munguia, A. *et al.* Production and purification of alternansucrase, a
glucosyltransferase from Leuconostoc mesenteroides NRRL B-1355, for the
synthesis of oligoalternans. *Enzyme and microbial technology* **15**, 77-85
(1993).
- 89 Robyt, J. F. & Walseth, T. F. Production, purification, and properties of
dextranucrase from Leuconostoc mesenteroides NRRL B-512F.
Carbohydrate research **68**, 95-111 (1979).
- 90 Yi, A.-R. *et al.* Cloning of dextranucrase gene from Leuconostoc citreum HJ-
P4 and its high-level expression in E. coli by low temperature induction.
Journal of microbiology and biotechnology **19**, 829-835 (2009).
- 91 Qiu, X., Pohl, E., Holmes, R. K. & Hol, W. G. High-resolution structure of the
diphtheria toxin repressor complexed with cobalt and manganese reveals an
SH3-like third domain and suggests a possible role of phosphate as co-
corepressor. *Biochemistry* **35**, 12292-12302 (1996).
- 92 Chludzinski, A. M., Germaine, G. R. & Schachtele, C. F. Purification and
properties of dextranucrase from Streptococcus mutans. *Journal of
bacteriology* **118**, 1-7 (1974).
- 93 del Moral, S., Olvera, C., Rodriguez, M. E. & Munguia, A. L. Functional role
of the additional domains in inulosucrase (IslA) from Leuconostoc citreum
CW28. *BMC biochemistry* **9**, 6 (2008).

- 94 Cheetham, N. W., Slodki, M. E. & Walker, G. J. Structure of the linear, low molecular weight dextran synthesized by a D-glucosyltransferase (GTF-S3) of *Streptococcus sobrinus*. *Carbohydrate polymers* **16**, 341-353 (1991).
- 95 Komatsu, H. *et al.* Kinetics of dextran-independent α -(1 \rightarrow 3)-glucan synthesis by *Streptococcus sobrinus* glucosyltransferase I. *The FEBS journal* **278**, 531-540 (2011).
- 96 Santos-Moriano, P. *et al.* Levan versus fructooligosaccharide synthesis using the levansucrase from *Zymomonas mobilis*: effect of reaction conditions. *Journal of molecular catalysis B: Enzymatic* **119**, 18-25 (2015).
- 97 Leathers, T. D. & Bischoff, K. M. Biofilm formation by strains of *Leuconostoc citreum* and *L. mesenteroides*. *Biotechnology letters* **33**, 517-523 (2011).
- 98 Lindberg, B., Lönngren, J. & Svensson, S. in *Advances in carbohydrate chemistry and biochemistry* Vol. 31 185-240 (Elsevier, 1975).
- 99 Miao, M. *et al.* Physicochemical characteristics of a high molecular weight bioengineered α -D-glucan from *Leuconostoc citreum* SK24. 002. *Food Hydrocolloids* **50**, 37-43 (2015).
- 100 Semyonov, D., Ramon, O., Shoham, Y. & Shimoni, E. Enzymatically synthesized dextran nanoparticles and their use as carriers for nutraceuticals. *Food & function* **5**, 2463-2474 (2014).
- 101 Aumelas, A., Serrero, A., Durand, A., Dellacherie, E. & Leonard, M. Nanoparticles of hydrophobically modified dextrans as potential drug carrier systems. *Colloids and Surfaces B: Biointerfaces* **59**, 74-80 (2007).
- 102 Xu, Y. & Du, Y. Effect of molecular structure of chitosan on protein delivery properties of chitosan nanoparticles. *International journal of pharmaceutics* **250**, 215-226 (2003).
- 103 Zhang, J., Elder, T. J., Pu, Y. & Ragauskas, A. J. Facile synthesis of spherical cellulose nanoparticles. *Carbohydrate Polymers* **69**, 607-611 (2007).
- 104 Mukasa, H., Shimamura, A. & Tsumori, H. Purification and characterization of cell-associated glucosyltransferase synthesizing insoluble glucan from *Streptococcus mutans* serotype c. *Microbiology* **135**, 2055-2063 (1989).
- 105 Konishi, N. *et al.* Structure and enzymatic properties of genetically truncated forms of the water-insoluble glucan-synthesizing glucosyltransferase from *Streptococcus sobrinus*. *The journal of biochemistry* **126**, 287-295 (1999).
- 106 Meng, X. *et al.* Characterization of the glucansucrase GTF180 W1065 mutant enzymes producing polysaccharides and oligosaccharides with altered linkage composition. *Food chemistry* **217**, 81-90 (2017).
- 107 Côté, G. L., Sheng, S. & Dunlap, C. A. Alternansucrase acceptor products. *Biocatalysis and biotransformation* **26**, 161-168 (2008).
- 108 Ortiz-Soto, M. E. *et al.* Impaired coordination of nucleophile and increased hydrophobicity in the +1 subsite shift levansucrase activity towards transfructosylation. *Glycobiology* **27**, 755-765, doi:10.1093/glycob/cwx050 (2017).

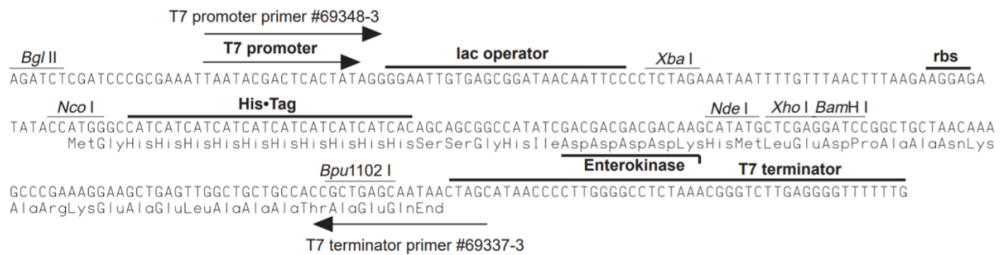
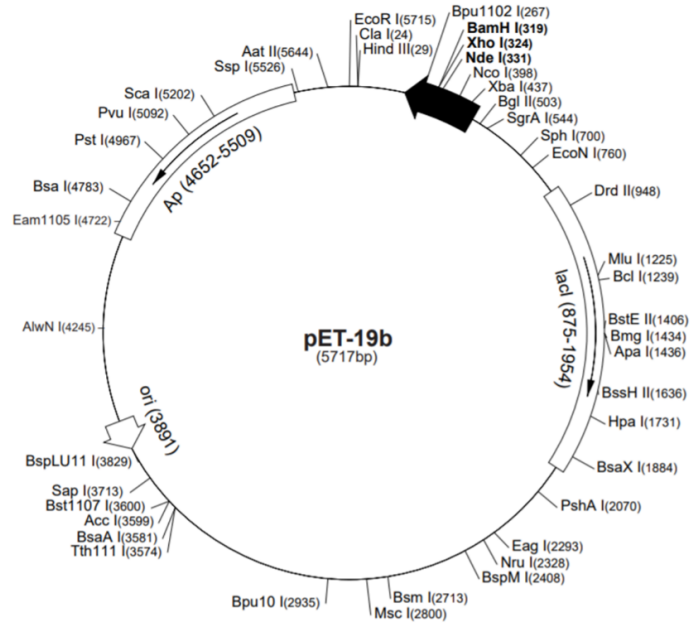
APPENDIX



จุฬาลงกรณ์มหาวิทยาลัย
CHULALONGKORN UNIVERSITY

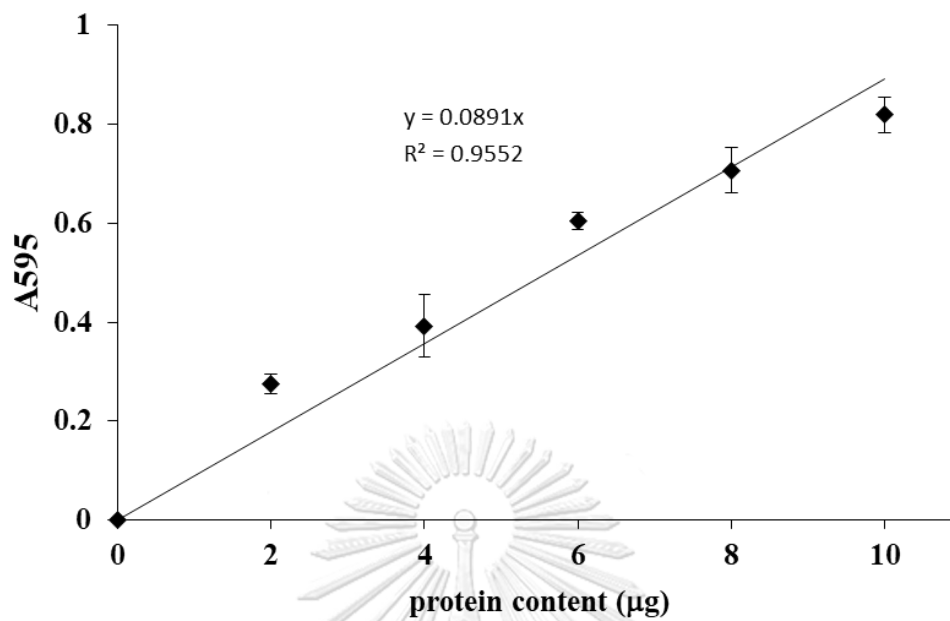
1. pET-19b vector

pET-19b sequence landmarks	
T7 promoter	472-488
T7 transcription start	471
His•Tag coding sequence	366-395
Multiple cloning sites (<i>Nde</i> I - <i>Bam</i> H I)	319-335
T7 terminator	213-259
<i>lac</i> I coding sequence	875-1954
pBR322 origin	3891
<i>bla</i> coding sequence	4652-5509

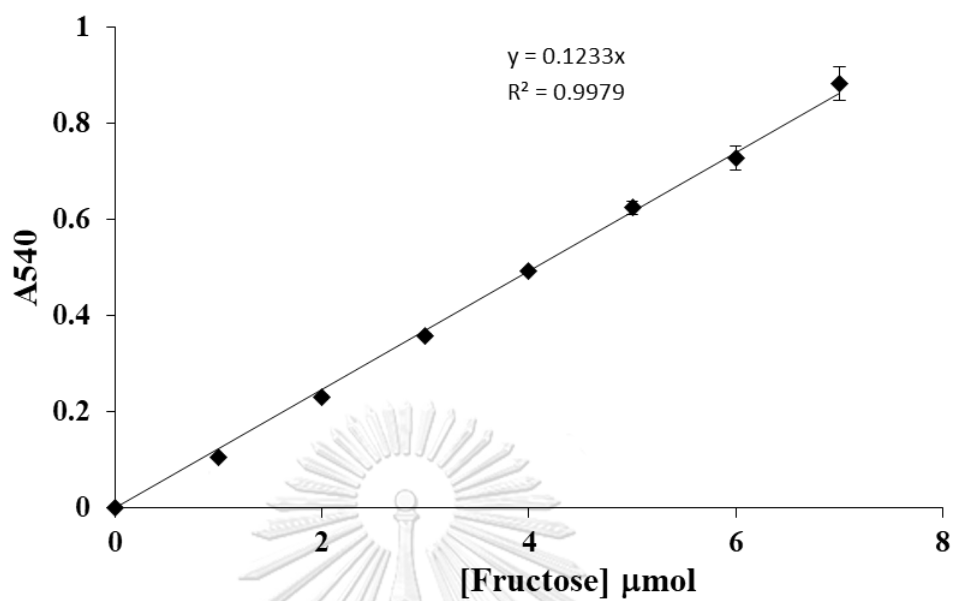


pET-19b cloning/expression region

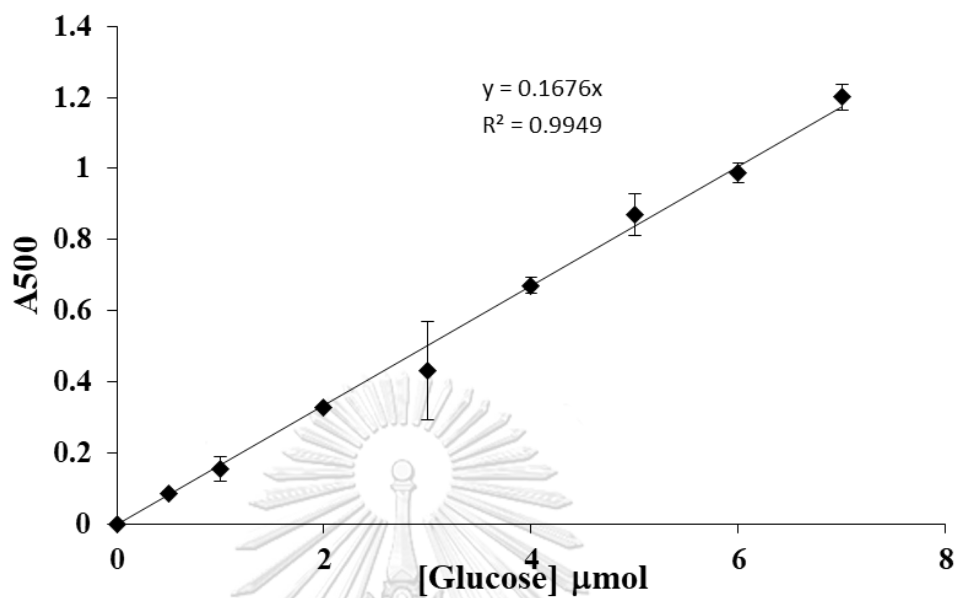
2. Calibration curve of protein (BSA) concentration (Bradford method)



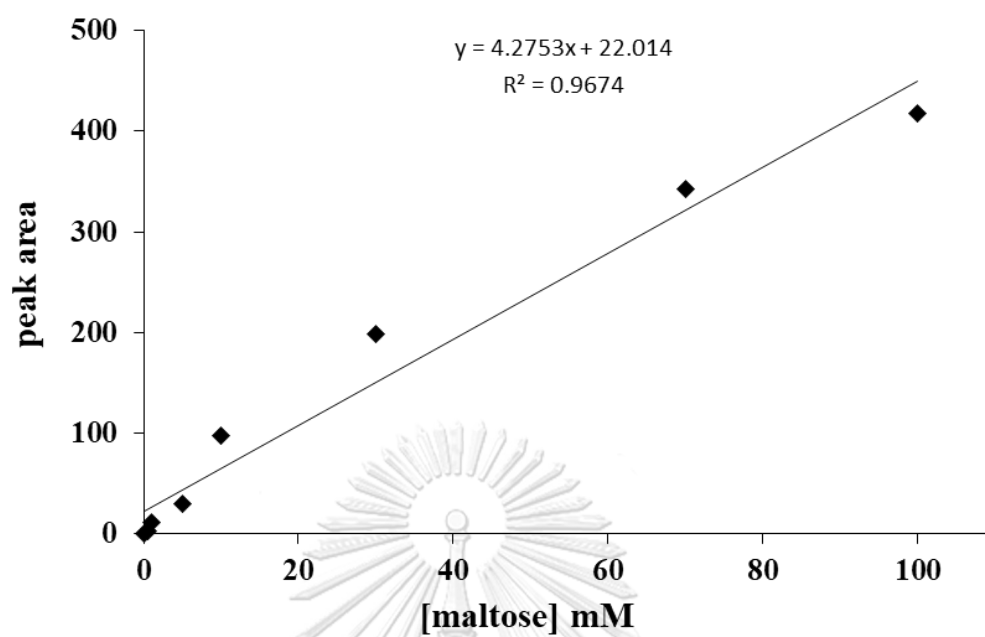
3. Calibration curve of total reducing sugar (DNS method)



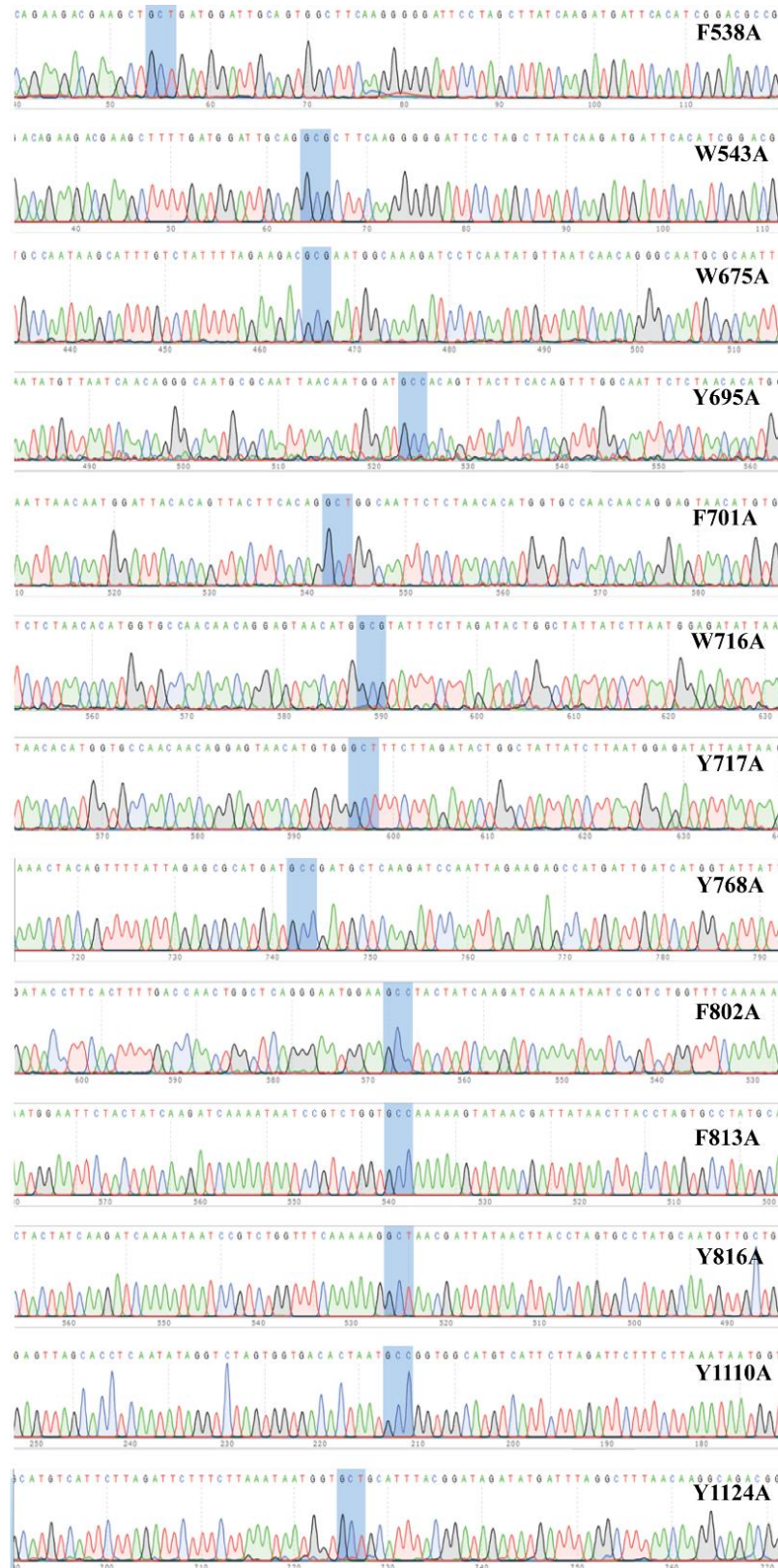
4. Calibration curve of glucose concentration (glucose oxidase assay)



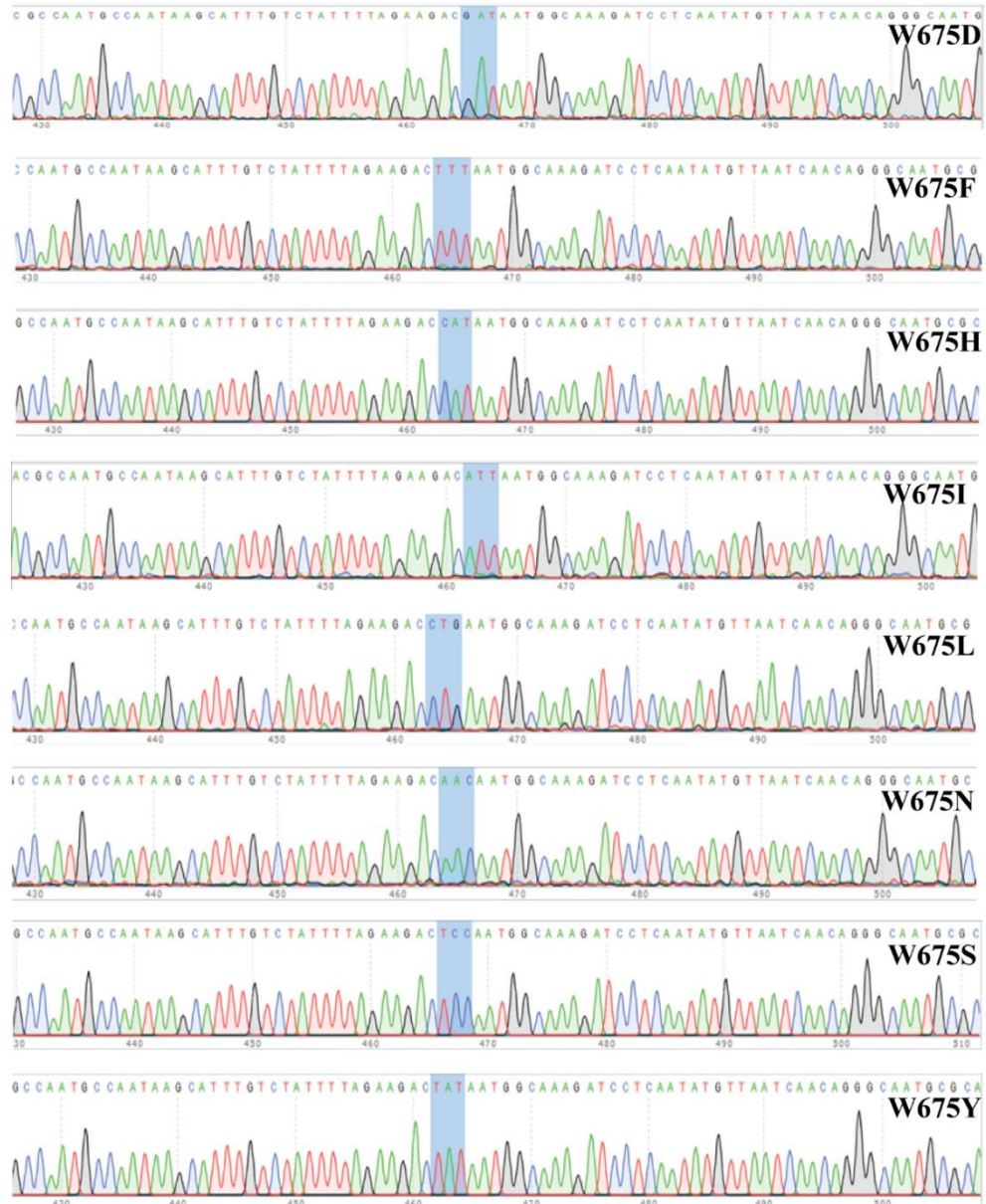
5. Calibration curve of maltose concentration (HPAEC-PAD)



6. Sequencing of 13 mutation alanine scanning, the F538A, W543A, W675A, Y695A, F701A, W716A, Y717A, Y768A, F802A, F813A, Y816A, Y1110A and Y1124A were generated by PCR driven overlapping extension method.



7. Sequencing of saturation mutagenesis at W675, W675D, W675F, W675H, W675I, W675L, W675N, W675S and W675Y were generated by PCR driven overlapping extension method.



VITA

Mr. Karan Wangpaiboon was born on 11 June, 1990 in Phitsanulok, Thailand. He finished secondary school from Phitsanulok Pittayakom School. He graduated with the Bachelor degree of Science from the Department of Biochemistry at Chulalongkorn University in 2011. He has studied for the degree of Doctor of Philosophy of Science at the program of Biochemistry and Molecular Biology, Faculty of Science, Chulalongkorn University since 2012.

